Integration of redox and light signals by the regulator protein AppA in *Rhodobacter sphaeroides*

Inaugural-Dissertation
zur Erlangung
des
Doktorgrades der Naturwissenschaften
(Dr. rer. nat.)

vorgelegt von

M.Sc.- Biol. Yuchen Han

aus
Jiangsu, P.R. China

angefertigt am Institut für Mikrobiologie und Molekularbiologie
Fachbereich Biologie und Chemie
Justus-Liebig-Universität Giessen

Giessen, Oktober 2006

Die vorliegende Arbeit wurde angefertigt am Institut für Mikrobiologie und Molekularbiologie des Fachbereiches 08 der Justus-Liebig-Universität Giessen in der Zeit von September 2002 bis Oktober 2006 unter der Leitung von Prof. Dr. Gabriele Klug.

1. Gutachterin:	**Prof. Dr. Gabriele Klug**
	Institut für Mikrobiologie und Molekularbiologie Justus-Liebig-Universität Giessen
2. Gutachter:	**Prof. Dr. Rainer Renkawitz**
	Institut für Genetik Justus-Liebig-Universität Giessen

Contents

Abbreviations

aa	amino acid
ADP	adenosinediphosphate
ALA	aminolevulinic acid
AMS	4-acetamido-4'-maleimidylstibene-2,2'-disulfonic acid
Ap	ampicillin
APS	ammoniumpersulfate
ATP	adenosinetriphosphate
BChl	bacteriochlorophyll
bp	base pair(s)
BSA	bovine serum albumin
cAMP	cyclic AMP
Ci	Curie
cpm	counts per minute
Crt	carotenoid
Cys	cysteine
°C	centigrade
Da	dalton
dATP	deoxyriboadenosine triphosphate
dCTP	deoxyribocytosine triphosphate
DEPC	diethyl-pyrocarbonate
dGTP	deoxyriboguanosine triphosphate
dITP	deoxyinosine triphosphate
DMSO	dimethyl sulfoxide
DNA	deoxynucleic acid
DNase	deoxyribonuclase
dNTP	deoxyribonucleotide triphosphate
ds	double strains
DTT	1, 4-dithiothreitol
dTTP	deoxyribothymidine triphosphate
E. coil	*Escherichia coil*
EDTA	ethylene diamine tetraacetic acid
e.g.	*exempli gratia* (for example)
et al.	*et alii* (and others)
etc.	*et cetera* (and other things)
EtOH	ethanol
FAD	flavin adenine dinucleotide
FC	flow chamber
FMN	flavin mononucleotide
g	gram
Gm	gentamycin
h	hour(s)
His	histidine
HTH	Helix-Turn-Helix
i.e.	*id est* (that is)
IPTG	isopropyl-β-D-thiogalactopyranoside
kb	kilo base pairs
kDa	kilodalton
Km	kanamycin
l	liter
LH I	light-harvesting complex I
LH II	light-harvesting complex II
LSD	salmon sperm DNA
M	molar (mol/l)
β-ME	β-Mercaptoethanol
mg	milligram
min	minute(s)
ml	milliliter
mmol	millimole
mM	millimolar
MOPS	morpholinopropansulfonic acid
mRNA	messenger RNA
µCi	microcurie
µg	microgram
µl	microliter
µm	micrometer
µM	micromolar
nm	nano meter
nt	nucleotide
OD	optical density

ORF	open reading frame
PAGE	polyacrylamide gel electrophoresis
PBS	phosphate-buddered saline
PCR	polymerase chain reaction
PMSF	phenylmethylsulfonyl fluorid
PNK	polynucleotide kinase
pO_2	partial oxygen pressure
PS	Photosynthesis
R. sphaeroides	*Rhodobacter sphaeroides*
RC	reaction center
RLU	relative light units
RNA	ribonucleic acid
RNase	ribonuclease
ROS	reactive oxygen species
rpm	revolution per minute
RT	room temperature
RU	resonance unit
sec	second(s)
SDS	sodium dodecyl sulfate
Sm	streptomycin
Sp	spectinomycin
SPR	surface plasmon resonance
Tc	tetracycline
TCA	trichloroacetic acid
TEMED	N,N,N',N'-tetramethylendiamine
Tris	Tris-hydroxymethylaminomethane
Tp	trimethoprim
UV	ultraviolet
V	volt

Publications

The following publications are based on this work:

Han, Y., Braatsch, S., Osterloh, L., and Klug, G. (2004) A eukaryotic BLUF domain mediates light-dependent gene expression in the purple bacterium *Rhodobacter sphaeroides* 2.4.1. *Proc. Natl. Acad. Sci. USA* 101: 12306-12311.

Han, Y., Meyer, M.H.F., Keusgen, M., and Klug, G. A heme cofactor is required for redox and light signaling by the AppA protein of *Rhodobacter sphaeroides*. Submitted.

Jäger, A., Braatsch, S., Haberzettl, K., Metz, S., Osterloh, L., **Han, Y.,** and Klug, G. Light signalling but not redox signalling by the AppA and PpsR proteins from *Rhodobacter sphaeroides* requires a balanced interplay to the PrrA response regulator. Submitted

1 Introduction

1.1 Blue light photoreceptors

Light is not only beneficial in processes such as photosynthesis, photo-repair and photosensing, but also harmful to living organism by leading the formation of singlet oxygen or other reactive oxygen species (ROS). The color of light is one of detectable quantities by living organism, it can activate a certain photoreceptor protein, which senses the incoming light at certain wavelength by the specific chromophore it carries. Blue light is the predominant light in aquatic ecosystem because of its ability to penetrate the water column. So it might be an ancient signal in the evolution of life. Furthermore, blue light photoreceptors may function as general response systems for high light intensities (*e.g.*, Kort *et al.*, 2000). Thus blue light absorbing photoreceptors are important for living organism. So far, blue light photoreceptors are found to distribute over three kingdoms of life – archaea, bactria and eukarya (Table 1.1). These can be divided into four families: LOV (light, oxygen, voltage) domain proteins (*e.g.*, phototropin), photolyase/cryptochrome, PYP (photoactive yellow protein) and BLUF [blue light using flavin adenine dinucleotide (FAD)] (Table 1.1).

1.1.1 LOV domain proteins

The LOV domain is a subset of the PAS superfamily involved in transducing light, oxygen or voltage signals (Taylor and Zhulin, 1999). Phototropin (NPH1) is one of well known example of this family. This protein undergoes a blue light dependent phosphorylation (Reviewed in Briggs *et al.*, 2001), and mediates photomovement responses in plants including phototropism, chloroplast relocation and stomatal opening (Briggs and Christie, 2002). Phototropin is a membrane protein, ranging from 114 to 130 kDa, which contains two input LOV domains and a serine/threonine kinase output domain (Table 1.1). LOV domains can serve as flavin-binding sites. Christie *et al.* (1999) demonstrated that both LOV domains of NPH1 are capable of binding the flavin-mononucleotide (FMN) when expressed as isolated domains in a heterologous expression system. LOV domains containing the photoactive flavin binding consensus sequence are also present in numerous bacteria. For example, YtvA in *Bacillus subtilis* is a phototropin-related blue light receptor (Reviewed in Braatsch and Klug, 2004). A

bacterial regulator of nitrogen fixation (NIFL) from *Azotobacter vinelandii* was the first to be identified as a flavoprotein containing FAD and serves as an oxygen sensor (Hill *et al.*, 1996). Recently, VVD, a LOV domain homologue as a small single protein (Table 1.1), containing 186 amino acids was identified from the fugus *Neurospora crassa* (Heintzen *et al.*, 2001). VVD defines a circadian clock–associated autoregulatory feedback loop that influences light resetting, modulates circadian gating of input by connecting output and input, and regulates light adaptation.

Table 1.1 Domain structure of blue light receptor families.

	Family	Chromophore	Distribution	Domain structure of example proteins		
I	LOV domain	Flavin	Bacteria Eukarya	NPH1 (*Arabidosis thaliana*)	LOV LOV S/T-kinase	996 aa
				VVD (*Neurospora crassa*)	LOV	186 aa
II	Photolyase/ cryptochrome	Flavin	Archaea Bacteria Eukarya	PhrA (*Rhodobacter sphaeroides*)	PHR FAD-binding	471 aa
				CRY1 (*Arabidosis thaliana*)	PHR FAD-binding	681 aa
III	Photoactive yellow protein (PYP)	Coumaric acid	Bacteria	PYP (*Rhodobacter sphaeroides*)	PAS	124 aa
				Ppr (*Rhodocista centenaria*)	PAS Phy-like H-kinase	884 aa
IV	BLUF domain	Flavin	Bacteria Eukarya	AppA (*Rhodobacter sphaeroides*)	BLUF Heme-binding	450 aa
				PACα (*Euglena gracilis*)	BLUF Adenylyl cyclase BLUF Adenylyl cyclase	1019 aa
				BlrB (*Rhodobacter sphaeroides*)	BLUF	140 aa

The distribution of blue light photoreceptors among the three kingdoms of life is based on the review in Braatsch and Klug (2004). The sequence analysis of each protein was done according to NCBI database (http://www.ncbi.nlm.nih.gov). PAS, Per-Amt-Sim, ubiquitous domain involved in sensory transduction either binding small cofactors or by protein-protein interactions (Zhulin *et al.*, 1997); LOV, light, oxygen, voltage, being a subset of the PAS superfamily, involved in transducing light,oxygen or voltage signals (Taylor and Zhulin, 1999); PHR, DNA photolyase domain; FAD-binding, flavin adenine dinucleotide binding domain; S/T-kinase, serine/threonine kinase; H-kinase, histidine kinase; Phy-like, phytochrome-like domain (Jiang *et al.*, 1999); BLUF, sensor of blue light using FAD (Gomelsky and Klug, 2002); Heme-binding, heme-binding domain, which is predicted as vitamin B_{12}-binding domain in AppA by SMART (http://smart.embl-heidelberg.de) and has been proved as heme-binding region in this work; Adenylyl cyclase: homologue with catalytic domains from class III adenylyl cyclase (Iseki *et al.*, 2002).

1.1.2 The photolyase/cryptochrome family

DNA photolyases (PHR) are ~55-65 kDa flavoproteins widely found in prokaryotes and eukaryotes, and catalyze blue/UV-A light-dependent repair of DNA damages resulting

from exposure to high-energy short-wavelength UV light (UV-B and UV-C) (Sancar, 1994). All the photolyases studied contain two chromophores (Table 1.1), a light-harvesting antenna chromophore, being either methenyltetrahydrofolate (MTHF), 8-hydroxy-7,8-didemethyl-5-deazariboflavin (8-HDF) or flavinmononucleotide (FMN), and a catalytic chromophore that is fully reduced flavin adenine dinucleotide ($FADH^-$) (Sancar, 2003). The light-harvesting chromophore absorbs blue light and transfers the excited energy in the nonradiative form to the $FADH^-$. The excited $FADH^-$ passes an electron to the cyclobutane pyrimidine dimers.

Cryptochromes (CRY) are flavoproteins in plants and animals that share structural similarity to DNA photolyase but lack photolyase activity. Cryptochromes act concurrently with phytochromes to mediate photomorphogenetic responses such as inhibition of stem elongation, stimulation of leaf expansion, control of photoperiodic flowing, entrainment of the circadian clock and regulation of gene expression (Cashmore *et al.*, 1999). Most plant cryptochromes are 70-80 kDa proteins with two recognizable domains, an N-terminal PHR domain that shares sequence homology with photolyases, and a C-terminal extension that has little sequence similarity to any known protein domain. Most residues known to be important for flavin-binding in photolyases are conserved in cryptochromes, whereas residues of photolyases that are critical for the binding of the second chromophore and DNA lesions are less well conserved in cryptochromes (Reviewed in Lin and Shilitin, 2003).

1.1.3 Photoactive yellow protein (PYP)

Because photoactive yellow protein (PYP) is a small and very water-soluble protein, it has been well-characterized in terms of structure and physical-chemical properties, although its function is poorly known. Like the LOV domain, it is a subfamily of the PAS domain family. PYP was first identified from *Ectothiorhodospira* (now called *Halorhodospira*) *halophila*. It is a yellow-colored protein and shown to be photoactive, hence it was named as Photoactive Yellow Protein (Meyer, 1985). It contains an anionic cinnamon derivative as chromophore (Hoff *et al.*, 1994) and plays a role in the process of bacterial phototaxis in an avoidance response to blue light (Sprenger *et al.*, 1993). Furthermore, proteins similar to PYP or PYP-containing proteins were found in a number of bacterial species belonging to the division of the proteobacteria. These proteins were grouped in the family of Xanthopsins. Different from other blue light photoreceptors, the proteins in this family contain 4-hydroxy-cinnamic acid as their photoactive chromophore

and their activation is based on light induced *E*/*Z* isomerization (Reviewed in Hellingwerf *et al.*, 2003). Until now no molecule acting downstream of PYP has been identified. The Ppr protein from *Rhodocista centenaria* (formerly called *Rhodospirillum centenum*) is a hybrid containing a PYP domain at the N-terminus and a phytochrome-like domain with a histidine kinase domain at the C-terminus (Table 1.1). Ppr regulates chalcone synthase gene expression in response to blue light with autophosphorylation inhibited *in vitro* by blue light. Phylogenetic analysis demonstrates that *R. centenaria* Ppr may be ancestral to cyanobacterial and plant phytochromes (Jiang *et al.*, 1999).

1.1.4 BLUF domain proteins

Recently a new family of blue light photoreceptor was identified, which noncovalently binds its chromophore FAD, hence it was designated BLUF for "sensors of blue light using FAD" (Gomelsky and Klug, 2002). Like LOV domains and PYP proteins, BLUF domain proteins can be divided into two categories (Figure 1.1): (i) "complex", multidomain proteins, *e.g.*, AppA from the purple bacterium *Rhodobacter sphaeroides*, and PACα/PACβ from eukaryote *Euglena gracilis* (Iseki *et al.*, 2002). In AppA, the BLUF domain is linked to a putative heme-binding domain sensing a redox signal (Table 1.1 and this work). BLUF domains in PAC show 27-32% sequence identity to AppA-BLUF and they are linked to the adenylyl cyclase domains (Table 1.1 and Figure 1.1); (ii) "short" proteins composed of a BLUF domain plus 30-70 additional amino acids (Figure 1.1), *e.g.*, ORF (open reading frame) 1328 in *Rhodopseudomonas palustris* (Gomelsky and Klug, 2002), BlrA (RSP4060) and BlrB (RSP1261, Table 1.1) in *Rhodobacter sphaeroides* (Jung *et al.*, 2005) and Slr1694 of *Synechocystis sp.* PCC6803 (Masuda *et al.*, 2004). In addition to the BLUF domain these small proteins contain C-termini showing no significant similarity to known protein motifs, so the hypothesis comes out that these "short" BLUF proteins are sensory modules that affect downstream processes through protein-protein interactions (Gomelsky and Klug, 2002).

Because the sequence and the predicted secondary structure of BLUF domains are dissimilar to those of PAS domains or DNA photolyase, BLUF domains or BLUF-containing proteins become a new family of blue light photoreceptor. And its small size and water-solubility make it a hot topic in the field of photoreceptors. While a number of biochemical studies have been done recently to gain some insights into blue light-mediated signal transduction, this work focuses on the physiological function of AppA

BLUF and signal transduction from input BLUF domain to output domain in *Rhodobacter sphaeroides*.

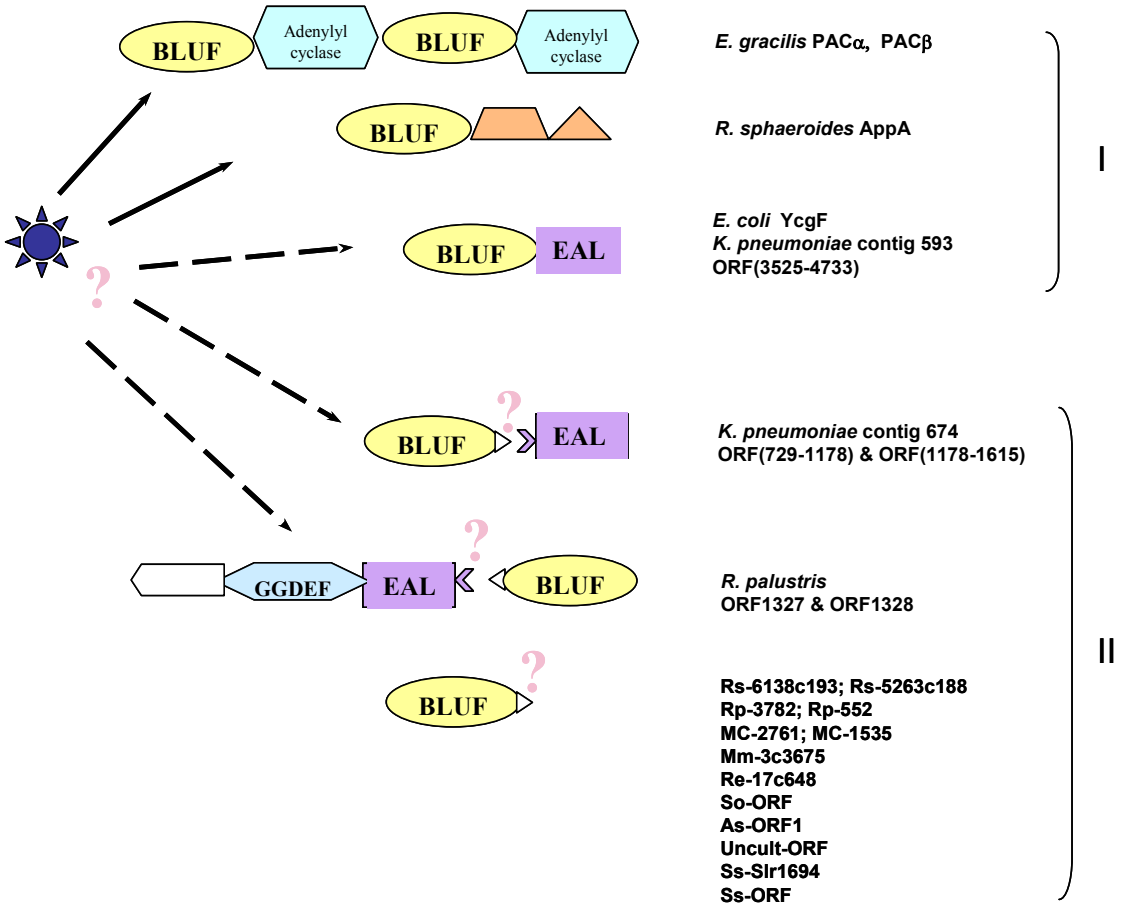

Figure 1.1 Architecture of the BLUF domain proteins.

The BLUF proteins shown in the figure are according to the SMART (http://smart.embl-heidelberg.de/) and Pfam databases (http://pfam.wustl.edu/). Group I includes 'complex' proteins, group II includes 'short' proteins. Putative domains that show no similarity to the protein domains in SMART or Pfam are shown in white. Abbreviations: BLUF, sensors of blue light using FAD; EAL, domain involved in c-di-GMP metabolism; GGDEF, putative diguanylate cyclase domain (Ausmees *et al.*, 2001); PAS, ubiquitous domain involved in sensory transduction by either binding small cofactors or protein-protein interactions (Zhulin *et al.*, 1997). (Modified from Gomelsky & Klug 2002)

1.2 Phylogenetics and physiology of *Rhodobacter sphaeroides*

The bacterium *Rhodobacter sphaeroides* is a facultative photoheterotroph belonging to the α-subdivision of the *Proteobacteria*. It is a non-sulfur purple bacterium living in aquatic environment. The *R. sphaeroides* 2.4.1 genome consists of two circular chromosomes, chromosome I (CI, ~3.0 Mbp), chromosome II (CII, ~0.9 Mbp), and five other replicons (Suwanto and Kaplan, 1989). This group of bacteria are among the most

metabolically diverse organisms known, being capable of growing in a wide variety of growth conditions. The energy acquiring mechanisms include anoxygenic photosynthesis in the presence of light under anaerobic conditions, fermentation, aerobic respiration and anaerobic respiration [*e.g.*, dimethyl sulfoxide (DMSO) as an electron acceptor]. It can also fix molecular nitrogen, assimilate carbon dioxide (Joshi and Tabita, 1996), and synthesize important tetrapyrroles, chlorophylls, heme, and vitamin B_{12} (Neidle and Kaplan, 1993).

1.3 Blue light photoreceptors in *Rhodobacter sphaeroides*

As other phototrophic bacteria, *Rhodobacter sphaeroides* can control its motility in response to light. And it can also regulate the formation of its photosynthetic complexes in response to light.

In *R. sphaeroides* the expression of the *puf* and *puc* operons encoding structural proteins of the light-harvesting complexes (LH I and LH II) and the reaction center (RC) is repressed to 50% (*pufBA*) and 20% (*pucBA*), respectively, by blue light under semi-aerobic (100μM dissolved oxygen) growth (Shimada *et al.*, 1992; Braatsch *et al.*, 2002). This response is mainly controlled by AppA-PpsR interaction. PpsR represses a subset of photosynthesis genes at high oxygen tension (Penfold and Pemberton, 1994; Gomelsky and Kaplan, 1995a). The flavoprotein AppA is known to function as PpsR antagonist, participating in the redox-dependent control of photosynthesis gene expression (Gomelsky and Kaplan, 1997). FAD, non-covalently attached to the BLUF domain of AppA was found to be the essential for the blue light dependent *puc* and *puf* expression (Braatsch *et al.*, 2002). BLUF can function as a single module independent of its C-terminus linked domain (Han *et al.*, 2004 and this work). Moreover, the three-dimensional dark state structure and the solution structure of the AppA BLUF domain reveal that BLUF is indeed a new class of flaving-binding proteins involved in light sensing (Anderson *et al.*, 2005; Grinstead *et al.*, 2006). Site-directed replacement of Tyr21 by Leu or Phe abolished the photochemical reaction implicating involvement of Tyr21 in the photocycle. Photochemical excitation of the flavin may result in strengthening of a hydrogen bond between the flavin and Tyr 21 leading to a stable local conformational change in AppA (Kraft *et al.*, 2003). Photoactivation could also break a hydrogen bond to the Trp104 side chain, which may be critical in induction of a global structural change in AppA (Anderson *et al.*, 2005). The details on the physiological

function of AppA BLUF and related signal transduction will be discussed in a later chapter (Chapter 1.4.2.2). In *R. sphaeroides* besides AppA BLUF, there are two short BLUF proteins present, *i.e.* RSP4060 (134 aa) and RSP1261 (140 aa), designated BlrA and BlrB (Table 1.1), respectively. Jung *et al.*, (2005) could show that purified BlrB contains noncovalently bound flavins and the major part of its crystal structure is similar to that of the BLUF domain from AppA. However, the function of BlrB has not been characterized yet.

In addition, the other three blue light receptor proteins or homologues were also found in *R. sphaeroides*. The *R. sphaeroides* 2.4.1 genome sequence (http://mmg.uth.tmc.edu/sphaeroides/) contains three ORFs (RSP2143, RSP1981 and RSP3077) similar to photolyase/cryptochrome like genes. According to DNA microarray studies, all three genes are transcribed (unpublished chipdata). Hendrischk *et al.* (unpublished) showed that RSP2143 (*phrA*) in contrast to RSP1981 or RSP3077 encodes a functional photolyase (PhrA, Table 1.1) and this *phrA* gene is regulated by singlet oxygen and peroxide in a σ^E dependent manner. Moreover, RSP2228 encodes a small LOV-homologous protein without any other functional domain linked. The knock-out mutant shows no significantly different phenotype comparing to wild type, so its function in *R. sphaeroides* is still mysterious. Interestingly, it was found that the RSP2228 product is strongly induced in the cells illuminated by blue light under semi-aerobic conditions (work of Anne-Kathrin Hendrischk, unpublished data). The *pyp* gene has been isolated from *Rhodobacter sphaeroides* RK1 by probing with a homologous PCR-product. This *pyp* gene encodes a 124 aa protein (Table 1.1) with 48% identity to the PYP from *Ectothiorhodospira halophila* and the typical PYP chromophore, 4-hydroxy-cinnamic acid, could be extracted from *Rhodobacter* (Kort *et al.*, 1998). So far, no physiological function of PYP could be assigned in *Rhodobacter*.

1.4 Regulation of photosynthesis genes by light and oxygen in *Rhodobacter sphaeroides*

1.4.1 The photosynthetic apparatus in *R. sphaeroides*

R. sphaeroides is extensively used for genetic studies of bacterial photosynthesis. It can transfer light energy into an electrochemical gradient of protons across the photosynthetic membrane to produce ATP without production of oxygen. The photosynthetic apparatus is only active and only expressed under anoxic or suboxic conditions, *i.e.* at reduced

oxygen tensions. *R. sphaeroides* has a respiratory system active in oxidative phosphorylation in the dark when oxygen and a suitable substrate are available. Generally, *R. sphaeroides* has the same growth rate under aerobic/dark or anaerobic/light conditions after adaptation to the respective growth conditions (Drews and Imhoff, 1991) .

The photosynthetic apparatus of *R. sphaeroides* is located in the vesicular intracytoplasmic membranes containing two light-harvesting complexes (LH I and LH II) and one photochemical reaction center (RC) (Figure 1.2A). The proteins of the RC and

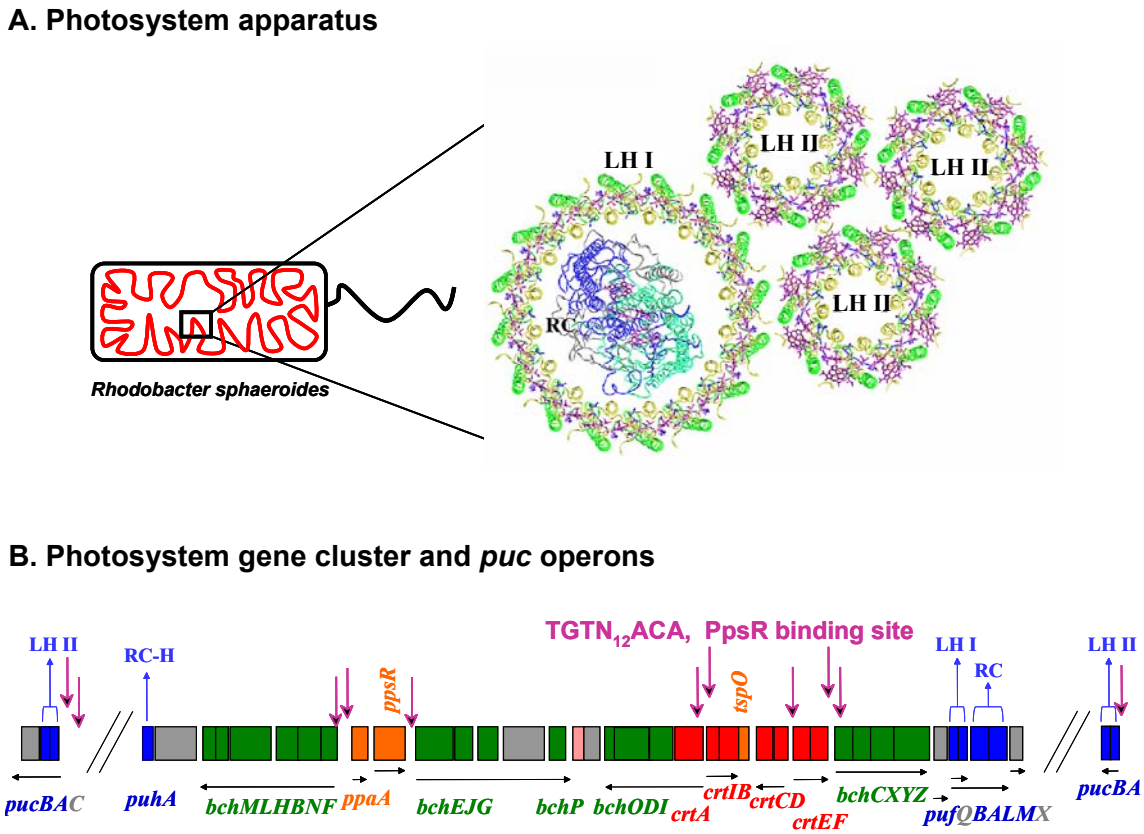

Figure 1.2 Scheme of photosynthetic apparatus (A) and photosynthesis gene cluster together with the *puc* operons (B) in *Rhodobacter sphaeroides*.

(A) Photosynthetic apparatus located in the vesicular intracytoplasmic membranes. LH, light-harvesting complex; RC, reaction center. (Modified from Osterloh, 2003)
(B) Photosystem gene cluster and *puc* operons. Putative transcripts are shown as black horizontal arrows, PpsR-binding sites are shown as purple vertical arrows and components of the photosynthetic apparatus are shown as blue vertical arrows. Colors: green, bacteriochlorophyll biosynthesis genes (*bch*); red, carotenoid biosynthesis genes (*crt)*; blue, genes encoding structural polypeptides of photosynthetic apparatus; gray, genes encoding assembly factors or proteins of unknown function; orange, genes encoding regulatory factors, *e.g. ppsR* (photopigment suppression), *ppaA* (photopigment and *puc* activation) and *tspO* (tryptophan-rich sensory protein); pink, genes encoding enzymes common to bacteriochlorophyll and ubiquinone biosynthesis. RC-H, H-subunit of RC. (Modified from Braatsch *et al.*, 2004)

LH complexes non-covalently bind bacteriochlorophyll (BChl), carotenoids and other cofactors in stoichiometric ratios (Drews, 1985). The absorbance maximum of BChl associated with the LH I is 875 nm, and those of BChl associated with the LH II complex are 800 and 850 nm. Colored carotenoids absorb in the range of 450 to 550 nm. The LH complexes serve to absorb light quanta and to transfer their excitation energy to the RC. In the RC, which is surrounded by the core antenna complex LH I (Figure 1.2A), the light-driven cyclic electron transport and the energy conservation take place. The pigment-binding proteins in LH II are encoded by part of the *puc* operon, the *puf* operon encodes the pigment-binding proteins in LH I and RC. The product of the *puhA* gene is the H-subunit of RC, which is a non-pigment-binding polypeptide and serves to stabilize the RC. The *puf* operon, the *puhA* gene and genes related to biosynthesis of carotenoids and BChl are clustered within a 45 kb DNA region of the *R. sphaeroides* genome and form a type of super operon as shown in Figure 1.2B (Drews and Imhoff, 1991). The expression of photosynthesis (PS) genes has been investigated in this work by determination of *puf* and *puc* expression.

1.4.2 Control of photosynthesis genes expression in *R. sphaeroides*

Generally, in *R. sphaeroides* the expression of PS genes is controlled by two major signals: oxygen and light. Under high oxygen tension, *R. sphaeroides* performs aerobic respiration and does not form photosynthetic apparatus. The simultaneous presence of oxygen and pigments creates the risk that ROS are generated. However, when the oxygen tension in the environment drops below a threshold value, the formation of photosystem is induced, even in the absence of light and still performing aerobic respiration (Reviewed in Gregor and Klug, 1999). In the absence of oxygen and the simultaneous presence of light, *R. sphaeroides* performs an anoxygenic photosynthesis using a single photosystem with cyclic electron transport. Under these growth conditions, the number of photosynthetic complexes formed depends on the light intensity. In addition, blue light represses the PS gene expression under intermediate oxygen tension (Shimada *et al.*, 1992; Braatsch *et al.*, 2002) and under anaerobic conditions (Happ *et al.*, 2005). In *R. sphaeroides*, oxygen and light controlled expression of PS genes is regulated by large numbers of regulatory proteins, such as the two-component PrrB/PrrA activation system, AppA/PpsR (antirepressor/repressor) system, FnrL, Spb, TrxA, IHF, PpaA, TspO (Figure 1.3).

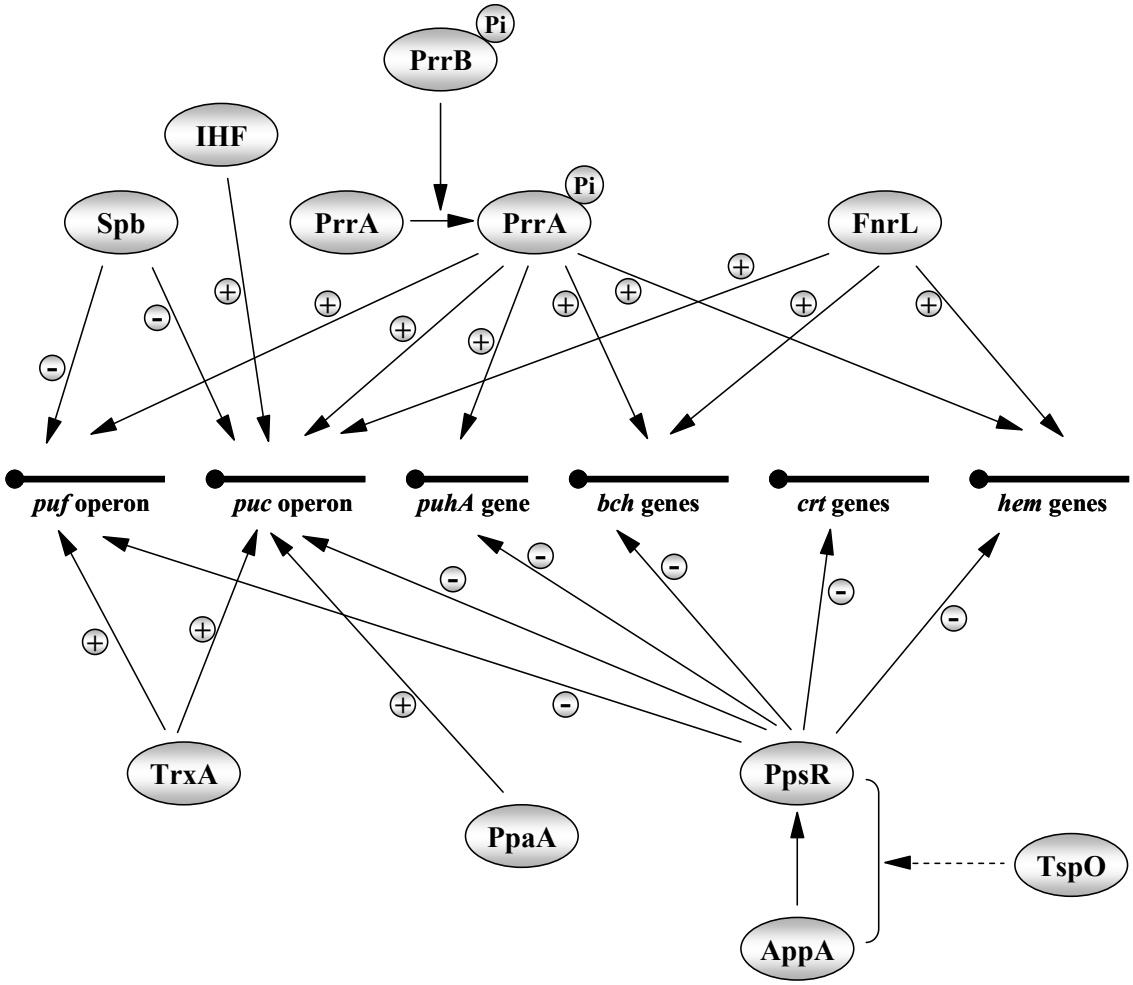

Figure 1.3 Schematic overview of proteins involved in the regulation of the transcription of photosynthesis genes in *Rhodobacter sphaeroides*.

Activation (+) and repression (-) of expression of representative PS genes are according to reported experimental results but not the prediction from sequence analysis. Solid line indicates direct regulation and dash line indicates indirect regulation. Not all proteins in regard to the expression of PS genes have been included for reasons of clarity.

Representative PS genes: *puf* operon, encodes structural proteins of the LH I antenna complex, the reaction center proteins and proteins involved in the assembly of these complexes; *puc* operon, encodes structural and regulatory proteins for the formation of the LH II antenna complex; *puhA* gene, encodes the non-pigment-binding subunit of the reaction center; *bch*, genes for bacteriochlorophyll synthesis; *crt*, genes for carotenoid synthesis; *hem*, genes for aminolevulinate synthesis and these genes are not located in the PS gene cluster.

Representative regulators: Spb, *R. sphaeroides puf*-binding protein; IHF, integration host factor; Prr, photosynthetic response regulator, at low oxygen tension the memberane-associated sensor kinase PrrB undergoes autophosporylation and transfers the phospho group to the corresponding response regulator PrrA; FnrL, fumarate nitrate regulator; TrxA, thioredoxin 1; PpaA, photopigment and *puc* activation; PpsR, photopigment suppression, a specific repressor of PS genes at high oxygen tension; AppA, activation of photopigment and *puc* expression, antagonist of PpsR, details in Figure 1.3; TspO, tryptophan-rich sensory protein, negatively affects the expression of PpsR-target genes by indirect modulation of the AppA/PpsR system.

1.4.2.1 The PrrB/PrrA two-component system

Prr, named for photosynthetic response regulator, is a signal transduction system involved in the activation of PS genes expression and the fixation of nitrogen and carbon (Joshi and Tabita, 1996). In *R. sphaeroides*, PrrA functions as a response regulator and PrrB functions as a sensor histidine-kinase/phosphatase. Those two proteins are also found in a *R. sphaeroides* related organism *R. capsulatus* and called RegA and RegB, respectively (Sganga and Bauer, 1992; Mosley, Suzuki, and Bauer, 1994). At low oxygen tension the memberane-associated sensor kinase PrrB undergoes autophosphorylation and transfers the phospho group to the corresponding response regulator PrrA (Oh and Kaplan, 2000). The phosphorylated DNA binding protein PrrA activates the transcription of several PS genes including those of the *puf* and *puc* operons (Eraso and Kaplan, 1996) (Figure 1.3). Under aerobic growth reductant flow through the cbb_3 oxidase, encoded by the *ccoNOQP* operon (cytochrome *c* oxidase), enhances the phosphatase activity of PrrB relative to its kinase activity thus preventing activation of PS genes by phosphorylated PrrA (Oh and Kaplan, 2001). A direct interaction between cbb_3 and PrrB was observed *in vitro* (Oh *et al.*, 2004). Recently, a redox-dependent light effect has been revealed in anaerobic *Rhodobacter* cultures. The light signal is transmitted via photosynthetic electron transport and components of the respiratory chain, and finally affects transcription through the PrrB/PrrA two component systems (Happ *et al.*, 2005). As a consequence, higher amounts of photosynthetic complexes are synthesized in the presence of light and absence of oxygen to allow an increased production of ATP.

PrrA is supposed to be a cytoplasmic protein and consists of a CheY-like receiver domain and a Fis-type Helix-Turn-Helix (HTH) domain. The PrrA binding site contains two GCGNC inverted repeats with variable half-site spacing and this consensus sequence was found present in the promoter region of both *puc* genes and *puf* genes (Laguri *et al.*, 2003). There is some evidence to suggest that different PS genes require different levels of active PrrA for their activation (Eraso and Kaplan, 1996). Moskvin *et al.* (2005) showed that the expression of *prrA*, upstream of which lacks PpsR binding sites, indirectly depends on PpsR. Additionally, PrrA is still active in a PrrB mutant (Eraso and Kaplan, 1994) and increases *puc* and *puf* expression when the oxygen tension decreases (This work). This further suggests that other phosphodonors are active in activating PrrA (Gomelsky and Kaplan, 1995b) or that PrrA can be activated without phosphorylation, and that PrrB may possess an intrinsic phosphatase activity (Eraso and Kaplan, 1996). The amino terminus

of PrrB comprises six hydrophobic membrane-spanning regions, which makes PrrB anchored in the membrane at its amino terminal half and with the kinase domain in the cytoplasm (Ouchane & Kaplan, 1999). Oxidation of the sensor kinase PrrB results in formation of an intracellular disulfide bond and converts the active dimer to an inactive tetramer (Swem *et al.*, 2003). In addition, the *prrC* gene was identified upstream of *prrA* with overlapping *prrA* by 8 bp (Eraso and Kaplan, 1995). Mutation study suggests that PrrC is located upstream of the two-component PrrB/PrrA activation system in the signal transduction pathway but downstream of the cbb_3 oxidase (Eraso and Kaplan, 2000).

1.4.2.2 The AppA/PpsR antirepressor/repressor system

PpsR (photopigment suppression), whose gene is located in the upstream regions of many *bch* and *crt* genes in the PS gene cluster (Figure 1.2B), is a specific repressor of PS genes at high oxygen tension (Penfold and Pemberton, 1994) (Figure 1.3). It possesses a C-terminal HTH motif, which plays a key role in DNA-binding as a tetramer (Gomelsky *et al.*, 2000; Masuda and Bauer, 2002). And the conserved binding motif TGT-N_{12}-ACA is located downstream of, or overlapping with, putative σ^{70}-type promoters of PS genes and *puc* operon (Choudhary and Kaplan, 2000) (Figure 1.2B). Inactivation of PpsR results in constitutive expression of PS genes even under aerobic conditions, thus making this $PpsR^-$ mutant genetically unstable under this condition (Gomelsky and Kaplan, 1997). The PpsR homolog from *R. capsulatus*, designated CrtJ, has been shown to bind to the same motif as a dimer and it undergoes a dithiol-disulfide switch when oxygen tension increases. Oxidized CrtJ shows lower DNA affinity (Ponnampalam and Bauer, 1997). In the central part of PpsR, there are two PAS domains critical for its proper conformation, repressor activity or protein-protein interaction (Gomelsky *et al.*, 2000). Until now, none of the PpsR proteins purified from *Escherichia coil* was found to contain any cofactors (Reviewed in Elsen *et al.*, 2005). Actually, DNA binding affinity of PpsR is under control of AppA through formation of AppA-PpsR complexes (Masuda and Bauer, 2002 and this work).

The flavoprotein AppA, activation of photopigment and *puc* expression, consists of 450 amino acids and antagonizes the repressor activity of PpsR. It is the only known protein that can transmit both redox and light signals. The N-terminal BLUF domain of AppA was identified as a new type of blue light phototreceptor and functions as single module independent of its C-terminal fused domain (Gomelsky and Klug, 2002; Han *et al.*, 2004 and this work). A cysteine-rich cluster (Cys-X5-Cys-Cys-X4-Cys-X6-Cys-Cys) at

carboxy-terminal part of AppA is previously supposed to sense the redox signal through the dithiol-disulfide switch. However, more evidences show that this part is not critical for the function of AppA (This work). In the central part of AppA, a vitamin B_{12}-binding sequence has been predicted at position of 274-393 amino acids (http://smart.embl-heidelberg.de/, Table 1.1). In fact, this work can show that there might be a heme-binding domain located at this region and transmitting redox signals. More results from this work suggest that light signal transmitted from BLUF domain and redox signals can influence the affinity between AppA and PpsR and consequently control DNA-binding activity of PpsR. It is not known how light signals are transmitted to the C-terminal part of AppA, and how changes in the light or redox signals from the C-terminal part affect the binding of AppA to PpsR.

A model of function of AppA is shown in Figure 1.4. At high oxygen tension, the AppA holoprotein is unable to release the repression of photosynthesis genes by PpsR in spite of light (Figure 1.4A). A decrease in oxygen tension to semi-aerobic conditions, in the absence of light, results in the transition of AppA into an active state and formation of a stable AppA-$PpsR_2$ complex (Figure 1.4B). This transition apparently does not involve the FAD cofactor of AppA. AppA in this state antagonizes PpsR and, therefore, PpsR-mediated repression of the *puf* and *puc* operons is released. When blue light is present, it excites FAD, facilitating reversion of AppA from the active state to the inactive state, thus leading to a tighter repression of the *puf* and *puc* operons. If oxygen tension is very low, blue light repression is still present through the AppA/PpsR system as that in intermediate oxygen conditions. However, this repression is covered by light induction through the PrrB/PrrA two component system, which can get light signal via photosynthetic electron transport and components of the respiratory chain under very low oxygen tension or anaerobic conditions (Happ *et al.*, 2005).

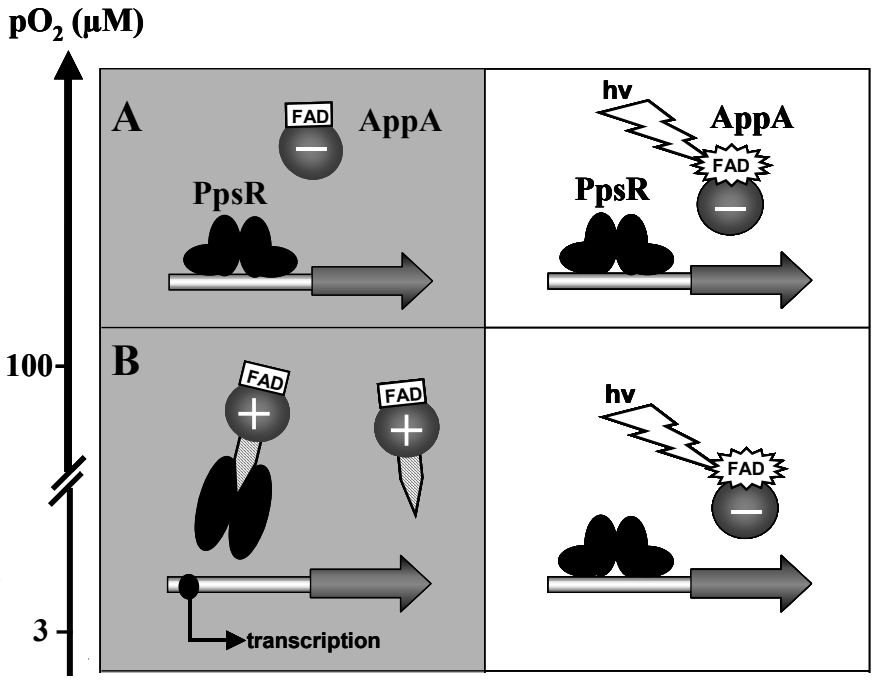

Figure 1.4 Model for function of AppA as an integrator of redox and light signals.

The oxygen and light dependent effect of AppA on *puc* expression is mediated by the transcriptional repressor PpsR (Gomelsky and Kaplan, 1998; Masuda and Bauer, 2002). **(A)** Under high oxygen tension, AppA is in an inactive conformation (−) independently of light. **(B)** During drop in oxygen tension, the AppA protein undergoes a transition to an active conformation (+) and forms a stable AppA-$PpsR_2$ complex that allows gene expression. Blue light-excited AppA (−) is incapable of inhibiting PpsR activity. The maintenance of the light dependent repression (Shimada *et al.*, 1992) is mediated by the FAD cofactor of the AppA protein (Braatsch *et al.*, 2002). (Modified from Braatsch and Klug, 2004)

1.4.2.3 Anaerobic regulator FnrL

FnrL which senses the redox state through its iron-sulfur cluster activates some photosynthesis genes at low oxygen tension (Zeilstra-Ryalls *et al.*, 1997; Zeilstra-Ryalls and Kaplan, 1998). The *fnrL* gene encodes the *R. sphaeroides* 2.4.1 homolog of Fnr (fumarate nitrate regulator), which is an anaerobic regulatory protein in *E. coli*. The N-terminal part of FnrL comprises the HTH DNA-binding domain and its consensus recognition sequence is TTGAT-N_4-ATCAA. Sequences similar or identical to this consensus sequence have been identified upstream of several genes involved in tetrapyrrole and BCh1 biosynthesis, including *hemA* (Neidle and Kaplan, 1993), *hemZ*, *hemF*, *hemN* (Zeilstra-Ryalls and Kaplan, 1995) and *bchE* (Zeilstra-Ryalls and Kaplan, 1998), as well as upstream of the *puc* operon (Lee and Kaplan, 1992). Under conditions of reduced oxygen tension, FnrL activates expression of *hemA* (Zeilstra-Ryalls and Kaplan, 1996) and the *puc* operon (Zeilstra-Ryalls and Kaplan, 1998), and it is also

involved in the anaerobic induction of *bchE*, *hemA* and *hemZ* (Oh, *et al.*, 2000) (Figure 1.3).

1.4.2.4 The *puf*-binding protein Spb

The histone-like nucleoid structuring protein (H-NS) from *R. sphaeroides*, termed Spb (*R. sphaeroides puf* operon-binding protein), contains a leucine-zipper motif, and the DNA-binding domain is located at the amino-terminal side of this motif (Shimada *et al.*, 1996). As its homolog *hvrA* in *R. capsulatus*, the *spb* gene is positioned immediately down stream of *prrA*. It was shown that Spb can bind upstream of the *puf* operon under various conditions and negatively controls the anaerobiosis-induced expression of the *puf* operon (Shimada *et al.*, 1993; 1996) (Figure 1.3). Nishimura *et al.* (1998) showed that Spb represses *puf* and *puc* expression under conditions of high light intensity. Spb may be involved in PS gene expression by facilitating the binding of other transcription factors, *e.g.* PrrA, RNA polymerase, *etc*.

1.4.2.5 Thioredoxin (Trx)

Thioredoxin is a small ubiquitous protein with a highly conserved active site sequence Cys-Gly-Pro-Cys. It is a part of the thioredoxin system, in which electrons are transferred from NADPH to thioredoxin reductase and finally to the thioredoxin. Thioredoxin together with the glutaredoxin is responsible for maintaining a cellular reducing environment and, thereby, can regulate the activity of enzymes (Reviewed in Zeller and Klug, 2006). Expression of the *trxA* gene in *R. sphaeroides* is regulated by oxygen level and oxidative stress at the transcriptional and post-transcriptional levels. All oxidative stress agents tested resulted in a moderate or strong increase of *trxA* mRNA levels, which was not due to increased mRNA stability (Li *et al.*, 2003). TrxA has been shown to affect the redox dependent expression of PS genes in *R. sphaeroides* (Pasternak *et al.*, 1999 and Figure 1.3). Furthermore, Li *et al.* (2004) presented a new signaling pathway by which oxygen can affect the expression of bacterial genes. Reduced TrxA increases the supercoiling activity of gyrase through binding to the gyrase B subunit, thus affecting PS gene expression. Inhibition of gyrase activity strongly reduces *puf* and *puc* expression. In *R. capsulatus*, another thioredoxin, TrxC, is present besides TrxA, and oxidized TrxC interacts with DNA gyrase and exerts a negative effect on the supercoiling activity of gyrase.

1.4.2.6 Other factors in photosynthesis genes expression

Besides the regulators discussed above, several additional elements have been observed to affect PS genes expression. The integration host factor (IHF) is a global regulatory protein which acts by binding DNA targets and bending the DNA so that looping occurs. Hence incontiguous regions of DNA can be brought together for interacting with DNA-binding regulatory proteins (Yang and Nash, 1989). Experimental results from Lee *et al.* (1993) suggest that the IHF-binding site is involved in repression of *puc* operon transcription by oxygen as well as modulation of *puc* operon transcription levels by incident light intensity (Figure 1.3). The *ppa* (photopigment and *puc* activation) gene is positioned immediately upstream of *ppsR* (Figure 1.2B). Its product, termed PpaA in *R. sphaeroides*, activates photopigment production and *puc* operon expression under aerobic conditions (Figure 1.3) and *ppaA* gene expression can be repressed by the repressor PpsR under high oxygen tension (Gomelsky *et al.*, 2003). The *tspO* (tryptophan-rich sensory protein) gene is also located within the PS gene cluster (Figure 1.2B). Its product TspO has been localized to the outer membrane of *R. sphaeroides* 2.4.1. TspO works through or modulates the AppA/PpsR system and acts upstream of the site of action of these regulatory proteins (Zeng and Kaplan, 2001 and Figure 1.3). In general, transcriptional regulation of PS genes by oxygen and light involves the coordinate action of many signal transduction pathways which form a complex regulatory network in *R. sphaeroides* (Figure 1.3). Some of these regulators are specific for PS genes and others are more global. Different PS genes are not all controlled by the same regulatory pathways, even these may overlap.

1.5 Objectives of this work

Many organisms are able to respond to different light qualities and light quantities. A number of photoreceptors have been identified and characterized in plant cells, however, much less is known about the perception of light in bacterial cells. The ancestors of *Rhodobacter* cells were the first cells to invent photosynthesis. This bacterium performs anoxygenic photosynthesis with only one cyclic photosystem under anaerobic conditions and in presence of light, and it also adapts to growth under aerobic conditions. When oxygen, light and pigments are present at the same time, harmful ROS are supposed to be generated. So at high oxygen tension less pigment-protein complexes are formed than at low oxygen tension. *R. sphaeroides* harbors a special light sensing molecule, AppA,

controlling blue light repression of *puf* and *puc* expression under semi-aerobic conditions through antagonizing the repressor activity of PpsR (Shimada *et al.*, 1992; Gomelsky *et al.*, 1998; Braatsch *et al.*, 2002). This work focuses on the physiological function of AppA, signals transduction between AppA and PpsR, and signals transduction between two functional domains of AppA.

AppA contains a novel type of FAD binding domain, which is named BLUF now (Gomelsky and Klug, 2002). It was published that this domain is also part of PAC protein in *Euglena gracilis* (Table 1.1). In the α-subunit and β-subunit of PAC, the BLUF domain is present in duplicate and fused to an adenylyl cyclase which shows blue light dependent activity (Iseki *et al.*, 2002). Besides AppA and PAC, sequence analysis suggests that the BLUF domain is also present as a short protein without any fused C-terminus (Gomelsky and Klug, 2002). This indicates that the BLUF domain could function as a module which can transduce a blue-light-dependent signal to certain output domains (or proteins), and this function does not depend on its fused C-terminal part. This work aims to give some experimental evidences on this assumption through expressing two functional parts of AppA separately or a hybrid PACα-AppA protein in *R. sphaeroides*.

AppA is unique in mediating light and redox signals. It contains two functional parts: the N-terminal BLUF domain sensing blue light and the C-terminal region mediating redox signaling. It is not known how light signals are transmitted to the C-terminal part of AppA, and how changes in the light or redox signals of the C-terminal part affect the binding of AppA to PpsR. This work should provide insights into the interaction of two functional domains of AppA and the interaction of AppA and PpsR through *in vitro* assays and *in vivo* analyses.

At high oxygen tension, PpsR can repress PS genes expression through binding to the consensus DNA sequence TGT-N_{12}-ACA. This sequence has been found in the promoter region of many PpsR-dependent genes but not in the *puf* operon, which encodes structural proteins and assembly factors of the RC and LH I complexes. This work should address a question: whether some other regulators integrate into blue light repression on *puf* expression. Many candidate factors, *e.g.* PrrB, FnrL, Spb, PpaA and TrxA, had been investigated in this work.

2 Materials

2.1 Chemicals and reagents

All other chemicals purchased from Carl-Roth (Germany) are not included in the list.

Products	Manufacturer
Agarose	FMC, Rockland USA
Ammonium peroxydisulfate (APS)	Sigma-Aldrich
4-acetamido-4'-maleimidylstibene-2,2'-disulfonic acid (AMS)	Molecular Probes
Bacto-Agar	Difco, Detroit USA
5-Bromo-4-chloro-3-indolyl-phosphate (BCIP)	Roche
Biotin	Serva
Boric acid (H_3BO_4)	Sigma-Aldrich
Bovines serum albumin (BSA)	Sigma-Aldrich
Bromophenol blue	Merck
Calcium chloride ($CaCl_2$)	Merck
Chloramphenicol	Sigma-Aldrich
Cobalt chloride ($CoCl_2$)	Sigma-Aldrich
Coomassie® brilliant blue R-250	Serva
Cupric chloride ($CuCl_2$)	Sigma-Aldrich
[α-^{32}P]dCTP [10 µCi/µl]	Amersham Pharmacia
[γ-^{32}P]ATP [10 µCi/µl]	Amersham Pharmacia
n-Decanal	Sigma-Aldrich
Dextran sulfate	Amersham Pharmacia
Diethyl-pyrocarbonate (DEPC)	Sigma-Aldrich
Dimethyl sulfoxide (DMSO)	Sigma-Aldrich
Ethidium bromide (EB)	Serva
Ficoll 400	Serva
Glucose	Merck
Glutathione (reduced)	Sigma-Aldrich
Glutathione Sepharose® 4B	Amersham Pharmacia
Hemin	Fluka
Hemin-agarose	Sigma-Aldrich
Imidazole	Sigma-Aldrich
1 kb Ladder	Invitrogen
Lithium acetate (LiOAc)	Sigma-Aldrich

Low range protein marker	New England Biolabs
Lumi-light western blotting substrate 1&2	Roche
Lysozyme	Serva
Magnesium sulfate ($MgSO_4$)	Merck
Mangnesium chloride ($MgCl_2$)	Roth
Manganese chloride ($MnCl_2$)	Sigma-Aldrich
Mangnesium sulfate ($MnSO_4$)	Sigma-Aldrich
Mineral oil	Sigma-Aldrich
4-Nitro blue tetrazolium chloride (NBT)	Roche
Niacinamide	Merck
Nickel sulfate ($NiSO_4$)	Sigma-Aldrich
Novobiocin sodium salt	Sigma-Aldrich
Ponceau S solution	Sigma-Aldrich
Potassium ferricyamide[$K_3Fe(CN)_6$]	Sigma-Aldrich
Prestained protein marker	New England Biolabs
Pyridine	Sigma-Aldrich
RNasin® plus RNase inhibitor	Promega
Standard I nutrient broth (STI-medium)	Merck
Sodium carbonate (Na_2CO_3)	Merck
Sodium dihydrogen phosphate (NaH_2PO_4)	Merck
Sodium dithionite ($Na_2S_2O_4$)	Fluka
Spermidine	Sigma-Aldrich
SYBR Green	Sigma-Aldrich
Tri-sodium citrate	Merck
Trace element (RÄ-medium)	Sigma-Aldrich
Vitamin B_{12}	Sigma-Aldrich
Vitamin B_{12}-agarose	Sigma-Aldrich
Xylene cyanol	Sigma-Aldrich
Yeast extract	Gibco

2.2 Enzymes

DNase I (RNase free)	Fementas or Invitrogen
DNA Topoisomerase I	Amersham Pharmacia
Lysozyme	Sigma-Aldrich
Proteinase K	Roth
Restriction endonucleases	New England Biolabs
RNase A	Roth
Taq DNA polymerase	QIAGEN
T4 DNA ligase	New England Biolabs
T4 polynucleotide kinase (T4 PNK)	New England Biolabs
Thrombin	Amersham Pharmacia

Vent DNA polymerase	New England Biolabs

2.3 Commercial reaction buffers

10×BSA for restriction endonucleases	New England Biolabs
0.1%BSA for Topoisomerase I	Amersham Pharmacia
10× NEB buffer (1, 2, 3, and 4)	New England Biolabs
5× Q-solution	QIAGEN
10× T4 PNK buffer	New England Biolabs
10× T4 ligase buffer	New England Biolabs
10× PCR buffer	QIAGEN
10× Topoisomerase I buffer	Amersham Pharmacia

2.4 Antibiotics

Table 2.1 Antibiotics. (Sterilized by 0.22 μm filter)

Antibiotics (Abbreviations)	Manufacturer	Solvent	Concentration (μg/ml)	
			E. coli	*Rhodobacter*
Ampicillin (Ap)	Carl-Roth	ddH_2O	100-200	---
Gentamycin (Gm)	Serva	ddH_2O	10	10
Kanamycin (Km)	Carl-Roth	ddH_2O	25	25
Spectinomycin (Sp)	Sigma-Aldrich	ddH_2O	10	10
Streptomycin (Sm)	Sigma-Aldrich	ddH_2O	100	25
Trimethoprim (Tp)	Sigma-Aldrich	Dimethyl-Formamide	---	50
Tetracycline (Tc)	Sigma-Aldrich	75% Ethanol	20	1.5

2.5 Molecular biological kits

E.Z.N.A. Plasmid Miniprep Kit II	Peqlab
Nick Translation Kit N 5500	Amersham Pharmacia
pGEM-T Vector System I	Promega
QIAEX II Gel Extraction Kit	QIAGEN
QIAquick Gel Extraction Kit	QIAGEN
QIAGEN OneStep RT-PCR Kit	QIAGEN
QIAGEN PCR Cloning Kit	QIAGEN
QIAquick PCR Purification Kit	QIAGEN
Reverse-iT™ One-Step RT-PCR Kit	ABgene
Total RNA isolation reagent	ABgene

2.6 Antibodies

RGS·His antibody	QIAGEN
Anti-His-AppAΔN	BioGenes and this work
Anti-PpsR	BioGenes and this work
Anti-Glutathione-S-Transferase (GST) (Peroxidase conjugate)	Sigma-Aldrich

Anti-Mouse IgG (whole molecule) (Alkaline phosphatase conjugate)
Sigma-Aldrich
Anti-Rabbit IgG (whole molecule) (Alkaline phosphatase conjugate)
Sigma-Aldrich
Anti-Rabbit IgG (whole molecule) (Peroxidase conjugate)
Sigma-Aldrich

2.7 Strains

Table 2.2 Strains.

Strain	Relevant features	References
E. coli		
JM109	*F' traD36 proA$^+$B$^+$ lacI^{q}Z Δ(lacZ)M15/ Δ(lac-proAB) glnV44 e14$^-$ gyrA96 recA1 relA1 endA1 thi hsdR17*	(Yanisch-Perron *et al.*, 1985)
JM110	F' *traD36 lacI^{q}ZΔ(lacZ)M15 proA$^+$B$^+$/rpsL* (Str^r) *thr leu thi lacY galK galT ara fhuA dam dcm glnV44 Δ(lac-proAB)*	Stratagene
M15 (pREP4)	Host strain for His-tag protein overexpression, Km^r	QIAGEN
S17-1	Tra$^+$ donor for diparental conjugation	(Simon *et al.*, 1983)
R. sphaeroides		
2.4.1	Wild-type	W.R. Sistrom
APP11	2.4.1 *ΔappA*::Tp^r	(Gomelsky and Kaplan, 1995)
JZ1678	2.4.1 *fnrL*::ΩKm^r	(Zeilstra-Ryalls and Kaplan, 1995)
L-7	2.4.1 *spb*::Km^r	(Nishimura *et al.*, 1998)
PPAXc	2.4.2 *ppaA(Xc)* (PpaA$^-$)	(Gomelsky *et al.*, 2003)
PPS1	2.4.1 *ppsR*::ΩKm^r	(Gomelsky and Kaplan, 1997)
PrrA2	2.4.1 *prrA* Δ*Bst*BI^b-*Pst*I^c::Ω Sm^r Sp^r PS$^-$ RC$^-$ B875$^-$ B800-850$^-$ Crt$^-$	(Eraso and Kaplan, 1995)
PrrB1	2.4.1 *prrB ΔNru*I-*Rsr*II::ΩSm^r Sp^r PS$^-$	(Eraso and Kaplan, 1995)
2.4.1*trxA*	Plasmid pPHURs*trxA*up was integrated into *R. sphaeroides* 2.4.1 chromosome to get single crossover recombination to generate *trxA* mutant. The chromosomal *trxA* is inactivated; one *trxA* is under control of IPTG inducible promoter. Tc^r	(work of Kuanyu Li, unpublished)

2.8 Plasmids

Table 2.3 Plasmids.

Plasmid	Relevant features	References
p484-Nco5	pRK415 derivative; contains full length *appA* with its own promoter	(Gomelsky and Kaplan, 1995)
P484-Nco50	pUC19 (*Sal*I, Pol) + 2.7-kb blunt-end *Nco*I fragment of p484-Sa (*appA* is in the same orientation as *lacZ*a)	(Gomelsky and Kaplan, 1995)
p484-Nco5-F	Site-directed mutant of *appA* in p484-Nco5; results in TG to AA (51, 52) substitution	(Braatsch *et al.*, 2002)
p484-Nco5Δ	In frame deletion of *appA* in p484-Nco5; results in loss of codon 5 to 190	(Gomelsky and Kaplan, 1998)
p484-Nco5ΔC	In frame deletion of *appA* in p484-Nco5; results in loss of codon 397 to450	Mark Gomelsky, unpublished
pBBR1MCS-2	Broad-host-range cloning vector, Km^r	(Kovach *et al.*, 1995)
pBBR1MCS-5	Broad-host-range cloning vector, Gm^r	(Kovach *et al.*, 1995)
pBBR2*pucluxAB*	pBBR1MCS-2 derivative, Sm^r Sp^r; Km^r, *puc* promoter fused to *luxAB* from *Vibrio harveyi*	(Braatsch, 2002; Happ, 2002; Han *et al.*, 2004)
pBBR2*pufluxAB*	pBBR1MCS-2 derivative, Sm^r Sp^r; Km^r, *puf* promoter fused to *luxAB* from *Vibrio harveyi*	(Kuphal, 2001)
pBBRAppA170	pBBR1MCS-5 derivative, Gm^r; contains truncated *appA* (codons 1 to 168) with its own promoter	(Han *et al.*, 2004; Osterloh, 2003)
pBluescript SK (+)	pUC19 derivative, Ap^r	Stratagene
pDrive	Cloning vector with U overhangs, *lacZα*, Ap^r, Km^r	QIAGEN
pGEX®-T	Cloning vector with T overhangs, *lacZ*, Ap^r	Promega
pGEMPACα	pGEM-T derivative, Ap^r; encoding sequence of PACα from *Euglena gracilis*	(Iseki *et al.*, 2002)
pGEX-4T-1	Cloning vector for GST-fusion protein overexpression, thrombin cleavage site, Ap^r	Amersham Pharmacia
pGEXAppAΔN	pGEX-4T-1::*appAΔ5-190*, Ap^r	This work
pGpps	pGEX-2TK::*ppsR*, Ap^r	(Gomelsky *et al.*, 2000)
pILA	pCSCM1 derivative, Ap^r, Km^r; source of *luxAB* genes from *Vibrio harveyi*	(Kunert et al., 2000)
pPHU281	Tc^r, *lacZ*, *mob*(RP4)	(Barany, 1985)
pQE30	Cloning vector for His-tag protein overexpression, Ap^r	QIAGEN
pQEAppA	pQE30::*appA*, Ap^r	This work
pQEAppAΔC	pQE30::*appAΔ397-450*, Ap^r	This work
pQEAppAΔN	pQE30::*appAΔ5-190*, Ap^r	This work

Plasmid	Relevant features	References
pQEAppAΔN9	pQE30::*appAΔ1-196* (V306A, A349V, P357L), Ap^r	This work
pQEAppAΔN14	pQE30::*appAΔ1-196* (P282Q, A314V), Ap^r	This work
pQEBLUF	pQE30::*BLUF*, Ap^r	This work
pRK415	Cloning vector, can replicate in *Rhodobacter*, *lacZ*α, IncP, Tc^r	(Keen *et al.*, 1988)
pRK4BLUF-*E.g.*	pRK415 derivative; encodes *Euglena gracilis* α1-BLUF –AppA fusion protein, Tc^r	(Han *et al.*, 2004) and this work
pRK*appA*ΔM	pRK415::*appA*Δ135-378, Tc^r	This work
RM3	pRK415::*appA* (L292R, A349V, P357L), Tc^r	This work
RM9	pRK415::*appA* (V306A, A349V, P357L), Tc^r	This work
RM12	pRK415::*appA* (V307G, A349V, P357L), Tc^r	This work
RM13	pRK415::*appA* (S348P, A349V, P357L), Tc^r	This work
RM14	pRK415::*appA* (P282Q, A314V), Tc^r	This work
RM17	pRK415::*appA* (I263T, A349V, P357L), Tc^r	This work
RM21	pRK415::*appA* (L204P, Q257R), Tc^r	This work
A	pRK415::*appA* (L204P), Tc^r	This work
B	pRK415::*appA* (P282Q), Tc^r	This work
C	pRK415::*appA* (P357L), Tc^r	This work
D	pRK415::*appA* (S348P), Tc^r	This work
E	pRK415::*appA* (A349V), Tc^r	This work
F	pRK415::*appA* (V306A), Tc^r	This work
G	pRK415::*appA* (V307G), Tc^r	This work
H	pRK415::*appA* (A314V), Tc^r	This work
I	pRK415::*appA* (A349V, P357L), Tc^r	This work
J	pRK415::*appA* (V306A, P357L), Tc^r	This work
K	pRK415::*appA* (V306A, A349V), Tc^r	This work

2.9 Oligonucleotides

All oligonucleotides were purchased from Carl-Roth (Germany).

Table 2.4 Oligonucleotides.

Name	Sequence (5'→3') and relevant features
A170down	CGG**GGTACC**TGTGCTGCAAGGCGATTA
	*Kpn*I, 623 to 640 of *BLUF* in plasmid pBBRAppA170, antisense
A314VF	AGCGTCGCGGTCCTGGCCG
	931 to 949 of *appA*, for AppA A314V mutation, sense
A314VR	CGGCCAGGACCGCGACGCT
	931 to 949 of *appA*, for AppA A314V mutation, antisense

Name	Sequence (5'→3') and relevant features
A349VF	TCGTCTCCGTGCTCAGGGCG 1037 to 1056 of *appA*, for AppA A349V mutation, sense
A349VR	CGCCCTGAGCACGGAGACGA 1037 to 1056 of *appA*, for AppA A349V mutation, antisense
appA 170	TGTCCG**TCTAGA**CGGGGGTAT *Xba*I, 499 to 520 of *appA*, introduce a stop codon, antisense
appA415	GCCGACAACACCAACATC 403 to 420 of *appA*, for sequencing of *appA*, sense
appA755	AGGTGACGCTGGCCTATT 743 to 760 of *appA*, for sequencing of *appA*, sense
AppACSph	CAT**GCATGC**GGCGCCGATGCCGGGTTC *Sph*I, 1135 to 1152 of *appA*, sense
AppA_down	CGG**GGTACC**GACGCTGCAAGAATC *Kpn*I, 1576 to 1593 of *appA*, antisense
appA*Eu*up	GGA**AGATCT**CAACACGACCTCGAGAAG *Bgl*II, 4 to 22 of *BLUF-E.g.-appA*, sense
appA*Eu*down	CCA**GGTACC**GTTCTCGTCTCGTTCATT *Kpn*I, 1467 to 1484 of *appA*, antisense
appA403F	GCCGACAACACCAACATCTTC 403 to 423 of *appA*, for RT-PCR, sense
appA755R	GAATAGGCCAGCGTCACCTG 742 to 761 of *appA*, for RT-PCR, antisense
AppAL	CAT**GCATGC**GCCGACAACACCAACATC *Sph*I, 403 to 420 of *appA*, sense
AppAR	TGC**TCTAGA**GGAGTCCTTCAGCTTCGA *Xba*I, 1117 to 1134 of *appA*, antisense
appA_up	CGGCGG**AAGCTT**AATCCGAGGTC *Hin*dIII, -364 to -342 of *appA*, sense
appAup2	GGA**AGATCT**CAACACGACCTCGAGGC *Bgl*II**,** 4 to 22 of *appA*, sense
appAup3	TGC**TCTAGA**TCGGAGGCCGACATGCGC *Xba*I**,** 335 to 352 of *appA*, sense
AppASph	CAT**GCATGC**CACCAGGCTGCGGCCCAC *Sph*I, 385 to 402of *appA*, antisense
C22	CCCAAGCTTGAGCGCCGAAGCGAT for *trxA* probe in Northern blot, sense

Name	Sequence (5'→3') and relevant features
AppAXba	TGC**TCTAGA**GGCGCCGATGCCGGGTTC
	*Xba*I, 1135 to 1152 of *appA*, sense
C23	GCGGATCCATGTCCACCGTTCCCG
	for *trxA* probe in Northern blot, antisense
DeltaCdown	CGG**GGTACC**AATTCAACGGGCGAGGG
	*Kpn*I, 1178 to 1194 of *appAΔC* in plasmid p484-Nco5ΔC, antisense
DeltaNup	GGA**AGATCT**CAACACGACCTCGACAAG
	*Bgl*II, 3 to 21 of *appAΔN* in plasmid p484-Nco5Δ, sense
DeltaNup2	GGA**AGATCT**GATCTGCTGAGCACCGAT
	*Bgl*II, 589 to 606 of *appA*, sense
DeltaNdown	TCC**CCCGGG**TCAGGCGCTGCGGCGG
	*Sma***I,** 1136 to 1353 of *appA*, antisense
H284AF	GTGCCGGGTGCCAAGCCGATC
	841 to 861 of *appA*, for AppA H284A mutation, sense
H284AR	GATCGGCTTGGCACCCGGCAC
	841 to 861 of *appA*, for AppA H284A mutation, antisense
KatE-F	CGCCGACAACCAGAACAC
	36 to 53 of *katE*, sense
KatE-R	CCTTGGCATGGACCACACGCTC
	142 to 163 of *katE*, antisense
L204PF	ACCGATCCGCCCGGTCGCCT
	601 to 620 of *appA*, for AppA L204P mutation, sense
L204PR	AGGCGACCGGGCGGATCGGT
	601 to 620 of *appA*, for AppA L204P mutation, antisense
M7	GCGGATAACAATTTCAC
	for sequencing of pRK415-insert, sense
MP6	GTTGGGTAACGCCAGGG
	for sequencing of pRK415-insert, antisense
OMEGA-F	ATCGCGGAAGAGACCCAGAG
	157 to 176 of *rpoZ*, for RT-PCR, sense
OMEGA-R	GAGCAGCGCCATCTGATCCT
	245 to 264 of *rpoZ*, for RT-PCR, antisense
P282QF	TCGCCGGCGTGCAGGGTCAC
	833 to 852 of *appA*, for AppA P282Q mutation, sense
P282QR	GTGACCCTGCACGCCGGCGA
	833 to 852 of *appA*, for AppA P282Q mutation, antisense

Name	Sequence (5'→3') and relevant features
P357LF	ACCGATCTTCTCGGCCTGAGC
	1060 to 1080 of *appA*, for AppA P357L mutation, sense
P357LR	GCTCAGGCCGAGAAGATCGGT
	1060 to 1080 of *appA*, for AppA P357L mutation, antisense
PACα1 up new	CCG**CTCGAG**AAGGGAGGAGAAACC
	135 to 149 of *PACα*, sense
PACα1 down	TGC**TCTAGA**GTGGGAGTCTTTCATGTG
	*Xba*I, 435 to 453 of *PACα*, antisense
pGEX5	GGGCTGGCAAGCCACGTTTGGTG
	for sequencing of pGEX-insert, sense, Amersham Pharmacia
pGEX3	CCGGGAGCTGCATGTGTCAGAGG
	for sequencing of pGEX-insert, antisense, Amersham Pharmacia
ppsR-F	AACCACATCGATCCGCGC
	265 to 282 of *ppsR*, for RT-PCR, sense
ppsR-R	ACACGTCGAGCACCACGC
	455 to 472 of *ppsR*, for RT-PCR, antisense
pQE Type III/IV	CGGATAACAATTTCACACAG
	for sequencing of pQE-insert, sense, QIAGEN
pQE Reverse	GTTCTGAGGTCATTACTGG
	for sequencing of pQE-insert, antisense, QIAGEN
puc-281	GGACGAGCAGCGTCAATTTC
	-281 to -262of *pucB*, sense
puc-23	ATCGACGGTTTGCGTGTAGG
	-42 to -23 of *pucB*, antisense
PUCA	TTACTCGGCCGCGACCGCA
	147 to 165 of *pucA*, for *puc* probe in Northern blot, antisense
PUCB	GTGACTGACGATCTGAACAAA
	0 to 18 of *pucB*, for *puc* probe in Northern blot, sense
Puc2AB-F	GGCAAAATCTGGCTCGTGGT
	10 to 29 of *pucA*, for RT-PCR, sense
Puc2AB-R	GGTGGTGGTCGTCAGCACAG
	98 to 117 of *pucA*, for RT-PCR, antisense
PUFA	TTACTCGGCGACGGCGACGC
	158 to 177 of *pufA*, for *puf* probe in Northern blot, antisense
PUFB	GGAGGATAGCATGGCTGATAA
	-10 to 10 of *pufB*, for *puf* probe in Northern blot, sense

Name	Sequence (5'→3') and relevant features
S348PF	TGCGGTTCGTCCCCGCGCTC
	1031 to 1050 of *appA*, for AppA S348P mutation, sense
S348PR	GAGCGCGGGGACGAACCGCA
	1031 to 1050 of *appA*, for AppA S348P mutation, antisense
V306AF	TCGACCTCGGCCGTGCATCC
	907 to 926 of *appA*, for AppA V306A mutation, sense
V306AR	GGATGCACGGCCGAGGTCGA
	907 to 926 of *appA*, for AppA V306A mutation, antisense
V307GF	ACCTCGGTCGGGCATCCCGA
	910 to 929 of *appA*, for AppA V307G mutation, sense
V307GR	TCGGGATGCCCGACCGAGGT
	910 to 929 of *appA*, for AppA V307G mutation, antisense

Nucleotides locations are relatively positioned from the start codon of the gene.
+ and – are designated from nucleotide position downstream from the start site in coding sequence and in the upstream sequence of gene, respectively.

2.10 Other materials and equipments

Bandpass filter BG12 (filter for blue light)	Schott
BIACORE® X	Biacore AB
Biodyne® A transfer membrane	Pall
Biodyne® B membrane	Pall
E. coil Pulser (electrotransformation)	Bio-rad
Flour-S™ *MultiImager*	Bio-rad
Gel blotting papers (Whatman papers)	Carl-Roth
310 Genetic Analyzer	ABI-Prism
Glutathione Sepharose® 4B	Amersham Pharmacia
Heat-absorbing filter KG1	Schott
Lamgda 12 (UV/VIS spectrometer)	Perkin Elmer
Light meter Li-189	Li-Cor
Liquid scintillation counter LS6500	Amersham Pharmacia
Lumat LB 9501	Berthold
Membrane filter (0.45µm, ø25mm)	Carl-Roth
Nickel-nitrilotriacetic acid (Ni-NTA) agarose	QIAGEN
Nick translation kit	Amersham Pharmacia
OxyScan Micro-Sauerstoffsensor 501	UMS
Phospho-imager for *Molecular Imager*® FX	Bio-Rad
Plasmonic® SPR system	HSS Systeme, Wallenfels
Primus 96 Thermocycler	MWG Biotech
ProbeQuant™ G-50 Micro-Column	Amersham Pharmacia
Protran® Nitrocellulose Transfer Membrane	Carl-Roth
Rotor-Gene™ 3000 Real Time Thermal Cycler	Corbett Research
Semidry-Blot- Apparatus	Amersham Pharmacia
Slide Projector (light source)	Carl Braun

Sonopuls GM70	Bandelin
Trio-Thermoblock	Biometra
UV-Stratalinker 1800 (UV-*crosslink*-Apparatus)	Stratagene
Vacuum-Blot-Apparatus	Appligene

3 Methods

3.1 Microbiological methods

3.1.1 Cultivation of *E. coli*

Standard I medium (STI) 25 g Standard I nutrient broth in 1 l H_2O, autoclaved

Agar plates 1.6% (w/v) Bacto-Agar in the media above, autoclaved

3.1.1.1 *E. coli* plating culture

Grow bacteria on the STI-agar in 9 cm diameter Petri dish at 37°C. When required, add antibiotics as Table 2.1.

3.1.1.2 *E. coli* liquid culture

Grow bacteria in a flask filled to 20-50% of total volume with STI-medium at 37°C on a shaker at a speed of 180 rpm. When required, add antibiotics as Table 2.1.

3.1.2 Cultivation of *R. sphaeroides*

RÄ-medium
3 g malate
0.2 g $MgSO4 \cdot 2H_2O$
1.2 g $(NH4)_2SO_4$
0.07 g $CaCl_2 \cdot 2H_2O$
1.5 ml trace elements
add H_2O to 1 l, pH 6.9 autoclaved
then add 8 ml vitamin solution & 20 ml phosphate solution

Vitamin solution
200 mg niacin
400 mg thiamin-HCl
200 mg nicotinamide
8.0 mg biotin
add H_2O to 1 l, filtered (0.2 μm)

Phosphate solution
0.9 g K_2HPO_4
0.6g KH_2PO_4, add H_2O to 1 l, autoclaved

Trace elements solution	500 mg Fe(II)-citrate 20 mg $MnCl_2 \cdot 2H_2O$ 5 mg $ZnCl_2$ 5 mg LiCl 2.5 mg KBr 2.5 mg KI 0.15 mg $CuSO_4$ 1 mg $NaMoO_4 \cdot 2H_2O$ 5 mg $CoCl_2 \cdot 6H_2O$ 0.5 mg $SnCl_2 \cdot 2H_2O$ 0.5 mg $BaCl_2$ 1.0 mg $AlCl_3$ 10 mg H_3BO_4 20 mg EDTA add H_2O to 1 l
Agar plates	1.6% (w/v) Bacto-Agar in the media above, autoclaved

3.1.2.1 *R. sphaeroides* plating culture

Grow bacteria on the RÄ-agar in 9 cm diameter Petri dish at 32°C. When required, add antibiotics as Table 2.1.

3.1.2.2 *R. sphaeroides* liquid culture

Aerobic culture

Grow bacteria in a baffle-flask filled to 40% of total volume with RÄ-medium at 32°C on a shaker at a speed of 140 rpm. When required, add antibiotics as Table 2.1.

Liquid culture under low oxygen conditions

Grow bacteria in a non-baffle-flask filled to 80% of total volume with RÄ-medium at 32°C on a shaker at a speed of 140 rpm. When required, add antibiotics as Table 2.1.

3.1.2.3 Blue light-shift experiments under semi-aerobic conditions

For semi-aerobic growth, oxygen concentration in the culture flasks is 104 ± 24 μM throughout the experiment. Monitor oxygen tension with a Pt/Ag-electrode (microoxygen sensor 501, Ums) and adjust it by varying the rotation speed of the shaker. The light source is the lamp of a slide projector (250 W, 24 V; Carl Braun). The light passes through a heat-absorbing filter (KG1; Schott) and a bandpass filter (BG12; Schott). The BG12 filter transmits blue light maximally at 400 nm; no light is transmitted above 500

nm. The irradiance produced by this light source measured at the culture level (Light Meter Li-189; Li-Cor) is 20 $\mu mol \cdot m^{-2} \cdot s^{-1}$. For light shift experiments, grow the cultures aerobically overnight. Then adapt the cultures to semi-aerobic conditions for one doubling time before illumination. When the optical density of cells reaches 0.1~0.3 at 660nm, transfer the cultures grown in the dark into the light at time zero. Wrap the flasks containing control cultures grown in the dark by aluminium foil.

3.1.2.4 Oxygen-shift experiment

Adjust oxygen tension by varying the rotation speed of the shaker. Grow the cultures aerobically overnight, dilute them to the optical density at 660 nm of 0.08 or 0.4 and grow them on a shaker at a speed of 100 rpm for one doubling time. Then decrease the speed of shaker to 40 rpm at time point zero. Wrap the flasks containing cultures in aluminium foil.

3.1.3 Preparation of glycerol stocks for the -80°C strain collection

Collect cells from liquid overnight culture of *E. coli* (4 ml) or *R. sphaeroides* (10ml) in late exponential growth phase by centrifugation at 4°C. Resuspend the pellet by 2 ml relevant medium without antibiotics and 1 ml 80% glycerol, transfer the suspension into two cryo-tubes, freeze them in liquid nitrogen and store at -80°C.

3.2 DNA preparation

3.2.1 Plasmid minipreparation by alkaline lysis

Lysis solution I	50 mM glucose 25 mM Tris-HCl (pH 8.0) 10 mM EDTA (pH 8.0) autoclaved and stored at 4°C
Lysis solution II	0.2 M NaOH 1% (w/v) SDS stored at room temperature
Lysis solution III	60 ml 5 M potassium acetate 11.5 ml glacial acetic acid 28.5 ml H_2O stored at 4°C

Perform plasmid minipreparation by alkaline lysis according to standard protocol (Sambrook and Russell, 2001). Inoculate 3 ml of STI-medium containing the appropriate

antibiotic with a single colony of bacteria. Incubate the culture overnight at 37°C with vigorous shaking. Pour 1.5 ml of the culture into a microfuge tube. Centrifuge at maximum speed for 30 sec in a microfuge. After centrifugation, remove the medium. Resuspend the bacterial pellet in 100 µl of ice-cold lysis solution I by vigorous votexing. Add 200 µl of lysis solution II to each bacterial suspension. Close the tube tightly, and mix the contents by invert the tube rapidly five times. Store the tube at the room temperature for 5 min. Add 150 µl of lysis solution III. Close the tube and disperse lysis solution III through the visous bacterial lysate by inverting the tube several times. Store the tube on ice for 15 min. Centrifuge the bacterial lysate at maximum speed for 10 min in a microfuge. Transfer the supernatant to a fresh tube. Add an equal amount of phenol:chloroform. Mix the organic and aqueous phases by votexing and then centrifuge the emulsion at maximum speed for 10 min in a microfuge. Transfer the aqueous upper layer to a fresh tube. Precipitate the nucleic acids from the supernatant by adding 2 volumes of ethanol. Mix the solution and then allow the mixture to stand at -80°C for 30 min. Collect the precipitated nucleic acids by centrifugation at maximum speed for 30 min in a microfuge. Remove the supernatant. Add 1 ml of 70% ethanol to the pellet and then collect the DNA by centrifugation at maximum speed for 10 min in a microfuge. Dissolve the nucleic acids in 50 µl of H_2O containing 20 µg/ml DNase-free RNase. Store the DNA solution at -20°C.

3.2.2 Plasmid midipreparation

Perform plasmid midipreparation by using E.Z.N.A. Plasmid Miniprep Kit II (Peqlab) according to the manufacturer's instruction.

3.2.3 Chromosomal DNA isolation

PBS (pH 7.4)	4 g NaCl 0.1 g KCl 0.72 g Na_2HPO_4 0.12 g KH_2PO_4 add H_2O to 500 ml, autoclaved
SET buffer	1.5 ml 5 M NaCl 5 ml 0.5 M EDTA (pH 8.0) 2 ml 1 M Tris (pH 7.5) add H_2O to 100 ml

Collect the cells (20 ml overnight liquid culture) by centrifugation at 8,000 rpm (using Sorvall® SS-34 rotor) for 10min at 4°C. Wash the pellet with 1 ml PBS, collect the cells by centrifugation at 8,000 rpm (using Sorvall® SS-34 rotor) for 5 min at 4°C, resuspend cells by 0.5 ml SET buffer containing 1 mg/ml lysozyme and incubate at 37°C for 30 min. Then add 50 µl 10% SDS and 25 µl 20 mg/ml proteinase K and incubate the mixture at 55°C for 2 h, invert several times during the incubation. Afterwards, add 1/3 volume 6 M NaCl and invert several times. Add 1 volume chloroform and incubate the mixture at room temperature for 30–60 min with end-over-end rotation. After centrifugation, precipitate the chromosomal DNA from the supernatant by 1 volume isopropanol and wash DNA with 75% ethanol. Then dissolve the dry DNA in 1 ml H_2O. Deactivate the DNase at 65°C for 10 min, store the chromosomal DNA at 4°C.

3.2.4 Gel extraction

Extract DNA fragment from the agarose gel by using QIAEX II Gel Extraction Kit or QIAquick Gel Extraction Kit (QIAGEN) according to the manufacturer's instruction.

3.2.5 Gel electrophoresis of DNA

TAE buffer	0.04 M Tris-acetate 0.001 M EDTA, pH8.0
TBE buffer	0.09 M Tris-borate 0.001 M EDTA, pH8.0
DNA blue marker	4 M urea 50% saccharose 50 mM EDTA (pH 8.0) 0.1% (w/v) bromphenol blue 0.1% (w/v) xylene cyanol
10% polyacrylamide gel (For DNA)	0.6 ml 10× TBE buffer 2.0 ml Rotiphorese® gel 30 24 µl 10% (w/v) APS 6 µl TEMED 3.4 ml H_2O

Perform the agarose gel electrophoresis in TAE buffer according to standard protocol (Protocol 5.1, Sambrook and Russell, 2001).

Perform 10% polyacrylamide gel electrophoresis in TBE buffer according to standard protocol (Protocol 5.9, Sambrook and Russell, 2001).

Stain the gel in ethidium bromide and detect the signals by UV illumination.

3.3 Molecular cloning

3.3.1 Polymerase chain reaction (PCR)

3.3.1.1 Standard PCR

Reaction components

100 ng template DNA
5.0 µl 10× amplification buffer
3.0 µl dNTP mix (4 mM each)
2.0 µl primers mix (50 pmol/µl each)
1~2 units thermostable DNA polymerase
add H_2O to 50 µl

Programme

96°C	8 min	
96°C	1 min	} 30 cycles
Annealing temperature	45 sec	
72°C	1 min/kb	
72°C	7 min	

Perform standard PCR either by *Vent* polymerase (New England Biolabs) or by *Taq* DNA polymerase (QIAGEN) according to the manufacturers' instruction.
Precipitate the PCR products by ethanol precipitation. Precipitate the nucleic acids by adding 1/10 volumes of sodium acetate (pH 4.5) and 5 volumes of ethanol. Mix the solution and then allow the mixture to stand at -20°C overnight. Collect the precipitated nucleic acids by centrifugation at maximum speed for 30 min in a microfuge. Remove the supernatant. Add 1 ml of 70% ethanol to the pellet and then collect the DNA by centrifugation at maximum speed for 10 min in a microfuge. Dissolve the nucleic acids in 50 µl of deionized H_2O containing 20 µg/ml DNase-free RNase. Store the DNA solution at -20°C.

3.3.1.2 Site-specific mutagenesis by overlap extension

Perform the site-directed mutagenesis by overlap PCR according to standard protocol (Protocol 13.6, Sambrook and Russell, 2001).

3.3.1.3 PCR-based random mutagenesis

Reaction components 100 ng template DNA

5.0 µl 10× PCR buffer
10.0 µl 5× Q-solution
3.0 µl dNTP mix (4 mM each)
1.0 µl dITP (10 mM)
5.0 µl DMSO
2.0 µl primers mix (50 pmol/µl each)
2 unit *Taq* DNA polymerase
add H_2O to 50 µl

Programme

96°C	8 min	
96°C	1 min	30 cycles
Annealing temperature	45 sec	
72°C	1 min/kb	
72°C	7 min	

3.3.2 Restriction

Perform the restriction according to the Catalog & Technical Reference of New England Biolabs®. Precipitate the restricted products by ethanol precipitation.

3.3.3 Ligation

3.3.3.1 Standard ligation

Reaction components

30 fmoles vector
30 fmoles insert
1 unit T4 DNA ligase
2 µl 10× T4 ligase buffer
add H_2O to 20 µl

Incubate the reaction mixture at 16°C overnight, then add 30 µl H_2O, inactivate the ligase at 65°C for 10 min, add 500 µl n-butanol, vigorously mix and centrifuge at maximum speed for 10 min in a microfuge. Dissolve the pellet in 10 µl H_2O.

3.3.3.2 Ligation using the pGEX®-T vector

Standard reaction

5 µl 2× rapid ligation buffer
1 µl pGEX®-T vector (50 ng/µl)
30 fmoles insert
1 unit T4 DNA ligase
add deionized water to 10 µl

Perform the ligation according to the manufacturer's instruction (Promega). Briefly centrifuge the pGEX®-T vector to collect contents at the bottom of the tube. Set up the

reaction as described above. Mix the reaction by pipetting. Incubate the reactions for 1 h at room temperature.

3.3.3.3 Ligation using the pDrive vector

Reaction components	5 µl 2× ligation master mix 1 µl pDrive vector (50 ng/µl) 30 fmoles insert add distilled water to 10 µl

Perform the ligation according to the manufacturer's instruction (QIAGEN® PCR Cloning Handbook, QIAGEN). Briefly mix the reaction components as described above and then incubate for 30 min at 16°C. Perform n-butanol precipitation before transformation.

3.3.4 Preparation of *E. coli* competent cells for electroporation

Inoculate the fresh overnight *E. coli* cells into 1 l STI-medium with 1:100 dilution and grow at 37°C with vigorous shaking until the optical density at 600 nm reaches 0.5~1.0. After chilling the cells on ice for 15~30 min, harvest cells by centrifugation in a cold rotor at 4,000×g for 15 min. Resuspend the pellet by 1 l cold sterile water, spin down; resuspend in 0.5 l cold sterile water, spin down; resuspend in 50 ml 10% ice-cold sterile glycerol, spin down; and resuspend in 6 ml 10% ice-cold sterile glycerol. Freeze the suspension in aliquots in liquid nitrogen and store at -80°C.

3.3.5 Transformation by electroporation

Mix 10-50 pg plasmid or 25 ng ligated DNA with 40 µl competent cells on ice. Sterilize the Gene Pulser® cuvette (Bio-rad) by UV-Stratalinker 1800 (Stratagene) using programme "Auto Crosslink" three times and chill it on ice before use. Apply a pulse of electricity (2.4 KV, 5 milliseconds) to the mixture using *E. coil* Pulser (Bio-rad). Afterwards transfer DNA/cell mixture to 1 ml STI-medium without any antibiotics. After incubation at 37°C with vigorous shaking for 1 h, plate 25 µl, 100 µl or 900 µl mixture on STI-agar plate containing appropriate antibiotics and incubate the agar-plates at 37°C overnight.

3.4 Extraction, purification and analysis of mRNA from *R. sphaeroides*

3.4.1 RNA isolation

3.4.1.1 Hot-phenol extraction

Solution I	0.3 M saccharose 0.01M NaOAc, pH 4.5
Solution II	0.01 M NaOAc, 2% (w/v) SDS
RNA storage buffer	500 mM Na_2HPO_4/ NaH_2PO_4 250 mM EDTA, pH 6.5
10× DNase buffer	200 mM Tris-HCl pH 8.3 20 mM $MgCl_2$ 500 mM KCl

Resuspend cell pellet by 125 µl RNA extraction solution I and 250 µl solution II. After vigorous mixing, incubate the suspension at 65°C for 1.5 min, add 400 µl Roti®-Aqua-Phenol, vortex, incubate at 65°C for 3min, freeze in liquid nitrogen for 30 sec, centrifuge 10 min at 10,000 × *g*. Repeat hot-phenol extraction three times. Then add 40 µl 3 M NaOAc (pH 4.5) and 1 ml ethanol to the upper phase and keep the mixture in liquid nitrogen for more than 30 min. After centrifugation (4°C, 10,000 × *g*, 30 min), wash the pellet with 1 ml 75% ethanol, dry in Speed Vac for 5 min and dissolve it in 180 µl DEPC-H_2O. Add 20 µl 10× DNase buffer and DNase (15 unit per 1 µg RNA), and incubate the mixture at room temperature for 20 min. Then add 200 µl Roti®-Phenol/Chloroform/Isoamylalcohol, votex and centrifuge (10,000 × *g*, 5 min). Treat the upper phase again with Roti®-Phenol/Chloroform/Isoamylalcohol. Add 20 µl 3 M NaOAc (pH 7.0) and 1 ml ethanol to the upper phase, and freeze the mixture in liquid nitrogen for more than 30 min. After centrifugation (4°C, 10,000 × *g*, 30 min), wash the pellet with 1 ml 75% ethanol, dry it in Speed Vac for 5 min and dissolve it in 50 µl DEPC-H_2O. Calculate the concentration of the total RNA as the following formula:

$C\ (mg/ml) = A_{260} \times \text{dilution factor} \times 40$

3.4.1.2 ABgene reagent

Perform the total RNA isolation with ABgene reagent according to the manufacturer's instruction.

3.4.2 Northern Blot

Formaldehyde agarose gel
1.43 g agarose
104 ml DEPC-H_2O
14.3 ml 10× MOPS
26 ml formaldehyde

RNA loading buffer
50 µl 10× MOPS
250 µl formamide
89 µl formaldehyde
111 µl DEPC-H_2O

Denaturing buffer
10 ml 1 M NaOH
6 ml 5 M NaCl
184 ml DEPC-H_2O

Neutralizing buffer
20 ml 1 M Tris-HCl (pH 7.5)
6 ml 5 M NaCl
174 ml DEPC-H_2O

50× Denhardt's reagent
1% (w/v) polyvinylpyrrolidone
1% (w/v) ficoll 400
1% (w/v) BSA

10× MOPS
41.8 g/L MOPS
10 mM EDTA
50 mM NaOAc
100 mM NaOH
pH 7.0

RNA blue marker
625 µl 80% glycerol
25 µl 250 mM EDTA (pH 8.0)
375 µl 1% bromophenol blue

20× SSC
1.5 M NaCl
150 mM sodium citritrate
pH 7.0

20× SSPE
3 M NaCl
20 mM EDTA
200 mM NaH_2PO_4
pH 7.0

Prehybridization buffer
(for DNA probes, 42°C for 5 h)
220 mg glycine
2.5 ml DEPC-H_2O
11 ml formamide
5.5 ml 20× SSPE
220 µl 10% (w/v) SDS
1.65 ml 50× Denhardt's
1.1 ml 5mg/ml LSD

Hybridization buffer
(for DNA probes, 42°C over night)
2.4 g dextransulfate
1.8 ml DEPC-H_2O
12.2 ml formamide
6.1 ml 20× SSPE
0.48 ml 0.2 M NaPPi
240 µl 10% (w/v) SDS
0.48 ml 50× Denhardt's
0.48 ml 5mg/ml LSD

Prehybridization buffer
(for oligonucleotides, 50°C for 3 h)
8.7 ml DEPC-H_2O
4.5 ml 20× SSC
750 µl 10% (w/v) SDS
750 µl 50× Denhardt's
0.3 ml 5mg/ml LSD

Hybridization buffer
(for oligonucleotides, 50°C over night)
9.45 ml DEPC-H_2O
4.5 ml 20× SSC
750 µl 10% (w/v) SDS
0.3 ml 5mg/ml LSD

Membrane wash buffer I
2× SSC
0.1% (w/v) SDS

Membrane wash buffer II
0.2× SSC
0.1% (w/v) SDS

Nick translation
4.5 µl dATP/dGTP/dTTP mixture
4.0 µl DNAfragment (~50 ng)
3.0 µl [α-^{32}P]-dCTP
3.0 µl enzyme
15.5 µl H_2O
incubated at RT for 20 min

Oligonucleotide labeling
1.0 µl oligonucleotide (10 pmol/ µl)
1.0 µl 10×T4 PNK buffer
3.0 µl [γ-^{32}P]-ATP
1.0 µl T4 PNK
4.0 µl H_2O
incubated at 37°C for 30 min

Dissolve total RNA (7–15 µg per lane) in 9 µl RNA loading buffer, incubate at 65°C for 10 min, add 1 µl RNA blue marker, run on a 1% (w/v) agarose 2.2 M formaldehyde gel in 1× MOPS at 100 V for around 3 h. Afterwards denature RNA by denaturing buffer (30~60 min), neutralize it by neutralizing buffer (30~60min) and transfer it to a nylon membrane (Biodyne® B membrane; Pall) by vacuum pressure blotting (under 50mbar for 45min) with transfer solution: 10× SSC in DEPC-H_2O. Fix the RNA on the membrane by UV crosslinking (UV-Stratalinker 1800; Stratagene). Radiolabel the specific DNA

fragments from *R. sphaeroides* with [α-^{32}P]-dCTP using Nick Translation Kit N 5500 (Amersham Pharmacia). The oligonucleotide used for hybridization with processed *Rhodobacter* 23S rRNA is 5'-CTTAGATGTTTCAGTTCCC-3' corresponding to the 23S rDNA positions 187–205 (*E. coli* numbering). Radiolabel the oligonucleotide at 37°C for 30~60 min with 20 μCi of [γ-^{32}P]-ATP using polynucleotide kinase. Purify the DNA fragments used for hybridizations by ProbeQuant™ G-50 Micro-Column. Denature 2 $\times 10^6$ c.p.m. (for DNA probe) or 6 $\times 10^5$ c.p.m. (for oligonucleotide probe) radiolabelled probe together with LSD at 95°C for 5 min before adding in hybridization tube. Incubate the membrane in the prehybridization buffer and then in the hybridization buffer as described above. Wash the membrane by the membrane wash buffer I and II (5 min each). Quantify the signals using a phosphoimaging system (*Molecular Imager*® FX; Bio-Rad) and the appropriate software (QUANTITY ONE; Bio-Rad).

3.4.3 RT-PCR

3.4.3.1 Semi-quantitative RT-PCR

QIAGEN OneStep RT-PCR Kit

Reaction components (15 μl)	1.5 μl RNA (40ng/μl) 3.0 μl 5× QIAGEN OneStep RT-PCR buffer 3.0 μl 5× Q-solution 0.6 μl dNTP mix (10 mM each) 0.6 μl QIAGEN OneStep RT-PCR enzyme mix 3.6 μl primers mix (5 pmol/μl each) 0.1 μl RNasin 2.6 μl RNase-free water		
Programme	50°C	30 min	
	96°C	15 min	
	96°C	30 sec	midexponential cycles
	Annealing temperature	30 sec	
	72°C	1 min/kb	
	72°C	5 min	

***Reverse*-iT™ One-Step RT-PCR Kit**

Reaction components (15 μl)	1.5 μl RNA (40 ng/μl) 7.5 μl 2× RT-PCR master mix 1.2 μl primers mix (5 pmol/μl each) 0.3 μl *Reverse*-iT™ RTase Blend (50 unit/μl) 4.5 μl RNase/DNase-free water

Programme	47°C	30 min	
	94°C	2 min	
	94°C	20 sec	midexponential cycles
	Annealing temperature	30 sec	
	72°C	1 min/kb	
	72°C	5 min	

Subject reaction products to electrophoresis on a 10% polyacrylamide gel and stain the gel by ethidium bromide afterwards. Quantify the signals using the Fluor-S™ *MultiImager* (Bio-Rad) and the appropriate software (QUANTITY ONE; Bio-Rad). Normalize mRNA levels to *rpoZ* mRNA, which encodes the ω-subunit of the *R. sphaeroides* RNA polymerase (Pappas *et al.*, 2004). Calculate the relative expression ratio (R) of a target gene as the following formula:

R = signal level of target gene / signal level of reference gene

3.4.3.2 Quantitative real-time RT-PCR

<u>*Reverse*-iT™ One-Step RT-PCR Kit</u>

Reaction components	2.0 µl RNA (20ngµl)		
(10 µl)	5.0 µl 2× RT-PCR master mix		
	0.8 µl primers mix (5 pmol/µl each)		
	0.2 µl SYBR Green		
	0.2 µl *Reverse*-iT™ RTase Blend (50 unit/µl)		
	1.8 µl RNase/DNase-free water		
Programme	47°C	30 min	
	94°C	2 min	
	94°C	20 sec	40 cycles
	Annealing temperature	30 sec	
	72°C	1 min/kb	
	72°C	5 min	

Perform quantitative real-time RT-PCR using a Rotor-Gene™ 3000 real time thermal cycler (Corbett Research) and quantify the relative mRNA transcripts by Rotor-Gene™ software version 6.0 (Corbett Research) and the method of Pfaffl (2001). Calculate the relative expression ratio (R) of a target gene based on real-time PCR efficiency (E) and the cross point (CP) for each transcript as the following formula:

$$R = \frac{(E_{ref})^{CP_{ref}}}{(E_{target})^{CP_{target}}}$$

The cross point (CP) is defined as the point at which the fluorescence rises appreciably above the background fluorescence. For determination of real-time PCR efficiencies (E) of reference gene and target genes, perform real-time PCR with different concentration of total RNA (final concentration: 8 ng/µl, 4 ng/µl, 2 ng/µl, 1 ng/µl and 0.5 ng/µl) at the same time using the relevant primer pairs. Calculate E and CP by Rotor-Gene™ software version 6.0 (Corbett Research). For *R. sphaeroides*, use *rpoZ* as reference gene, which encodes the ω-subunit of the *R. sphaeroides* RNA polymerase (Pappas *et al.*, 2004).

3.5 Protein techniques

3.5.1 Protein purification

3.5.1.1 *E. coli* culture growth for preparative purification (1 liter)

Inoculate 20 ml of STI broth containing appropriate antibiotics. Grow at 37°C overnight with vigorous shaking. Inoculate a 1 liter culture 1:50 with the noninduced overnight culture. Grow at 37°C with vigorous shaking until an OD_{600} of 0.6 is reached. Induce expression by adding IPTG to the final concentration of 0.5~1 mM. Incubate the culture at 25°C for an additional 8 h, or at 17°C overnight (for the detail of each protein, refer the relevant chapter). Harvest the cells by centrifugation at 4,000 × *g* for 20 min. Freeze the cell pellets at -20°C.

3.5.1.2 Purification of His-tagged proteins

Purification under native conditions

Lysis buffer	50 mM NaH_2PO_4 300 mM NaCl 10 mM imidazole 20 mM β-mercaptoethanol 1% Triton X-100 adjust pH to 8.0
Wash buffer	50 mM NaH_2PO_4 300 mM NaCl 20 mM imidazole 20 mM β-mercaptoethanol 1% Triton X-100 adjust pH to 8.0
Elution buffer	50 mM NaH_2PO_4 300 mM NaCl

50-250 mM imidazole
adjust pH to 8.0

Perform the purification according to the manufacturer's instruction (QIAGEN). Thaw the cell pellet for 15 min on ice and resuspend the cells in lysis buffer at 2~5 ml per gram wet weight. Add lysozyme to 1 mg/ml and incubate at 4°C for 30 min with end-over-end rotation or sonicate on ice using a sonicator equipped with a microtip (use six 30 s bursts at 200~300 W with a 30 s cooling period between each burst). If the lysate is very viscous, add RNase A (10 μg/ml) and DNase I (5 μg/ml) and incubate on ice for 10~15 min. Centrifuge lysate at 10,000 × *g* for 20~30 min at 4°C to pellet the cellular debris. Add 1 ml of the 50% Ni-NTA slurry to 10 ml cleared lysate and mix gently by end-over-end rotation at 4°C for 60 min. Load the lysate-Ni-NTA mixture into a column (Polypropylene columns, 5 ml, QIAGEN) with the bottom outlet capped. Remove bottom cap and collect the flow-through. Wash six times with 10 ml wash buffer. Elute the protein 6~10 times with 0.5~2 ml elution buffer.

Purification under denaturing conditions

Buffers for eluting protein by an imidazole gradient

Lysis buffer
7 M Urea
30 mM Tris (pH 7.5)
20 mM imidazole
20 mM β-mercaptoethanol
1% Triton X-100

Wash buffer
7 M urea
30 mM Tris (pH 7.5)
50 mM imidazole
20 mM β-mercaptoethanol
1% Triton X-100

Elution buffer
7 M urea
30 mM Tris (pH 7.5)
100-500 mM imidazole
20 mM β-mercaptoethanol
1% Triton X-100

Buffers for eluting protein by pH gradient

Lysis buffer
8 M Urea
10 mM Tris
100 mM NaH_2PO_4
20 mM β-mercaptoethanol
1% Triton X-100
adjust pH to 8.0 using NaOH

Wash buffer
8 M Urea
10 mM Tris
100 mM NaH_2PO_4
20 mM β-mercaptoethanol
1% Triton X-100
adjust pH to 6.3 using HCl

Elution buffer
8 M Urea
10 mM Tris
100 mM NaH_2PO_4
20 mM β-mercaptoethanol
1% Triton X-100
adjust pH to 4.5 using HCl

Perform the purification according to the manufacturer's instruction (QIAGEN). Thaw the cell pellet for 15 min on ice and resuspend in lysis buffer at 5 ml per gram wet weight. Lyse cells for 15~60 min at room temperature by end-over-end rotation until the solution becomes translucent. Centrifuge lysate at 10,000 × *g* for 20~30 min at room temperature to pellet the cellular debris. Add 1 ml of the 50% Ni-NTA slurry to 10 ml lysate and mix gently by end-over-end rotation for 60 min at room temperature. Load lysate-resin mixture carefully into an empty column (Polypropylene columns, 5 ml, QIAGEN) with the bottom cap still attached. Remove the bottom cap and collect the flow-through. Wash six times with 10 ml wash buffer. Elute the recombinant protein 6~10 times with 0.5~2 ml elution buffer.

3.5.1.3 Purification of GST fusion proteins

PBS (pH 7.3)
140 mM NaCl
2.7 mM KCl
10 mM Na_2HPO_4
1.8 mM KH_2PO_4

Lysis and wash buffer
PBS containing 20 mM β-mercaptoethanol and 1% Triton X-100

Elution buffer
50 mM Tris-HCl (pH 8.0)
10 mM glutathione

Perform the purification according to the manufacturer's instruction (Amersham Pharmacia).

For preparation of matrix, gently shake the bottle of Glutathione Sepharose 4B to resuspend the medium. Use a pipet with a wide-bore tip to remove sufficient slurry for use and transfer the slurry to an appropriate container/tube. Sediment the medium by

centrifuging at 500 × *g* for 5 min. Carefully decant the supernatant. Wash the Glutathione Sepharose 4B by adding 10 ml of cold (4 °C) PBS per 1.33 ml of the original slurry of Glutathione Sepharose 4B dispensed. Invert to mix. Sediment the medium by centrifuging at 500 × *g* for 5 min. Decant the supernatant. For each 1.33 ml of the original slurry of Glutathione Sepharose 4B dispensed, add 1 ml of PBS. This results in a 50% slurry. Mix well prior to subsequent pipetting steps.

Thaw the cell pellet for 15 min on ice and resuspend the cells in lysis buffer at 2~5 ml per gram wet weight. Add lysozyme to 1 mg/ml and incubate at 4°C for 30 min with end-over-end rotation. Add 1 ml of the 50% slurry of Glutathione Sepharose 4B equilibrated with PBS to each 10 ml of lysate. Incubate for 30 min at room temperature with end-over-end rotation. Sediment the medium by centrifuging at 500 × *g* for 5 min. Carefully decant the supernatant (= flow-through). Wash the medium with 10 bed volumes (Bed volume is equal to 0.5× the volume of the 50% Glutathione Sepharose slurry used.) of PBS. Invert to mix. Sediment the medium by centrifuging at 500 × *g* for 5 min. Carefully decant the supernatant (= wash). Repeat wash steps six times. Elute the bound protein from the sedimented medium by adding 1.0 ml of elution buffer per 1 ml bed volume of the original slurry. Mix gently to resuspend the medium. Incubate at room temperature for 10 min with end-over-end rotation to elute the fusion protein from the medium. Sediment the medium by centrifuging at 500 × *g* for 5 min. Carefully decant the supernatant (= eluted protein) into a fresh centrifuge tube. Repeat elution steps 6-10 times and save the supernatant.

If necessary, remove GST by thrombin cleavage as description of the manufacturer's instruction (GST fusion system handbook, Amersham Pharmacia). Wash the fusion-protein-bound Glutathione Sepharose with 10 bed volumes of PBS. Centrifuge the suspension at 500 × *g* for 5 min, decant the supernatant. Prepare a mixture of 80 µl (80 units) of thrombin and 920 µl of 1× PBS. For each ml of Glutathione Sepharose bed volume, add 1 ml of thrombin mixture Glutathione Sepharose pellet. Gently shake or rotate the suspension. Incubate at room temperature (22–25 °C) for 2–16 h. Following incubation, centrifuge the suspension at 500 × *g* for 5 min to pellet the Glutathione Sepharose. Carefully transfer the eluate to a tube. The eluate will contain the protein of interest and thrombin, while the GST portion of the fusion protein will remain bound to the Glutathione Sepharose medium. Remove the thrombin either using centricon (MILLIPORE) or using HiTrap Benzamidine FF (Amersham Pharmacia)

3.5.1.4 Storage of proteins

Storage buffer (pH 7.3)
250 mM NaCl
2.7 mM KCl
10 mM Na_2HPO_4
1.8 mM KH_2PO_4
15% Glycerol

Dialyze the eluted protein in storage buffer and store at 4°C.

3.5.2 Bradford protein concentration assay

Reaction components
5 µl protein
900 µl deionized water
250 µl Roti®-Quant (Carl-Roth)

Gently invert the mixture several times, incubate at room temperature for 3~5 min and record the absorbance of the sample at 595 nm. Use BSA as standard.

3.5.3 SDS-polyacrylamide gel electrophoresis

Resolving gel (30 ml)
7.5 ml 1.5 M Tris-HCl (pH 8.8)
various amount of Rotiphorese® gel 30*
0.3 ml 10% (w/v) SDS
0.3 ml 10% (w/v) APS
12 µl TEMED
add H_2O to 30 ml

Stacking gel (8 ml)
1.0 ml 1.0 M Tris-HCl (pH 6.8)
1.3 ml Rotiphorese® gel 30
80 µl 10% (w/v) SDS
80 µl 10% (w/v) APS
8 µl TEMED
5.5 ml H_2O

Running buffer
3 g Tris
14.4 g glycine
10 ml 10% (w/v) SDS
add H_2O to 1000 ml

4× SDS gel-loading buffer
15% (v/v) glycerol
4% (w/v) SDS
200 mM β-mercaptoethanol

* 8.0 ml, 10.0 ml, 12.0 ml and 15.0 ml of Rotiphorese® gel 30 for 8%, 10%, 12% and 15% SDS-polyacrylamide gel, respectively.

125 mM Tris-HCl (pH6.8)
0.2% (w/v) bromophenol blue

Mix the protein sample with 4× SDS gel-loading buffer in a ratio of 4:1 (v/v) and denature the protein at 95°C for 5 min. Load the sample in an SDS-polyacrylamide gel of appropriate percentage and run the gel at 150~200 volts for 3~5 hours. Stain the gel either with silver salt or with Coomassie brilliant blue.

3.5.4 Staining of SDS-polyacrylamide gels

3.5.4.1 Silver staining of SDS-polyacrylamide gels

Fixation solution
50% (v/v) methanol
12% (v/v) acetic acid
0.05% (v/v) formaldehyde

Solution I
0.1 g $Na_2S_2O_3 \cdot 5H_2O$
add H_2O to 500 ml

Solution II
0.4 g $AgNO_3$
187.5 µl formaldehyde
add H_2O to 250 ml

Solution III
15 g Na_2CO_3
125 µl formaldehyde
5 ml solution I
add H_2O to 250 ml

Fix the gel by gently agitation in fixation solution for 45 min. Soak the gel three times in 50% ethanol, 20 min each. Then incubate the gel in solution I for 1 min, wash three times with deionized water, 20 sec each. Place the gel in solution II for 20 min and wash three times with deionized water, 20 sec each. Then place in solution III. Stop the reaction by acetic acid when the desired degree of banding has been observed.

3.5.4.2 Coomassie blue staining of SDS-polyacrylamide gels

Staining solution
0.1% (w/v) Coomassie® brilliant blue R-250
50% (v/v) methanol
10% (v/v) acetic acid
filtered

Destaining solution
50% (v/v) methanol
10% (v/v) acetic acid

Stain the gel with staining solution for 45 min on a shaker, rinse it with deionized water and destain the gel by destaining solution until the background is nearly clear.

3.5.5 Western Blot

Transfer buffer	5% (v/v) methanol 50 mM Tris (pH 7.9) 40 mM glycine 0.04% (w/v) SDS
TBS	50 mM Tris (pH 7.4) 0.2 M NaCl
Blocking agent	5% (w/v) milk powder in TBS
Substrate solution (detection of alkaline phosphatase)	100 mM Tris (pH 9.5) 100 mM NaCl 50 mM $MgCl_2$

Separate the protein samples by SDS-polyacrylamide gel electrophoresis and transfer them to Protran® nitrocellulose transfer membrane (Carl-Roth). Perform the electrophoretic transfer using western blotting machine (Amersham Pharmacia) at 0.8 mA/cm^2 for 45 min. Use the Whatman paper saturated with transfer buffer as a reservoir. Rinse the blot briefly in TBS and sock it in blocking agent at 4°C overnight. Incubate the blot with specific antibody in TBS containing 2.5% (w/v) milk powder on a shaker at room temperature for 2 hours, and then wash it by shaking in TBS three times, 5 min each. Then incubate the blot with the second antibody conjugated with enzyme (*e.g.* alkaline phosphatase or peroxidase) in TBS containing 2.5% (w/v) milk powder on a shaker at room temperature for 2 hours, and then wash it by shaking in TBS three times, 5 min each. For detection of alkaline phosphatase, apply the fresh prepared substrate solution containing NBT (4.5 µl/ml) and BCIP (3.5 µl/ml) on the blot in the dark until the colored products can be seen. For detection of peroxidase, apply lumi-light western blotting substrate 1 and 2 (v:v=1:1) on the blot, and capture the chemiluminescence on an X-ray film. Quantify the signals by software QUANTITY ONE (Bio-Rad).

3.5.6 Preparation of proteins for producing antibody

Subject the interested protein on an SDS-polyacrylamide gel. Then soak the gel in ice-cold 3 M NaCl until the visible signals appear. Cut the gels containing the target protein

(100~200 μg/gel), wash gels in deionized water and send them to BioGenes (Germany) for producing the antibody from rabbits.

3.5.7 Determination of protein stability in cells

Grow bacteria to late exponential growth phase. Then block the translation by adding chloramphenicol (final concentration is 500 μg/ml) into the culture. Harvest cells just before adding chloramphenicol, 1 hour and 3 hours after adding chloramphenicol. Detect interested protein from cell-free extracts by Western Blot according to chemiluminescence detection system (Roche).

3.5.8 Reconstitution with hemin or vitamin B_{12}

Dialysis buffer	250 mM NaCl 2.7 mM KCl 10 mM Na_2HPO_4 1.8 mM KH_2PO_4 15% glycerol
Hemin stock solution	5 mg/ml hemin in 0.1 M NaOH, store at 4°C
Vitamin B_{12} stock solution	5 mg/ml vitamin B_{12} in ddH_2O, store at 4°C

Put the purified protein in dialysis tubing with appropriate pore size. Dialyse them in the dialysis buffer containing 10 mg/l hemin or 2 mg/l vitamin B_{12} at 4°C overnight with low agitation. Then alter the buffer to dialysis buffer without hemin or vitamin B_{12}. Continue the dialysis at 4°C overnight and replace with the same volume of fresh dialysis buffer twice. Record the absorbance spectrum of the sample from 280 nm to 900 nm. Use the last dialysis buffer as blank.

3.5.9 Thiol-redox state analysis

4-Acetamido-4'-maleimidylstibene-2, 2'-disulfonic acid (AMS; Molecular Probes) was used for *in vitro* modification of free thiol groups. The addition of AMS leads to the alkylation of free thiol groups, present in the reduced but not in the oxidized protein. The addition of the high-molecular-mass AMS moiety to the reduced but not to the oxidized protein allows separation of the two forms by gel electrophoresis.

Precipitate the protein sample on ice for 30 min by 10% (final concentration) trichloroacetic acid (TCA). Collect the precipitated protein by cool centrifugation at a speed of 10,000 × *g* for 20 min and wash the pellet with 500 mM Tris (pH 8.0). Dissolve the pellet in a 20 µl buffer containing 15 mM AMS, 50 mM Tris (pH 8.0) and 0.1% SDS. Incubate them at 32°C for 3 hours and separate them in an appropriate percentage SDS-PAGE. Detect the protein either by silver staining or by Western Blot.

3.5.10 Gel mobility shift analysis

5× binding buffer	250 mM Tris/HCl (pH 7.0) 5 mM EDTA 750 mM NaCl 50% glycerol
TAE buffer	0.04 M Tris-acetate 0.001 M EDTA, pH8.0
4% TAE-polyacrylamide gel	4.6 ml Rotiphorese® gel 30 0.68 ml 50× TAE buffer 210 µl 10% (w/v) APS 34 µl TEMED 28.5 ml H_2O
Oligonucleotide labeling	4.0 µl oligonucleotide (963 nM) 2.0 µl 10×T4 PNK buffer 4.0 µl [γ-^{32}P]-ATP 2.0 µl T4 PNK 8.0 µl H_2O incubated at 37°C for 30min purified by ProbeQuant^{TM} G-50 Micro-Column

Incubate treated protein or protein-protein mixture with a ^{32}P-labeled DNA fragment at 30°C for 40 min in 20 µl binding solution containing 4 µl 5× binding buffer, 1 µg bovine serum albumin and 1 µg salmon sperm DNA. Subject the mixture on a 4% polyacrylamide gel electrophoresis (30 mA for 2.5 hours) in TAE buffer. Dry the gel on a gel dryer for more than 30 min. Analyze the signals using a phosphoimaging system (*Molecular Imager*® FX; Bio-Rad) and the appropriate software (QUANTITY ONE; Bio-Rad).

3.5.11 Surface plasmon resonance (SPR)-based protein-protein interaction analysis

Surface plasmon resonance (SPR) is an optical tool used for monitoring the binding processes between proteins, antigen-antibodies or other complexes. Although belonging to the optical sensors, the sample colour and medium have no influence on this special type of detection, because the laser beam does not cross the sample. Using SPR allows therefore a totally label-free technique for *in vitro* interaction studies of proteins (Lee *et al*, 2005).

3.5.11.1 BIACORE® X system

The protein-protein binding can be studied by using a BIACORE® X biosensor system (Biacore AB; Uppsala). To immobilize His_6-AppAΔN on the NTA-biosensor surface, first bind Ni^{2+} to the NTA-surface of both flow chambers (FCs) through injection of 10 µl of a 0.5 mM $NiSO_4$ solution at a flow rate of 10 µl/min. Then, inject His_6-AppAΔN four times to FC2 in a volume of 50 µl at a concentration of 1 µM in the running buffer (10 mM Na_2HPO_4, 1.8 mM KH_2PO_4, 2.7 mM KCl, 1M NaCl, pH 7.3) at a flow rate of 10 µl/min. This results in an increase of resonance units (RUs, a resonance unit is arbitrarily definited as 1/3,000 of a degree in the angular change.) of approximately 1000. To detect the PpsR binding to the His_6-AppAΔN surface, inject PpsR at 25°C in the running buffer described as above at a different flow rate. Remove PpsR from the His_6-AppAΔN surface by injecting 10 µl of 0.05 M glycine-HCl (pH 3.0) at a flow rate of 10 µl/min. Regenerate the sensor chip according to the manufacturer's instruction.

3.5.11.2 Plasmonic® SPR system

The protein-protein binding can also be studied by using a SPR spectroscope (Plasmonic®, HSS Systeme, Wallenfels, Germany). The spectroscope is used in normal autosampler modes. One of the main advantages of using Plasmonic® SPR system is the micro-cuvette technology. Up to eight measurements can be performed at the same time.
Dissolve or dilute all reagents and proteins in phosphate buffered saline (PBS, 0.25 M NaCl, pH 7.3). Perform each measurement at least twice at a temperature of 22.0°C. To illuminate the samples with light, place a strong light (1500 W, white light) in the SPR machine at an adequate height (30 cm) over the sample tray. Samples should be illuminated for 10 minutes prior to application.

Protein immobilization can be performed by using a non-specific binding surface modification of the gold chip. The hydrophobic C18-surface can be created using Octadecyltrimethoxysilane on a previously cleaned gold surface according to the procedure from Hartmann (2004). After protein immobilisation, all further binding residues are saturated using a high-concentrated BSA solution. After blocking the remaining binding sites, wash the surface of cuvette and chip using PBS buffer. Finally, apply the second protein to the cuvette and study interactions of second protein to the immobilized one on the chip surface.

Measuring different concentrations of one protein with a constant concentration of the immobilized interacting partner allows the determination of the association constant (k_{ass}) for these two proteins. For this purpose, the method of Edwards and Leatherbarrow (1997) has been used. This method is based on the assumption that this kinetic parameter of an interaction process can be determined from the initial binding rates and the maximum binding capacity. Plotting the initial binding rate against the corresponding protein concentration gives a linear relationship. k_{ass} is determined graphically from the equation $X_{slope} = R_{max} \times k_{ass}$, where X_{slope} is the slope, and R_{max} is the maximum binding capacity at the highest protein concentration.

3.6 Enzyme assays

3.6.1 Supercoiling assay for determination of gyrase activity

Plasmid relaxation reaction components

5 µg plasmid pBluescript SK (+)
10 µl 10× Topoisomerase I buffer
10 µl 0.1% BSA
1 µl Topoisomerase I
add deionized water to 100 µl

Sonication buffer

25 mM Tris-HCl pH 7.5
150 mM KCl
10% glycerol
2 mM PMSF

5× supercoiling buffer

250 mM Tris-HCl pH 7.5
100 mM KCl
50 mM $MgCl_2$
10 mM DTT
25 mM spermidine
250 µg/ml BSA

Gyrase introduces negative supercoils, while topoisomerase I relaxes them (Messer, 1999). To determination of gyrase activity, a plasmid relaxed by topoisomerase I can be used as substrate. Since the supercoiled plasmid is more compact than the relaxed one, it migrates more rapidly during gel electrophoresis. Therefore, the plasmids in different degree of supercoiling can be separated by gel electrophoresis. Because DNA gyrase catalyzes the ATP-dependent supercoiling of covalently circular DNA, the high amounts of supercoiled plasmids indicate the high supercoiling activity of gyrase.

To produce the relaxed plasmids for the supercoiling assay, incubate the plasmid relaxation mixture at 37°C for 2 hours, inactivate topoisomerase I at 75°C for 10 min and keep the mixture on ice. To prepare the cell free extracts, resuspend *R. sphearoides* cell pellet by 500 µl sonication buffer, break the cells by sonication and ultracentrifuge at 4°C for 30 min at a speed of 100,000 rpm (using Beckman® TLA100.1 rotor). Determine the amount of total protein in the supernatant by Bradford assay (Bradford, 1976). Incubate 0.1 µg of total protein at 37°C for 2 h in 20 µl buffer containing 4 µl 5× supercoiling buffer, 3.0 mM ATP and 0.1 µg of relaxed plasmid pBluescript DNA. Add SDS (final concentration is 0.2%) to stop the reaction, and analyze the samples by the 0.8% agarose gel electrophoresis.

3.6.2 Luciferase-activity assay for analysis of gene expression *in vivo*

Stock solution (100 mM) 19.5 µl n-Decanal
980.5 µl methanol

A plasmid harboring the *Vibrio harveyi luxAB* gene under control of the promoter of target gene can be transferred into interested host cell by conjugation. The activity of luciferase indicates the transcript levels of target gene. The bacterial luciferase catalyzes the following reaction:

$$FMNH_2 + RCHO + O_2 \longrightarrow FMN + RCOOH + H_2O + hv$$

Therefore, the luciferase activity can be measured by means of the total light produced.

For the colonies of reporter strain on the agar-plate, spread 150 µl stock solution on the lid of plate, then seal the plate by Parafilm. Detect the bioluminescence by Fluor-S™ *MultiImager* (Bio-Rad). For liquid culture, resuspend 0.1 ml of reporter strain culture in 0.9 ml of fresh media and supplement the mixture with decanal to a final concentration of 1 mM. Record the light emission by bioluminescence in a photomultiplier-based

luminometer (Lumat LB9501, Berthold, Nashua, NH). The mean value of 10 data around the maximum of the peak is used as the luminescence output. Normalize all readings to the optical density of the cultures at 660 nm. Measurements should be performed three times on independent cultures.

3.7 Other methods

3.7.1 Transfer plasmid into host cell by diparental conjugation

PY medium

10g bacto-tryptone
0.5g yeast extract
0.4M $CaCl_2$
0.4M $MgCl_2$
0.5% $FeSO_4$
add H_2O to 1 l, pH 7.0, autoclaved

Inoculate 3 ml of STI-medium containing the appropriate antibiotic with *E. coli* S17-1 (donor strain) containing target plasmid. Incubate the culture overnight at 37°C with vigorous shaking. Mix 500 µl of *E. coli* S17-1 (donor strain) culture and 500 µl *Rhodobacter* acceptor strain in exponential growth phase by repeated pipetting. Collect the cells by centrifugation at maximum speed for 2 min in a microfuge. Resuspend the cell pellet by 100 µl RÄ-medium, transfer the suspension onto membrane filter (0.45µm, ø25mm, Carl-Roth) and incubate cell mixture on a PY agar plate at 32°C for 4 hours. Afterwards, wash the cells out of the membrane by 1 ml RÄ-medium and dilute them from 1:10 to $1:10^6$. Apply 100 µl of each on RÄ agar plates with appropriate antibiotics. Incubate at 32°C for more than two days.

3.7.2 *In situ* hybridization for *Rhodobacter*

STE buffer

10 mM Tris-HCl pH 8.0
1 mM EDTA
25% saccharose
autoclaved

Denaturing buffer

0.5 M NaOH
1.5 M NaCl

Neutralizing buffer

1 M Tris-HCl, pH 7.5
1.5 M NaOH

20× SSC

1.5 M NaCl,
150 mM sodium citritrate, pH 7.0

50× Denhardt's reagent	1% (w/v) polyvinylpyrrolidone 1% (w/v) ficoll 400 1% (w/v) BSA
Pre- & hybridization buffer	4.3 ml DEPC-H_2O 3 ml 20× SSC 0.5 ml 10% (w/v) SDS 2 ml 50× Denhardt's 0.2 ml 5mg/ml LSD
Nick translation	4.5 µl dATP/dGTP/dTTP mixture 4.0 µl DNAfragment (~50 ng) 3.0 µl [α-^{32}P]-dCTP 3.0 µl enzyme 15.5 µl H_2O incubated at RT for 20 min

Incubate the Biodyne® A transfer membrane with cells in STE buffer (7 ml for ø140 mm membrane, 3 ml for ø80 mm membrane) containing 2 mg/ml lysozyme for 15 min at room temperature and dry for 5 min on Whatman paper; incubate the membrane in denaturing buffer for 15 min and dry for 5 min; incubate the membrane in the neutralizing buffer for 15 min and dry for 5 min; incubate the membrane in 2× SSC for 5 min and dry for 5 min. Fix the DNA on the membrane by UV crosslinking (UV-Stratalinker 1800; Stratagene). Then incubate the membrane in 3× SSC and 0.1% SDS at 55°C for 2 h. Radiolabel the specific DNA fragments from *R. sphaeroides* with [α-^{32}P]-dCTP using Nick Translation Kit N 5500 (Amersham Pharmacia) and purify them by ProbeQuant^{TM} G-50 Micro-Column. Denature the labeled DNA (2.5 ×10^5 c.p.m. per hybridization reaction) and LSD at 95°C for 5 min before using. After prehybridization (60°C for 1 h) and hybridization (60°C overnight), wash the membrane in 5× SSC for 5 min, 5× SSC and 0.5% (w/v) SDS for 20 min, 2× SSC and 0.5% (w/v) SDS for 20 min. Quantify the signals using a phosphoimaging system (*Molecular Imager*® FX; Bio-Rad) and the appropriate software (QUANTITY ONE; Bio-Rad).

3.7.3 Spectroscopy analysis on cell-free lysate

Grow *R. sphaeroides* cells to an OD_{660} of 0.7~0.9 under low oxygen concentration ($pO_2 \approx$ 3 µM) in the dark, and then harvest cells by centrifugation. Resuspend the cell pellet by RÄ-medium and break the cells by sonication. Determine the amount of total protein in the supernatant by Bradford assay (Bradford, 1976). Perform spectral analyses on the

crude cell-free lysates containing 600 μg of protein per ml using a spectrophotometer (Lambda 12, PerkinElmer).

3.7.4 Spectroscopy analysis of pyridine hemi- and hemochromes

Storage buffer
250 mM NaCl
2.7 mM KCl
10 mM Na_2HPO_4
1.8 mM KH_2PO_4
15% glycerol

Reagent A
0.2 M NaOH
50% (v/v) pyridine

Hemes in the hemoproteins have been assigned to three groups:
Heme *a* - the iron is chelate of cytoporphyrin IX;
Heme *b* - protoheme (the iron chelate of protoporphyrin IX) as prosthetic group but which lack a covalent bond between the porphyrin and the protein;
Heme *c* - the covalent thioether linkages between either or both of the vinyl side chains of protoheme side chains and the protein.
Hemes *a*, *b* and *c* can be determined from pyridine hemochrome spectra. A hemochrome is defined as a complex of ferroporphyrin with a nitrogenous base. If the iron is in the ferric state the compound is a hemichrome (Berry & Trumpower, 1987). For hemes *a, b* and *c*, the positions of the α-band of the pyridine Fe(II) hemochrome are listed in Table 3.1. Because the noncovalently associated hemes can be extracted by acid acetone (Table 3.1), the heme *b* and *c* can be separated by acetone-HCl precipitation.

Table 3.1 Practical criteria for determining the hemes in the hemoproteins.

	α-band of pyridine ferrohemochrome in alkaline solution	Solubility of product from treatment of hemoprotein with acetone-HCl in ether
Heme *a*	580-590 nm	Soluble
Heme *b*	556-558 nm	Soluble
Heme *c*	549-551 nm (two thioether links) 553 nm (single thioether link)	Insoluble, while still attached to the peptide

* Requires elaborate precautions to prevent decomposition to an insoluble product.

For preparing pyridine hemochrome or pyridine hemichrome, mix the protein solution (the concentration of protein is 0.2-1.6 mg/ml) with an equal volume of freshly prepared reagent A. Immediately add potassium ferricyanide [$K_3Fe(CN)_6$, final concentration is 0.5

mM] for producing pyridine hemichrome. To produce pyridine hemochrome, immediately add a few grains of solid sodium dithionite ($Na_2S_2O_4$) after adding the reagent A, mix well. Record the absorbance spectrum of the sample from 250 nm to 700 nm. Use the mixture of storage buffer and reagent A (v:v = 1:1) as blank. Because the formation of reduced pyridine hemochrome critically depends on the amount of sodium dithionite added to the sample, add a few additional grains of sodium dithionite and immediately record the absorbance spectra several times in order to ensure maximal chromogen formation.

To dissociate the heme *b* from the protein, precipitate the protein by addition of 9 volumes of 4°C acetone containing 2% (v/v) concentrated HCl. After 10 min on ice, collect the precipitates by centrifugation, dry, and resolve in the storage buffer.

3.7.5 Bacteriochlorophyll measurement

Grow *R. sphaeroides* cell to an OD_{660} of 0.7~0.9 under low oxygen concentration ($pO_2 \leq 3$ μM) in the dark. Collect cells from 4 ml liquid culture by centrifugation. Extract photopigments with 1 ml acetone-methanol (7:2 vol/vol) from cell pellets, and record the absorption at 770 nm. The bacteriochlorophyll (BChl) concentration can be calculated as following by using an extinction coefficient at 770 nm of 76 $mM^{-1} \cdot cm^{-1}$ if 1cm-cuvette has been used in the experiment:

$$BChl\ (\mu M) / OD_{660} = (OD_{770} \times 1000 \times V_{acetone\text{-}methanol}\ ml) / (76\ mM^{-1} \cdot cm^{-1} \times 1\ cm \times V_{cell}\ ml \times OD_{660})$$

4 Results

4.1 Role of the BLUF domain in photosynthesis (PS) gene expression in *Rhodobacter sphaeroides* 2.4.1

The AppA protein of *Rhodobacter sphaeroides* was originally described as part of a major redox signal chain (Gomelsky and Kaplan, 1997) controlling, together with the PrrB/PrrA two component system, FnrL and thioredoxin 1 (TrxA), the oxygen dependent expression of photosynthesis (PS) genes (Reviewed in Zeilstra-Ryalls and Kaplan, 2004). Among these PS genes, *puf* and *puc* operons encode pigment binding proteins and additional proteins involved in the formation of photosynthetic complexes. It was known that the high *puf* and *puc* transcript levels of wild type cells in the dark and their strong decrease after blue light irradiation at intermediate oxygen tension depend on the AppA protein (Braatsch *et al.*, 2002). Thus, AppA does not only respond to an oxygen dependent redox signal but is also a blue light photoreceptor (Braatsch *et al.*, 2002; Masuda and Bauer, 2002; Braatsch and Klug, 2004).

The AppA primary structure consists of an N-terminal FAD binding domain (Gomelsky and Kaplan, 1998 and Figure 4.1), named BLUF (Gomelsky and Klug, 2002). FAD noncovalently attaches to the BLUF domain and senses the blue light. Recently the AppA photo-excitation process was studied in detail. Kraft *et al.* (2003) proposed that photochemical excitation of the flavin results in strengthening of a hydrogen bond between the flavin and Tyr 21 leading to a stable local conformational change in AppA. The Gln63 side chain and the Trp104 side chain surround the flavin chromophore and are critical in induction of a global structural change in AppA (Anderson *et al.*, 2005; Masuda *et al.*, 2005). Furthermore, the mutant analysis showed that Thr51 and Gly52 are essential for FAD-binding and required to maintain maximal repression of *puf* and *puc* operon during the continuous blue light illumination (Braatsch *et al.*, 2002).

The AppA protein functions as an antagonist of the repressor PpsR, which represses the PS gene expression at high oxygen tension by binding the consensus sequence, TGT-N_{12}-ACA, present in the promoter region of several PS genes (Figure 1.2B). At intermediate oxygen concentrations, light determines whether AppA releases the repressing effect of PpsR or not (Braatsch *et al.*, 2002). So far, AppA is the only known protein that transduces and integrates both light signals and redox signals.

The BLUF domain also occurs in several other bacterial proteins, mainly in cyanobacteria and α-proteobacteria (Gomelsky and Klug, 2002), but the function of these other bacterial BLUF domain proteins has not been elucidated. Four BLUF domains are found in Eukarya, more precisely in the photoactivated adenylyl cyclase (PAC) of the unicellular flagellate *Euglena gracilis*, where PAC mediates a photophobic response (Iseki *et al.*, 2002). Two BLUF domains belong to the α-subunit of the enzyme, PACα, and two to the PACβ subunit (Figure 4.1). The BLUF domains of the *R. sphaeroides* AppA and the *E. gracilis* PAC proteins share an identity of 28-32%. In this work, the PACα1-BLUF domain was fused to the C-terminal domain of the AppA protein (Table 4.1) to test whether the BLUF domain represents a module, which can mediate a light response in different molecular and cellular environments. In addition, the AppA BLUF domain or the AppA C-terminal domain were expressed alone or in combination in *R. sphaeroides* and the functions of those proteins have been tested in this work.

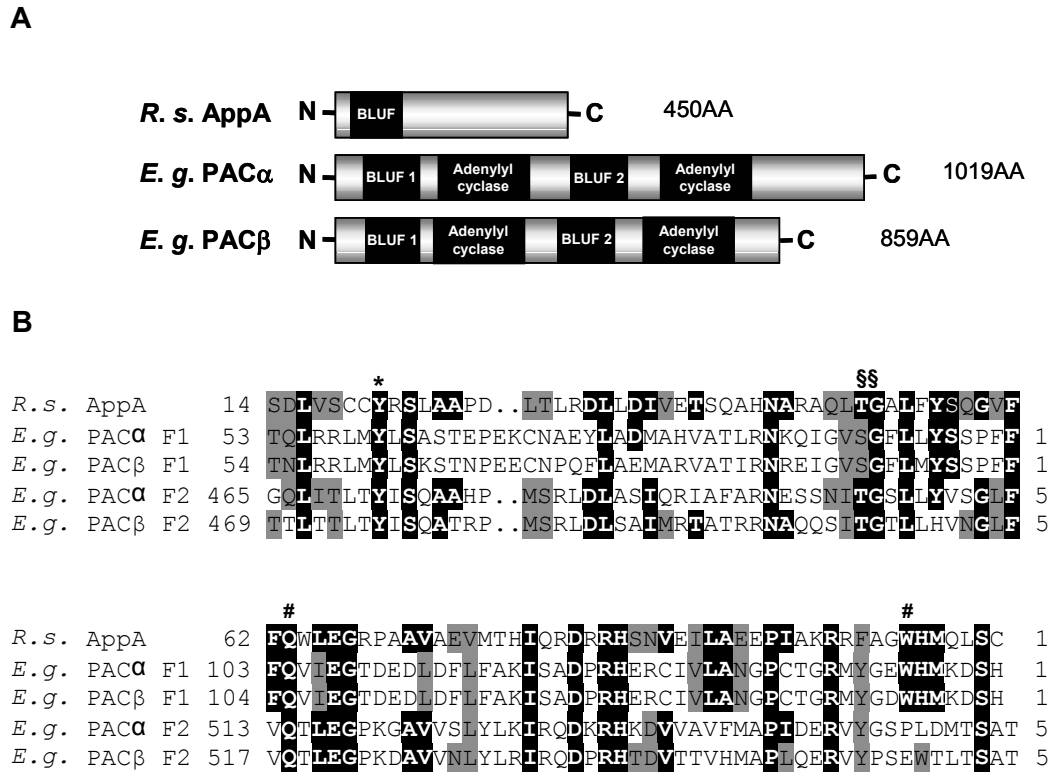

Figure 4.1 The BLUF domains in AppA and PAC proteins.

The functions of two proteins containing BLUF domains have been tested experimentally. Similar to the BLUF domain in *R. sphaeroides* AppA, the BLUF domains from the photoactivated adenylyl cyclase (PAC) from *E. gracilis* are also involved in blue-light-sensing (Iseki *et al.*, 2002). **(A)** Domain structure of the polypeptides. AA, amino acids; **(B)** Sequence alignment, regions identical (black) and similar (grey) to amino acid residues from AppA are highlighted. Tyr21 (*) in AppA is involved in the photocycle of the BLUF domain (Kraft *et al.*, 2003). Thr51 (§) and Gly52 (§) in AppA are essential for FAD-binding (Braatsch *et al.*, 2002). Glin63 and Trp104 (#) are critical in induction of a global structural change in AppA (Anderson *et al.*, 2005; Masuda *et al.*, 2005). (Modified from Braatsch, 2002)

4.1.1 Light- and redox-dependent regulation of PS genes in the control strains: APP11 and APP11(p484-Nco5)

In order to study the function of different AppA-derived proteins, a number of plasmids were constructed and expressed in *R. sphaeroides* strain APP11 (Gomelsky and Kaplan, 1995) (strains 1-6, Table 4.1). This mutant strain lacks the AppA antirepressor protein and is therefore unable to release the PpsR repressor protein from its DNA targets. As a consequence of the strong repression of photosynthesis genes by PpsR, the cells are virtually unpigmented even when grown in the presence of ≤ 3 μM oxygen (Table 4.1 and Figure 4.2) or under anaerobic growth conditions (Gomelsky and Kaplan, 1995). No expression of the *puc* genes is detected in the strain APP11 by Northern blot analysis (Figure 4.3), even at low oxygen tension when *puc* mRNA levels in the wild type are high (Hunter *et al.*, 1987). However, a plasmid borne *appA* copy (Gomelsky and Kaplan, 1995)[strain 2: APP11(p484-Nco5), Table 4.1] restored functional redox dependent gene regulation as indicated by pigmentation (Table 4.1 and Figure 4.2) and *puc* expression levels at low oxygen tension (Figure 4.3 and Figure 4.5). When grown at intermediate oxygen level, the strain APP11(p484-Nco5) showed normal light dependent repression of *puc* mRNA levels (Braatsch *et al.*, 2002 and Figure 4.8).

Table 4.1 Light and redox dependent *puc* expression and BChl contents of APP11 derived strains.

No.	Strain	AppA domain structure	Regulatory function		rel. Bchl
			Light (% Inhibition)	Redox	(μM/OD_{660})
1	APP11		n.d.	n.d.	≤ 0.01
2	APP11 (p484-Nco5)	FAD BLUF Cys	73	+	0.64 ± 0.02
3	APP11(pRK4BLUF-*E.g.*)	FAD *E.g.* BLUF Cys	85	+	0.56 ± 0.02
4	APP11(pBBRAppA170)	FAD BLUF	n.d.	n.d.	≤ 0.01
5	APP11(p484-Nco5Δ)	Cys	0	+	0.60 ± 0.05
6	APP11(pBBRAppA170) (p484-Nco5Δ)	FAD BLUF Cys	60	+	0.61 ± 0.03

The parental strain APP11 is impaired in the production of both photopigments and structural protein components of the photosystem due to an insertional inactivation of the chromosomal *appA* gene (Gomelsky and Kaplan, 1995). A schematic alignment of AppA proteins expressed from the listed strains is shown. AppA mediated light and redox dependent *puc* expression levels are summarized as detected by Northern blot analyses. Relative BChl concentrations shown represent the mean ± standard deviation of three independent measurements of low oxygen (pO_2 ≈ 3 μM) grown cultures. *puc* inhibition under semiaerobic conditions was shown in percentage = 100 × (1- signal level in light irradiated cells / signal level in dark cells); +, significant increase in *puc* signal intensity due to a decrease in oxygen concentration; n.d., no detectable *puc* signal by Northern blot analysis under all oxygen concentrations tested. (Han *et al.*, 2004)

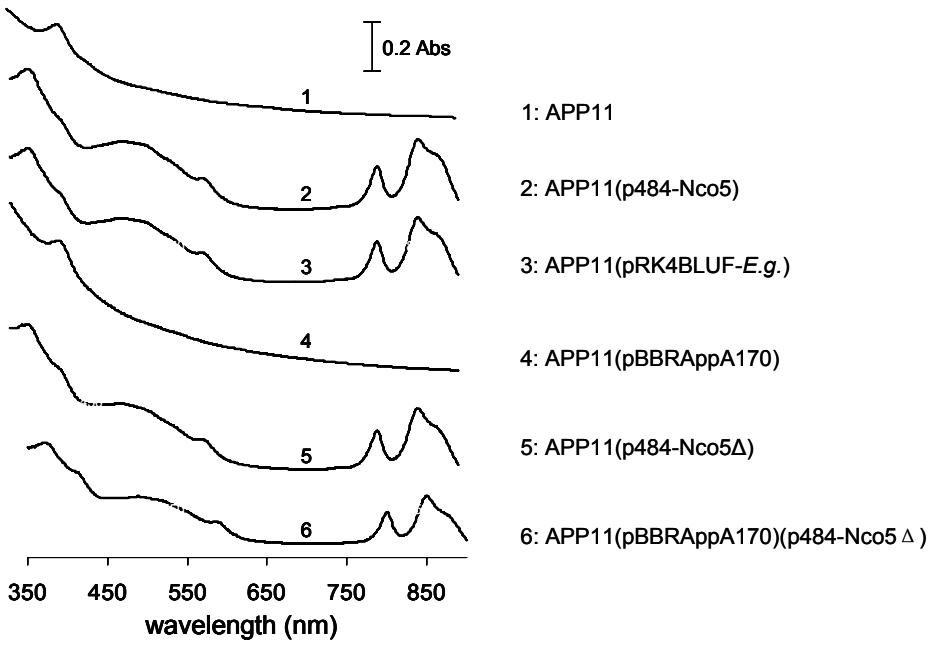

Figure 4.2 Absorbance spectra of the cell extracts from exponentially grown APP11 derived strains under low (pO2 ≈ 3 μM) oxygen tension.
The absorbance maximum of BChl associated with the light harvesting complex (LH) I is 875 nm, and those maxima of BChl associated with the LH II complex are 800 and 850 nm. Colored carotenoids absorb in the range of 450 to 550 nm. (Han *et al.*, 2004)

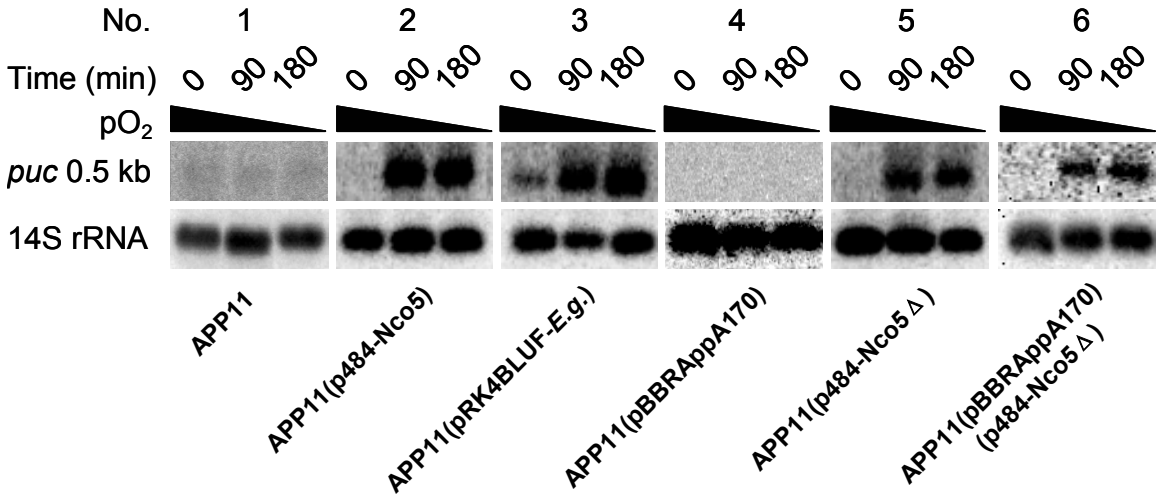

Figure 4.3 Redox dependent regulation of *puc* gene expression in strain APP11 complemented with plasmid constructs listed in Table 4.1.

During the time course of the experiments, the concentration of dissolved oxygen in the media was decreased from 200 µM to ≤ 3 µM. Total RNA was isolated at indicated time points and *puc* transcript levels were monitored by RNA gel blot analyses. A 14S rRNA specific probe (14S rRNA is a product of 23S rRNA *in vivo* processing) (Kordes *et al.*, 1994) was used to show relative RNA loadings. Numbers refer to the strain constructs shown in Table 4.1. (Han *et al.*, 2004)

4.1.2 Light- and redox-dependent regulation of PS genes in the strain expressing the PACα1-AppA hybrid protein [strain APP11(pRK4BLUF-*E.g.*)]

4.1.2.1 Construction of strain APP11(pRK4BLUF-*E.g.*)

A DNA fragment encoding the BLUF-domain PACα1 (BLUF1 in PACα, Figure 4.1) from *E. gracilis* was PCR-amplified (primer pair: PACα1 up new/ PACα1 down, Table 2.4) from pGEMPACα (contains the coding sequence of PACα1) and cloned into p484-Nco50 (contains wild type *appA* with its own promoter) replacing *appA* codons 7-450. Subsequently a DNA fragment encoding the C-terminal AppA domain was PCR-amplified (using primers: AppAup3/AppA_down, Table 2.4) and fused in frame. The resulting recombinant *appA* gene and wild type promoter sequence was subcloned into pRK415 yielding pRK4BLUF-*E.g.* (Figure 4.4). Due to the cloning procedure, additional amino acids serine and arginine were introduced between PACα1 and the C-terminal AppA domain at position 113 and 114 of the hybrid protein. The plasmid pRK4BLUF-*E.g.* was introduced in *R. sphaeroides* strain APP11 by diparental conjugation, resulting in strain APP11(pRK4BLUF-*E.g.*).

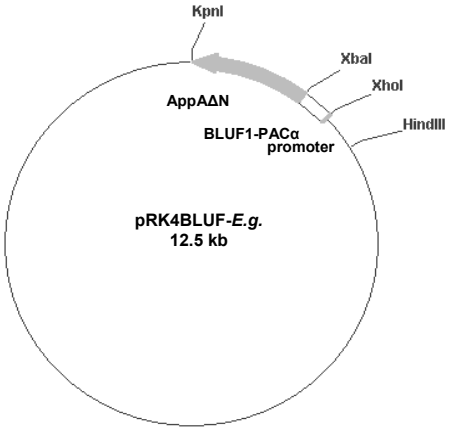

Figure 4.4 Schematic map of plasmid pRK4BLUF-*E.g.*

4.1.2.2 Redox-dependent regulation of PS genes in strain APP11(pRK4BLUF-*E.g.*)

Rhodobacter cells expressing the PACα1-AppA hybrid protein [strain 3: APP11(pRK4BLUF-*E.g.*)] exhibit similar BChl concentrations and spectroscopic characteristics as those of control strain APP11(p484-Nco5) when grown under low oxygen tension (Table 4.1 and Figure 4.2), indicating a normal redox-dependent antirepression of photosynthesis genes. This assumption was confirmed by monitoring *puc* expression after a shift from high to low oxygen tension by Northern blot analysis. Both strains showed a strong increase in *puc* mRNA levels after decrease of oxygen tension (Figure 4.3, strain 2 and 3).

The *puc* expression levels were also quantified by applying a quantitative luciferase assay. The reporter plasmid pBBR2*pucluxAB* was conjugationally transferred into the strains under investigation. This plasmid replicates in *Rhodobacter* and has the *Vibrio harveyi luxAB* genes transcriptionally fused to the *puc* promoter region followed by the *pucBA* genes (Braatsch, 2002; Happ, 2002; Han *et al.*, 2004). 0.1 ml of cell suspension was supplemented with the substrate *n*-decanal and the light emission by bioluminescence was recorded by a luminometer. As shown in Figure 4.5, when the oxygen tension decreases, the luciferase activity increases around threefold in presence of both wild type AppA protein [strain APP11(p484-Nco5)] and PACα1-AppA hybrid protein [strain APP11(pRK4BLUF-*E.g.*)].

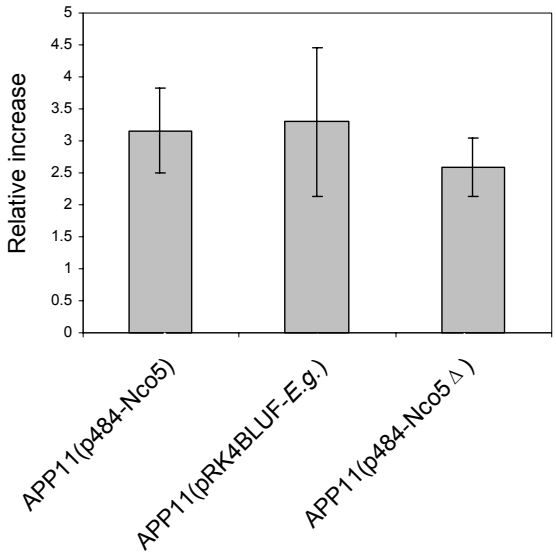

Figure 4.5 Fold increase of the luciferase activity in *R. sphaeroides* APP11 derived strains after oxgen-shift.

The luciferase was encoded by plasmid pBBR2*pucluxAB* in each strain and the expression of the luciferase is under the control of the *puc* promoter. The relative light units were normalized to the optical density of the cultures at 660nm, and the values after five-hour-shift were used to compare to the ones at time point zero, resulting in the increasing fold. Each column and bar indicate the mean and the standard deviation, respectively, of three independent experiments.

4.1.2.3 Light-dependent regulation of the *puf* and *puc* genes in strain APP11(pRK4BLUF-*E.g.*)

The luciferase-activity assay was also performed to analyze the light-dependent regulation of gene expression. A plasmid pBBR2*pufluxAB*, which expresses the luciferase under control of the *puf* promoter (Kuphal, 2001), was used to determine the *puf* expression levels in *R. sphaeroides* 2.4.1 (wild type) and strain APP11(pRK4BLUF-*E.g.*). The cell suspension was spread equally on the RÄ-agar plate and the light emission by bioluminescence of the colonies was detected by Fluor-S™ *MultiImager* (Bio-Rad). In wild-type 2.4.1, the illuminated cells showed much lower luciferase activity compared to the cells kept in dark, indicating that the *puf* expression is significantly repressed by blue light (Figure 4.6A). This blue light repression can also be detected in strain APP11(pRK4BLUF-*E.g.*) (Figure 4.6B). And such repression can be released after switching off the light (Figure 4.6C). These results suggest that the PACα1-AppA hybrid protein behaves the same as wild-type AppA protein in the response of blue light.

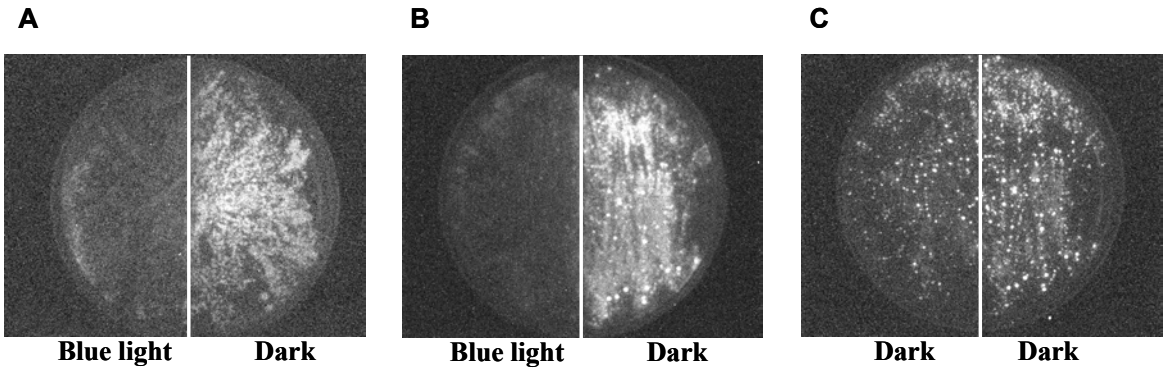

Figure 4.6 Bioluminescence of *R.sphaeroides* 2.4.1(pBBR2*pufluxAB*) (A) and *R.sphaeroides* APP11(pRK4BLUF-*E.g.*)(pBBR2*pufluxAB*) colonies (B&C).

Each strain harbors a plasmid pBBR2*pufluxAB*, which expresses the luciferase in *Rhodobacter* under control of the *puf* promoter. **(A)** The cell suspension of *R.sphaeroides* 2.4.1(pBBR2*pufluxAB*) was spread equally on the RÄ-agar plate. After incubated in dark for two days, the half of plate was illuminated by blue light for 1.5 h, while the other half was covered by aluminum foil; **(B)** The *R.sphaeroides* APP11(pRK4BLUF-*E.g.*)(pBBR2*pufluxAB*) cells were treated the same as described in (A); **(C)** The same plate from (B) was kept in dark for additional 2 h after illumination by blue light.

Upon blue light illumination at 104 ± 24 µM dissolved oxygen, the strain APP11(pRK4BLUF-*E.g.*) showed about 65% of *puf* inhibition and up to 85% of *puc* inhibition as determined by RNA gel blots (Figure 4.7). Similar values of inhibition were reported in the presence of the wild type AppA protein (Braatsch *et al.*, 2002 and Table 4.1, strain 2).

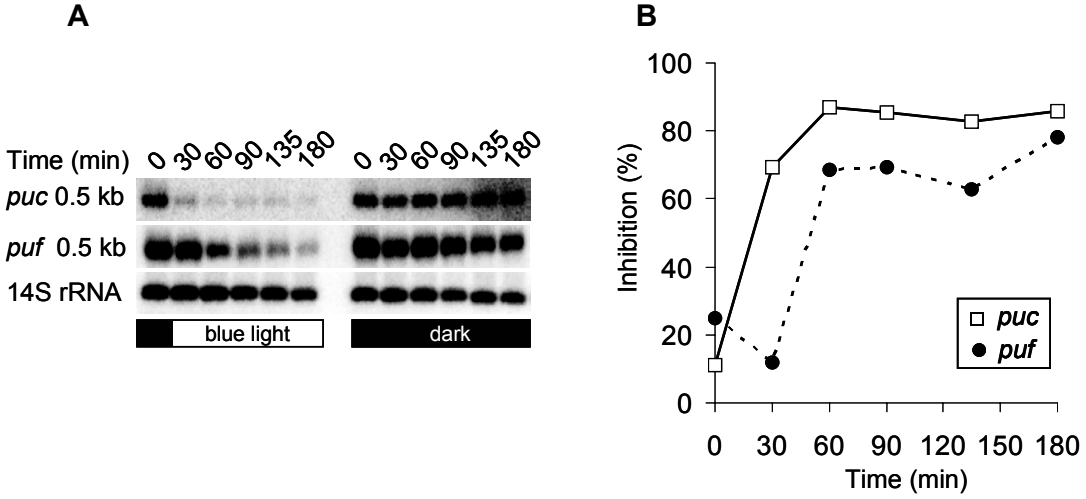

Figure 4.7 Kinetics of *puf* and *puc* expression in strain *R. sphaeroides* APP11(pRK4BLUF-*E.g.*) caused by blue light irradiation.

Cells grown at 104 ± 24 µM dissolved oxygen were shifted from the dark into blue light or kept in the dark. **(A)** *puc* and *puf* expression changes determined by RNA gel blot analyses. A 14S rRNA specific probe was used to show relative RNA loadings. **(B)** The intensities of mRNA signals were quantified and normalized to the intensities of the rRNA signals. Percent of inhibition of normalized *puc* (open squares) and *puf* (filled circles) mRNA levels were plotted [inhibition in % = 100 × (1- mRNA level in light irradiated cells / mRNA level in dark cells)]. (Han *et al.*, 2004)

The blue light-dependent regulation of *puc* expression was also quantified by the luciferase-activity assay using a reporter plasmid pBBR2*pucluxAB*, which contains 334bp *puc* promoter region upstream of the *Vibrio harveyi luxAB* genes. In the presence of the wild type AppA protein [strain APP11(p484-Nco5)] and the PACα1-AppA hybrid protein [strain APP11(pRK4BLUF-*E.g.*)], luciferase activity drops after illumination, approaching a very low level that is also observed in the strain APP11 (Figure 4.8A). The luciferase assays performed with strains expressing the PACα1-AppA hybrid protein [strain APP11(pRK4BLUF-*E.g.*)] or wild type AppA [strain APP11(p484-Nco5)] confirmed the RNA gel blot results and demonstrate that all *cis* regulatory elements involved in blue light repression of *puc* genes are contained within the 334 bp promoter upstream region present on the reporter plasmid pBBR2*pucluxAB*. Average repression rates during blue light illumination of both semiaerobically grown cultures were 80% (Figure 4.8B), well reflecting the 73-85% inhibition as determined by RNA gel blots (Figure 4.7).

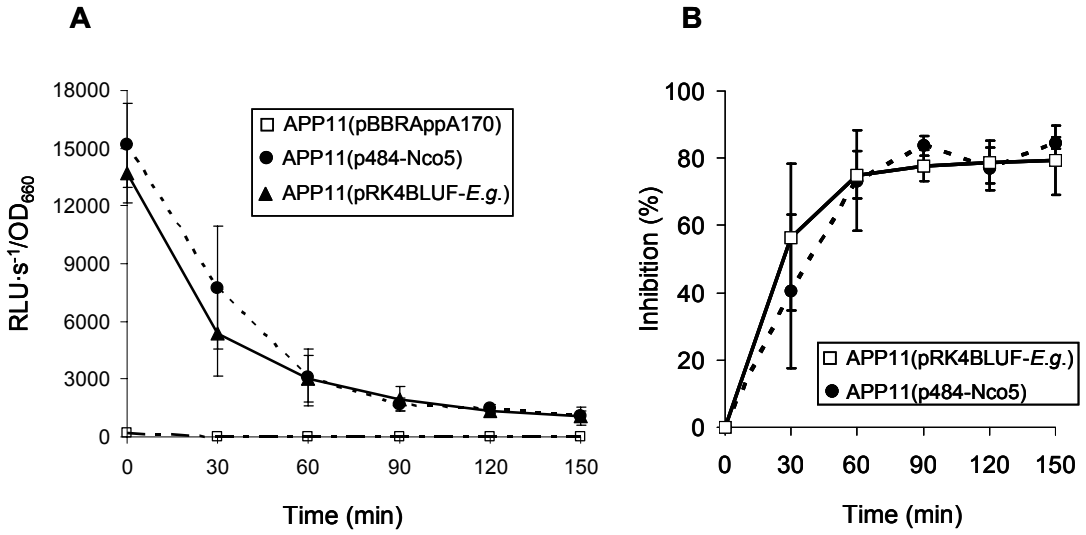

Figure 4.8 Kinetics of *puc* expression in *R. sphaeroides* APP11 derived strains caused by blue light irradiation.

Cells grown at 104 ± 24 µM dissolved oxygen were shifted from the dark into blue light or kept in the dark. Each strain listed in this figure harbours a plasmid pBBR2*pucluxAB*, which can express the luciferase in *Rhodobacter* under control of the *puc* promoter. **(A)** Luciferase activity assays for *puc* expression in strains APP11(pBBRAppA170) (open squares), APP11(p484-Nco5) (filled circles) and APP11(pRK4BLUF-*E.g.*) (filled triangles). The relative light units ($RLU \cdot s^{-1}$) of light irradiated cells were plotted after normalization to the optical density of the cultures at 660 nm. Each point and bar shows the mean and the standard deviation, respectively, of three independent experiments. **(B)** Luciferase activity assays for *puc* expression in strains APP11(pRK4BLUF-*E.g.*) (open squares) and APP11(p484-Nco5) (filled circles). The relative light units of light irradiated and dark cells were normalized to the optical density of the cultures at 660 nm and plotted as percent of inhibition. Each point and bar shows the mean and the standard deviation, respectively, of three independent experiments. (Modified from Han *et al.*, 2004)

These data reveal that the eukaryotic BLUF domain of the PACα1-AppA fusion protein can fully replace the AppA BLUF domain from *R. sphaeroides* in light signaling and does not interfere with the redox signaling function.

4.1.3 Light- and redox-dependent regulation of PS genes in the strain only expressing the BLUF domain [strain APP11(pBBRAppA170)] and the strain only expressing the C-terminal domain of AppA [strain APP11(p484-Nco5Δ)]

To better understand the functions of the AppA domains in redox and light signaling, the BLUF domain or the C-terminal domain of AppA was separately expressed in *R. sphaeroides* (Table 4.1, strains 4 and 5). The absorption spectrum and the relative BChl concentration of the strain harbouring the AppA BLUF domain [strain 4: APP11(pBBRAppA170)] were identical to that of the parental strain APP11 (Table 4.1 and Figure 4.2). As in the strain APP11, no *puc* mRNA was detected by Northern Blot analysis in the strain APP11(pBBRAppA170) under all growth conditions tested (Figure 4.3). The luciferase activity in this strain is also at very low level (Figure 4.8A). The lack of *puc* expression could be due to the fact that the BLUF domain is not stable when expressed separately. However, as shown below (Figure 4.9), the separated BLUF domain is able to transmit the blue light signal when expressed together with the C-terminal domain of AppA, which requires expression of a stable protein. Thus, these results show that the BLUF domain alone is not able to release the repressing effect of PpsR.

Strain APP11(p484-Nco5Δ) harbours the C-terminal domain of AppA (Table 4.1, strain 5). Its BChl concentration and absorption spectrum are identical to that of control strain APP11(p484-Nco5) which expresses the wild type AppA protein (Table 4.1 and Figure 4.2). Northern Blot analysis and luciferase activity assays after a transition from high oxygen tension to low oxygen tension confirmed a normal redox dependent increase of the *puc* mRNA levels (Figures 4.3 and 4.5). *puc* expression was, however, independent of blue light (Table 4.1, strain 5). These results indicate that the C-terminal domain of AppA is sufficient for redox regulation but not for light regulation. Since the BLUF domain alone is unable to transmit the light signal and to release the PpsR repressing effect, it is suggested that the PpsR repressor protein should interact with the C-terminal AppA domain and that the BLUF domain might influence this interaction in dependence of blue light.

4.1.4 Light- and redox-dependent regulation of PS genes in the strain expressing the BLUF domain and the C-terminal part of AppA separately [strain APP11(pBBRAppA170)(p484-Nco5Δ)]

The results obtained with the hybrid AppA protein containing the *Euglena* BLUF domain suggested that the BLUF domain is able to signal to different output domains. Some bacteria encode proteins just consisting of the BLUF domain (Gomelsky and Klug, 2002), but the function of these proteins has not been elucidated. It is conceivable that these BLUF proteins transfer a light-dependent signal to other proteins by protein-protein interactions without the necessity of a covalent linkage. To test this hypothesis, the N-terminal BLUF domain of AppA and the C-terminal AppA domain were separately expressed in one strain APP11(pBBRAppA170)(p484-Nco5Δ) (Table 4.1, strain 6). This strain showed the same BChl concentration and absorption spectrum as control strain APP11(p484-Nco5) (Table 4.1 and Figure 4.2). It also showed the same *puc* expression as the control strain in the response to oxygen concentration (Figure 4.3). RNA gel blot analysis revealed a light-dependent *puc* and *puf* inhibition by 50-60% (Figure 4.9 and Osterloh, 2003). Based on the significant blue light dependent gene repression by the separated domains, the conclusion is that the BLUF domain functions as a module, which can transduce a light dependent signal to a C-terminally fused output domain or to a separately expressed protein.

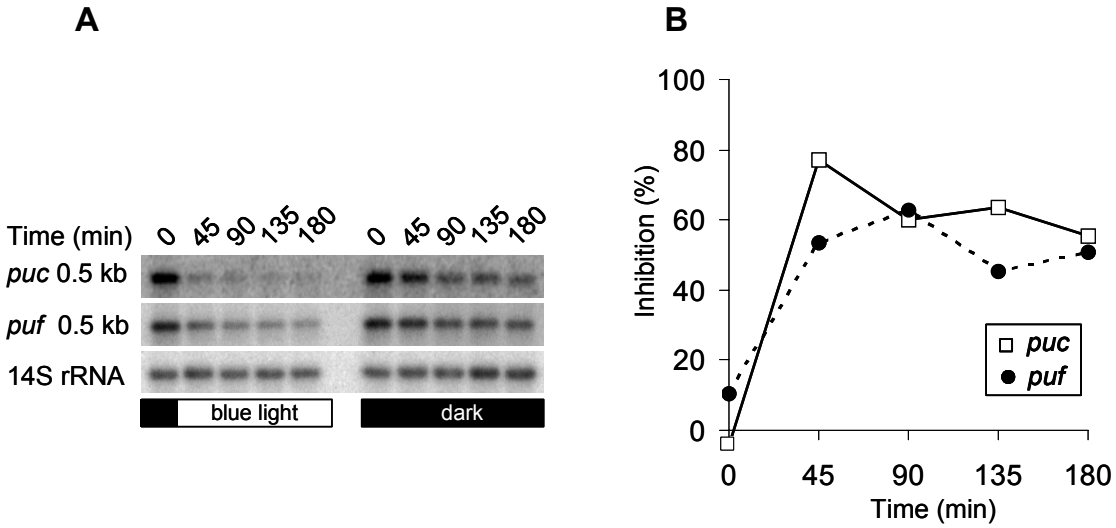

Figure 4.9 Kinetics of *puf* and *puc* expression in *R. sphaeroides* APP11(pBBRAppA170)(p484-Nco5Δ) caused by blue light irradiation.

Cells grown at 104 ± 24 µM dissolved oxygen were shifted from the dark into blue light or kept in the dark. **(A)** *puc* and *puf* expression changes as determined by RNA gel blot analyses. A 14S rRNA specific probe was used to show relative RNA loadings. **(B)** Quantification of *puc* (open squares) and *puf* (filled circles) inhibition. The evaluation was performed as described in the legend to Figure 4.6. (Osterloh, 2003 and Han *et al.*, 2004)

4.2 Role of the C-terminal domain of AppA in light- and redox-dependent regulation

The flavoprotein AppA from the facultatively phototroph *Rhodobacter sphaeroides* 2.4.1 controls the expression of PS genes in response to changes in oxygen tension as well as in light intensity and quality. Signal transmission involves interaction of AppA with PpsR, which can repress PS genes through binding to the consensus sequence TGT-N_{12}-ACA found in tandem in the promoter regions of most PS genes.

AppA integrates light and redox signals. The BLUF domain, which is located at the N-terminus of AppA, functions as blue light receptor. Mutant analysis revealed that the C-terminal domain of AppA is sufficient for redox regulation; however, light signaling requires the BLUF domain together with the C-terminal domain of AppA (Chapter 4.1.3). This suggests that PpsR should bind to the C-terminal domain of AppA, not to the BLUF domain. Furthermore, the BLUF domain and the C-terminal domain of AppA can transmit the light signal even when expressed as separated domains (Chapter 4.1.4). This implicates that the BLUF domain is fully modular and can relay signals to the C-terminal domain of AppA and that there should be an interaction between BLUF and the C-terminal domain of AppA. Therefore, the C-terminal domain of AppA plays a key role not only in redox-dependent regulation but also in the light-dependent regulation.

4.2.1 Role of the cysteine-rich cluster of AppA in light- and redox-dependent regulation

4.2.1.1 Light- and redox-dependent regulation of PS genes in the strain expressing the truncated AppA lacking the cysteine-rich cluster [strain APP11(p484-Nco5ΔC)]

The sequence analysis indicates that AppA contains a cysteine-rich cluster (Cys-X5-Cys-Cys-X4-Cys-X6-Cys-Cys) at the carboxy-terminal region. Moreover, two cysteine residues are conserved in PpsR protein of *R. sphaeroides* and CrtJ protein in *R. capsulatus*. CrtJ is a PpsR homologue (75% homology) and undergoes a dithiol-disulfide switch when oxygen tension changes. The oxidized CrtJ shows a higher DNA binding affinity (Masuda *et al.*, 2002). It thus seems possible that the cysteine-rich cluster of AppA is involved in the oxidation/reduction of PpsR (Masuda & Bauer, 2002). To better understand the function of the cysteine-rich domain of AppA in redox and light signaling,

the plasmid p484-Nco5ΔC, expressing the truncated AppA lacking the cysteine-rich cluster, was introduced in the *appA*$^-$ strain *R. sphaeroides* APP11 by diparental conjugation, resulting strain APP11(p484-Nco5ΔC). The absorption of cell extract from strain APP11(p484-Nco5ΔC) at 800 nm, 850 nm and 875 nm was less than that of control strain APP11(p484-Nco5) having wild type *appA* sequence on a plasmid (Figure 4.10), indicating that strain APP11(p484-Nco5ΔC) forms less photosynthetic apparatus than the control strain. Strain APP11(p484-Nco5ΔC) also accumulated much lower amounts of BChl than the control strain [0.23 ± 0.02 μM/OD_{660} in strain APP11(p484-Nco5ΔC), 0.69 ± 0.04 μM/OD_{660} in strain APP11(p484-Nco5)] when the cells are grown at low oxygen conditions (pO2 ≈ 3 μM).

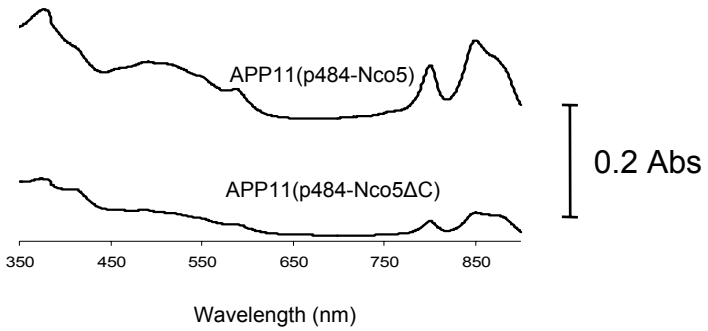

Figure 4.10 Absorbance spectra of the cell extracts from exponentially grown strain APP11(p484-Nco5) and strain APP11(p484-Nco5ΔC) under low oxygen tension (pO2 ≈ 3 μM).

The absorbance maximum of BChl associated with the light harvesting complex (LH) I is 875 nm, and those of BChl associated with the LH II complex are 800 and 850 nm. Colored carotenoids absorb in the maxima of 450 to 550 nm.

However, this truncated AppA can still transduce redox and light signals as the wild type does. After blue light illumination under semi-aerobic conditions, the level of *puf* mRNA decreased to 30% of the level present in the dark control, whereas the *puc* mRNA was no longer detectable by Northern blot analysis (Figure 4.11A). When the oxygen tension decreased, the *puc* mRNA level increased significantly (Figure 4.11B). This implicates that the cysteine-rich domain at the very C-terminus of AppA might influence the basal expression of PS genes, but does not affect the redox and light signaling.

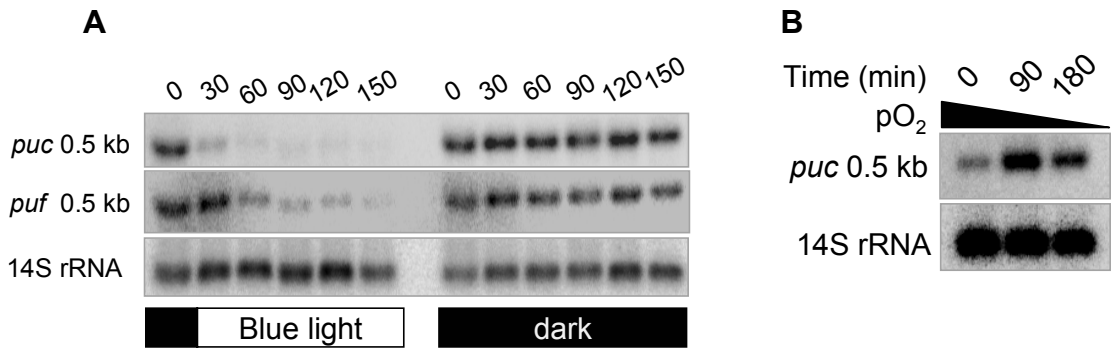

Figure 4.11 *puf* and *puc* expression in strain APP11(p484-Nco5ΔC).

(A) Cells were grown at 104 ± 24 μM dissolved oxygen and shifted from the dark into blue light or kept in the dark; **(B)** Cells were grown in the dark and the concentration of dissolved oxygen in the medium was decreased from 200 μM to ≤3 μM during the time course of the experiment. Total RNA was isolated at indicated time points, and *puf* and *puc* transcript levels were monitored by RNA gel-blot analyses. A 14S rRNA-specific probe was used as internal standard.

4.2.1.2 Expression and purification of AppA and AppAΔC

In order to test the role of the cysteine-rich domain *in vitro*, the full-length AppA and a truncated AppA lacking the cysteine-rich domain (AppAΔC) were overproduced in *E. coli* cells. Because Gomelsky & Kaplan (1998) failed to produce soluble GST-AppA from *E. coli* cells, a His-tagged AppA was overexpressed in this work. The 1.59 kb *Bgl*II-*Kpn*I DNA fragment, containing full length *appA* sequence, was amplified by PCR (primers: appAup2 and AppA_down, Table 2.4) and cloned into the *Bam*HI and *Kpn*I sites of vector pQE30. The recombinant plasmid designated pQEAppA was transformed into *E. coli* JM109. The His-AppA fusion protein was produced in *E. coli* JM109(pQEAppA) cells induced under variable conditions and the cells always turned into yellow color after induction. However, His-AppA (49.8 kDa) was always produced in insoluble form (Figure 4.12), *i.e.* as inclusion bodies, which were yellow. This phenomenon was also found in the study of Gomelsky & Kaplan (1998) and implicates that AppA does bind to the flavin.

For overexpression of AppAΔC, the 1.2 kb *Bgl*II-*Kpn*I DNA fragment, containing *appA* codons 1-396, was amplified by PCR (primers: appAup2 and DeltaCdown, Table 2.4) using plasmid p484-Nco5ΔC as template and cloned into the *Bam*HI and *Kpn*I sites of vector pQE30. The recombinant plasmid designated pQEAppAΔC was transformed into *E. coli* JM109. The His-AppAΔC fusion protein was produced in *E. coli* JM109(pQEAppAΔC) cells induced under variable conditions and the cells always turned

into yellow color after induction. Unfortunately, His-AppAΔC (43.7 kDa) was always produced in insoluble form (Figure 4.13), *i.e.* as inclusion bodies, which were yellow. This phenomenon implicates that AppAΔC can also bind to the flavin and the cysteine-rich domain does not affect the BLUF domain to bind FAD.

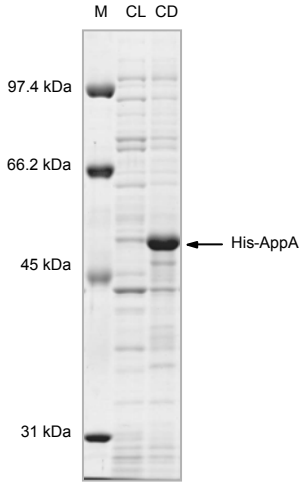

Figure 4.12 AppA-enriched inclusion bodies.

AppA protein was overproduced in *E. coli* JM109(pQEAppA). The clear lysate (CL) and cell debris (CD) were loaded on a 10% SDS-polyacrylamide gel, and the signals were analyzed by Coomassie blue staining. The molecular mass standards (M) are shown in the left of figure.

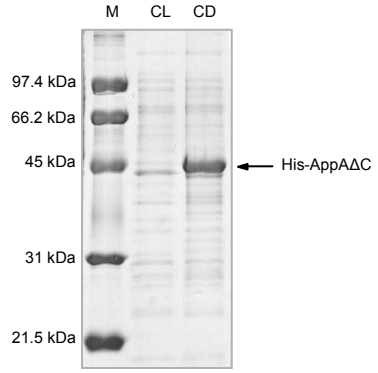

Figure 4.13 AppAΔC-enriched inclusion bodies.

AppAΔC protein was overproduced in *E. coli* JM109(pQEAppAΔC). The clear lysate (CL) and cell debris (CD) were loaded on a 15% SDS-polyacrylamide gel, and the signals were analyzed by Coomassie blue staining. The molecular mass standards (M) are shown in the left of figure.

4.2.2 The *in vivo* redox states of the two cysteines of PpsR

The cysteine-rich cluster at carboxy-terminal part of AppA and two cysteines at the position 251 and 424 of PpsR were previously supposed to sense the redox signal through a dithiol-disulfide switch. The CrtJ protein in *R. capsulatus* is a PpsR homologue (75% homology) and its DNA binding activity was proved to be redox controlled by formation/disruption of disulfide bonds within the protein (Masuda *et al.*, 2002). However, the *in vivo* data showed that the cysteine-rich cluster is not involved in redox- and light-dependent regulation (Chapter 4.2.1). Furthermore, the PpsR mutant (C251S/C424S) showed similar activity as wild-type PpsR in regulation of PS gene expression (Moskvin *et al.*, 2005), suggesting that AppA interacts with PpsR irrespective of the disulfide bond. Therefore, the redox states of the two cysteines of PpsR were determined *in vivo* by AMS modification.

4.2.2.1 Expression and purification of PpsR

For the control of the experiment, the PpsR protein was gotten after the thrombin cleavage through purified GST-PpsR fusion protein. The GST-PpsR fusion protein was expressed in *E. coli* JM109(pGpps) cells. Optimal production of a soluble GST-PpsR fusion occurred when mid-log cells (OD_{600} = 0.6), grown at 25°C, were induced with 0.1 mM isopropyl-β-D-thiogalactopyranoside (IPTG) for 8 h. The purification was performed using Glutathione Sepharose® 4B and GST-PpsR (76 kDa) was eluted by glutathione (Figure 4.14A). To remove the GST-tag, the GST-PpsR-bound Glutathione Sepharose was incubated with thrombin (50 units per 0.5 ml Glutathione Sepharose) at room temperature overnight with end-over-end rotation. Then PpsR (51.1 kDa) was eluted by PBS (250 mM NaCl, pH 7.3) (Figure 4.14B). The late eluates were collected and dialyzed in storage buffer (Chapter 3.5.1) for raising antibody and for *in vitro* assays.

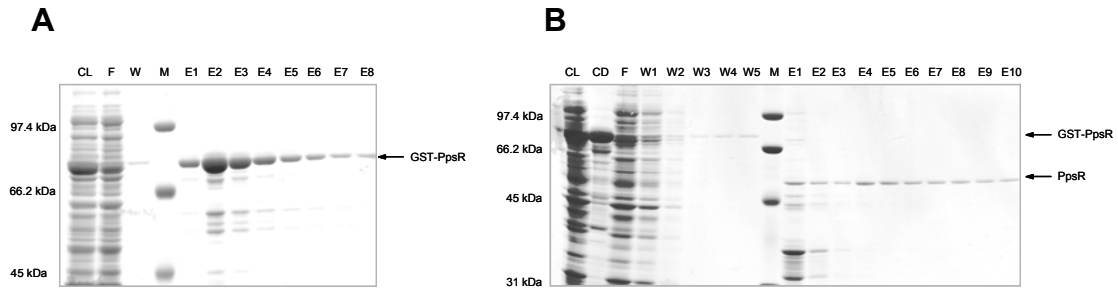

Figure 4.14 Purification of PpsR from crude extract of *E. coli* JM109(pGpps).

(A) Purification of GST-PpsR using Glutathione Sepharose® 4B. Proteins were loaded on a 10% SDS-polyacrylamide gel, and the signals were analyzed by Coomassie blue staining; **(B)** Thrombin cleavage to remove the GST-tag. Proteins were loaded on a 12% SDS-polyacrylamide gel, and the signals were analyzed by Coomassie blue staining. Abbreviations: M, molecular mass standards (also shown in the left of figures); CL, clear lysate; CD, cell debris; F, flow-through; W, wash fraction; E, eluate.

4.2.2.2 Determination of the *in vivo* redox states of the two cysteines of PpsR

To determine the *in vivo* redox states of PpsR in *R. sphaeroides* grown at different oxygen tension, the two cysteines were modified by AMS, which can modify the free thiol groups *in vitro*. The addition of AMS leads to the alkylation of free thiol groups, present in the reduced but not in the oxidized protein. The addition of the high-molecular-mass AMS moiety to the reduced but not to the oxidized protein allows separation of the two forms by gel electrophoresis. As shown in Figure 4.15A, treatment of reduced PpsR with AMS resulted in slower electrophoretic migration than AMS-treated oxidized PpsR. There is no

difference in electrophoretic migration pattern between oxidized PpsR treated with AMS and non-AMS-treated PpsR. These results indicate that oxidized PpsR has no available cysteine for AMS modification, which is contrasted by reduced PpsR that does have AMS-modifiable cysteine sulfhydryl groups.

To test the disulfide bond status of PpsR *in vivo*, the whole-cell proteins were precipitated by direct treatment with trichloroacetic acid (TCA). Since TCA denatures proteins, the oxidized and reduced states of cellular proteins are effectively fixed with TCA. Whole-cell TCA-precipitated proteins were then treated with AMS and subsequently separated by SDS-PAGE. The electrophoretic mobility of PpsR was then detected by Western blot analysis. As shown in Figure 4.15B, the mobility of PpsR from anaerobically, semi-aerobically and aerobically grown cells that were TCA precipitated and then treated with AMS had the same electrophoretic mobility. All of them had retarded mobility in comparison of non-AMS-treated PpsR, indicating that each thiol group of the two cysteines in PpsR exits in a reduced state irrespective of oxygen. This result is in agreement with previously published data (Cho *et al.*, 2004).

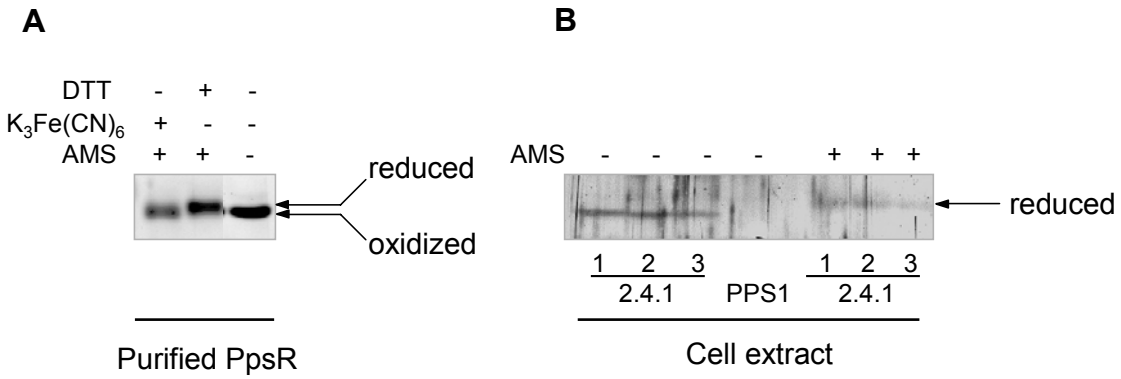

Figure 4.15 Examination of disulfide bond formation in PpsR by AMS modification.

(A) Purified PpsR treated with either DTT or $K_3Fe(CN)_6$, and then treated with AMS; **(B)** PpsR in cell extracts of wild-type strain 2.4.1 grown under anaerobic conditions (lane 1), semi-aerobic conditions (lane 2), and aerobic conditions (lane 3). Strain PPS1 is the *ppsR*- mutant. The PpsR proteins were detected by Western blot using the PpsR-specific antibody.

4.2.3 Inhibition of the PpsR DNA-binding activity by the C-terminal part of AppA

4.2.3.1 Expression and purification of GST-AppAΔN

A previous *in vivo* analysis strongly suggested that it is the C-terminal part of AppA that binds PpsR and inhibits the DNA-binding activity of PpsR (Han *et al.*, 2004 and Chapter

4.1.3). In order to directly prove this assumption, an N-terminally truncated AppA (amino acids 5-190 deleted) was expressed in a GST-tagged version in *E. coli*. The 0.8 kb *Bgl*II-*Sma*I DNA fragment was amplified by PCR (primers: DeltaNup and DeltaNdown, Table 2.4) using plasmid p484-Nco5Δ as template and cloned into the *Bam*HI and *Sma*I sites of vector pGEX-4T-1. The recombinant plasmid designated pGEXAppAΔN was transformed into *E. coli* JM109. The GST-AppAΔN fusion protein was produced in *E. coli* JM109(pGEXAppAΔN) cells induced at 25°C with 0.5 mM IPTG for 8 h. The purification was performed using Glutathione Sepharose® 4B and GST-AppAΔN (56.3 kDa) was eluted by glutathione (Figure 4.16). The pattern of multiple bands is most likely due to partial degradation of the protein (see later chapter).

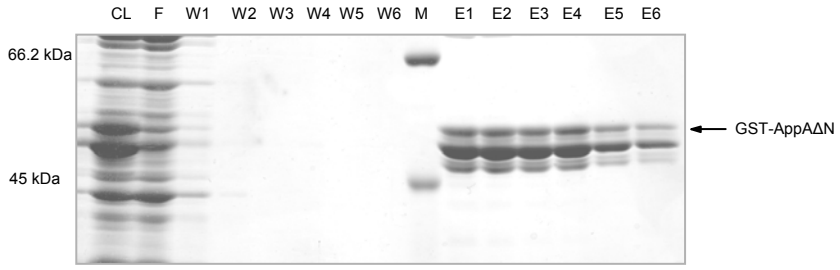

Figure 4.16 Purification of GST-AppAΔN from crude extract of *E. coli* JM109(pGEXAppAΔN).

Purification of GST-AppAΔN was performed using Glutathione Sepharose® 4B. Proteins were loaded on a 10 % SDS-polyacrylamide gel, and the signals were analyzed by Coomassie blue staining. Abbreviations: M, molecular mass standards (also shown in the left of figure); CL, clear lysate; F, flow-through; W, wash fraction; E, eluate.

4.2.3.2 The C-terminal part of AppA inhibits the PpsR DNA-binding activity

The interaction of the C-terminal part of AppA (AppAΔN) with the PpsR protein was studied by analyzing the interference of AppAΔN with DNA binding of the PpsR protein by gel retardation analysis. When a 259 bp DNA fragment (amplified by PCR using primers: puc-281 and puc-23, Table 2.4) spanning the *puc* promoter region was incubated with increasing concentrations of GST-PpsR, the migration of the DNA fragment in a native gel was retarded (Figure 4.17A). The addition of 9 pmol of PpsR shifted the DNA fragment completely.

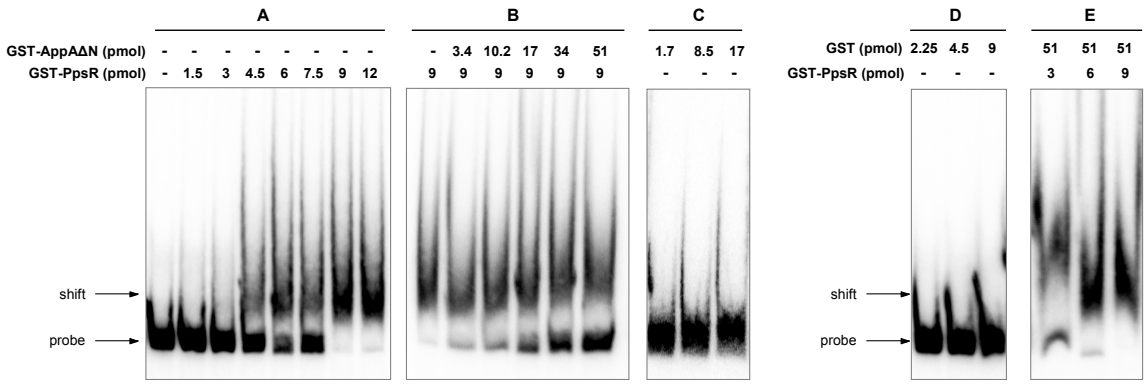

Figure 4.17 Inhibition of the PpsR DNA-binding activity by AppAΔN.

Reduced PpsR (amount as indicated in the figure) was preincubated without AppAΔN **(A)** or with AppAΔN **(B)** at room temperature for one hour and then incubated for further 40min at 30°C with the ^{32}P-labeled *puc* DNA probe. For the control, AppAΔN alone **(C)**, GST alone **(D)**, and PpsR preincubated with GST **(E)** were incubated with the same amount of ^{32}P-labeled *puc* DNA probe at the same condition described above. The samples were then analyzed on a 4% native polyacrylamide gel.

When the DNA fragment (15.4 fmol) was incubated with 9 pmol of PpsR and increasing amounts of GST-AppAΔN, increasing amounts of non retarded DNA were observed (Figure 4.17B), indicating that AppAΔN interferes with DNA binding of the PpsR protein. Part of the DNA was retarded even when AppAΔN was present in a 5.7-fold excess over PpsR. The GST alone did not result in retardation of the DNA fragment (Figure 4.17D) nor interfere with PpsR-DNA binding (Figure 4.17E), and the GST-AppAΔN did not result in retardation of the *puc* promoter DNA fragment (Figure 4.17C). These *in vitro* data support the conclusion based on *in vivo* experiments (Han *et al.*, 2004) that PpsR interacts with the C-terminal part of AppA.

The Pfam data base predicted that the C-terminal part of AppA contains a putative vitamin B_{12} binding domain. However, Oh & Kaplan (2001) suggested that AppA possibly contains a heme as redox prosthetic group. Therefore, the functions of vitamin B_{12} and heme were also studied by gel retardation analyses in the present of vitamin B_{12} or hemin. As shown in Figure 4.18A, increasing amounts of vitamin B_{12} resulted in decreasing amounts of retarded DNA, suggesting vitamin B_{12} might increase the activity of AppAΔN in the inhibition of the PpsR DNA-binding activity. However, vitamin B_{12} alone also inhibited the DNA-binding activity of PpsR (Figure 4.18B). The same phenomenon showed up when hemin was added in this assay (Figure 4.18C). Therefore, it could be possible that vitamin B_{12} and hemin influence the DNA-binding activity of

PpsR or that vitamin B_{12} and hemin unspecifically change the mobility of DNA in such assays.

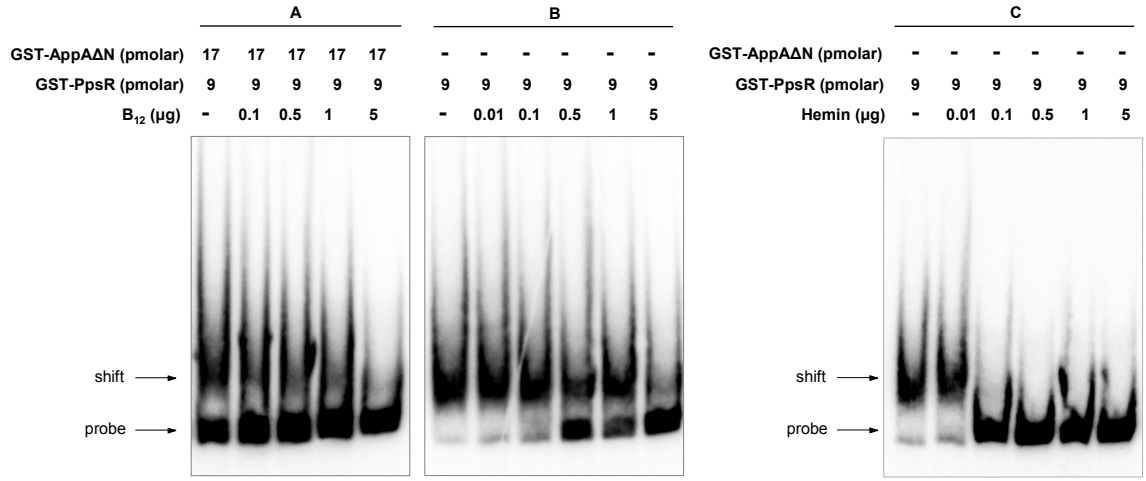

Figure 4.18 Effect of vitamin B_{12} and hemin on the PpsR DNA-binding activity.

Reduced PpsR (amount as indicated in the figure) was preincubated with AppAΔN **(A)** or without AppAΔN **(B)** at room temperature in the presence of vitamin B_{12} for one hour and then incubated for further 40min at 30°C with the ^{32}P-labeled *puc* DNA probe; **(C)** Reduced PpsR was preincubated with hemin at room temperature for one hour and then incubated with the same amount of ^{32}P-labeled *puc* DNA probe at the same condition described above. The samples were then analyzed on a 4% native polyacrylamide gel.

4.2.4 The C-terminal part of AppA encompasses a heme binding domain

As described above, vitamin B_{12} and heme could be two candidate cofactors carried by the C-terminal part of AppA (AppAΔN). To find out which cofactor the C-terminal part of AppA carries, the binding of vitamin B_{12} or heme to the AppAΔN protein was tested.

4.2.4.1 Expression and purification of His-AppAΔN

The AppAΔN was produced in *E. coli* cells with His-tag at the N-terminus. The 1.04 kb *Bgl*II-*Kpn*I DNA fragment was amplified by PCR (primers: DeltaNup and AppA_down, Table 2.4) using plasmid p484-Nco5Δ as template and cloned into the *Bam*HI and *Kpn*I sites of vector pQE30. The recombinant plasmid designated pQEAppAΔN was transformed into *E. coli* JM109. His-AppAΔN was produced in *E. coli* JM109(pQEAppAΔN) cells induced at 17°C overnight with 0.5 mM IPTG. The purification was performed by Ni-NTA agarose either under native conditions (Figure 4.19A) or under denaturing conditions (Figure 4.19C).

When AppAΔN was purified under native conditions and analysed in SDS-polyacrylamide gel, there were always multiple bands showing up close to expected position (calculated size: 29.7 kDa). The Western blots using the specific antibody against either His-tag (Figure 4.19B) or AppAΔN (Figure 4.33) suggest that the pattern of multiple bands is most likely due to partial degradation of the protein.

In order to get high amounts of AppAΔN for raising antibody, His-AppAΔN was purified under denaturing conditions and eluted from Ni-NTA agarose by pH gradient (Figure 4.19C). The AppAΔN-specific antibody was raised in a rabbit against the gel-purified His-AppAΔN. Fortunately, the AppA protein could be detected by this antibody from the cell extracts of *R. sphaeroides*. Therefore, this AppAΔN-specific antibody was used in this work to determine the AppA protein and AppA variants by Western blot.

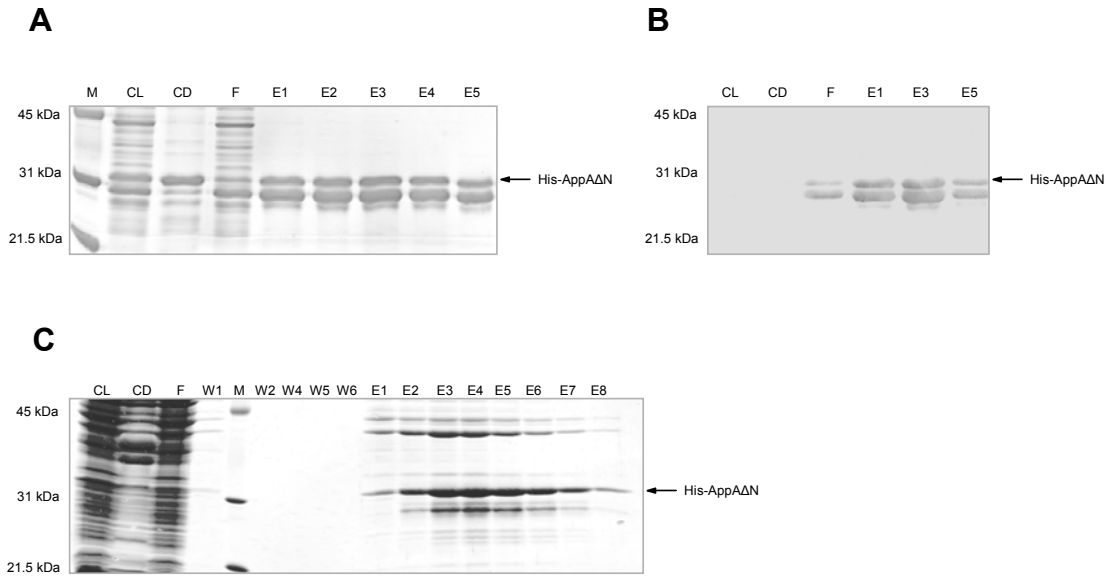

Figure 4.19 Purification of His-AppAΔN from crude extract of *E. coli* JM109(pQEAppAΔN).

His-AppAΔN was purified under native conditions. Proteins were loaded on a 12% SDS-polyacrylamide gel, and the signals were analyzed by Coomassie blue staining **(A)** and Western blot **(B)** using a specific antibody against His-tag; **(C)** Purification of His-AppAΔN under denaturing conditions. Proteins were eluted by pH gradient and loaded on a 12% SDS-polyacrylamide gel. The signals were analyzed by Coomassie blue staining. Abbreviations: M, molecular mass standards (also shown in the left of figures); CL, clear lysate; CD, cell debris; F, flow-through; W, wash fraction; E, eluate.

4.2.4.2 Reconstitution of His-AppAΔN with hemin

When His-AppAΔN was purified from the *E. coli* expression strain under native conditions, it was only very lightly colored, suggesting that only very low amounts of the tetrapyrrole cofactor were bound. Spectral analysis revealed a peak at around 410 nm (Figure 4.20A), as known for protein bound heme. It was reported that the heme

saturation increases when the expression cells are grown in the medium containing the δ-aminolevulinic acid (δALA), which is a heme precursor (Kery *et al.*, 1995; Smart & Bauer, 2006). Unfortunately, δALA did not significantly increase the binding of AppAΔN to heme, even though the *E. coli* expression cells were grown in the δALA-supplemented (final concentration: 10 mM) medium. After incubating the protein with hemin and removing any unbound cofactor by dialysis, the protein fraction showed absorbance at 411 nm as is typical for bound heme (Figure 4.20B). After adding sodium dithionite, the reduced form gave a spectrum with a Soret peak at 424 nm and absorption maximum at 556nm (Figure 4.20B). The reduced pyridine hemochrome gave a spectrum with peaks at 556 nm and 524 nm (Figure 4.20C). These data indicate that the bound heme is redox active. No significant absorbance was detected after reconstitution of the protein with vitamin B_{12} (Figure 4.20D) and the heme precursor protophorphyrin IX (data not shown).

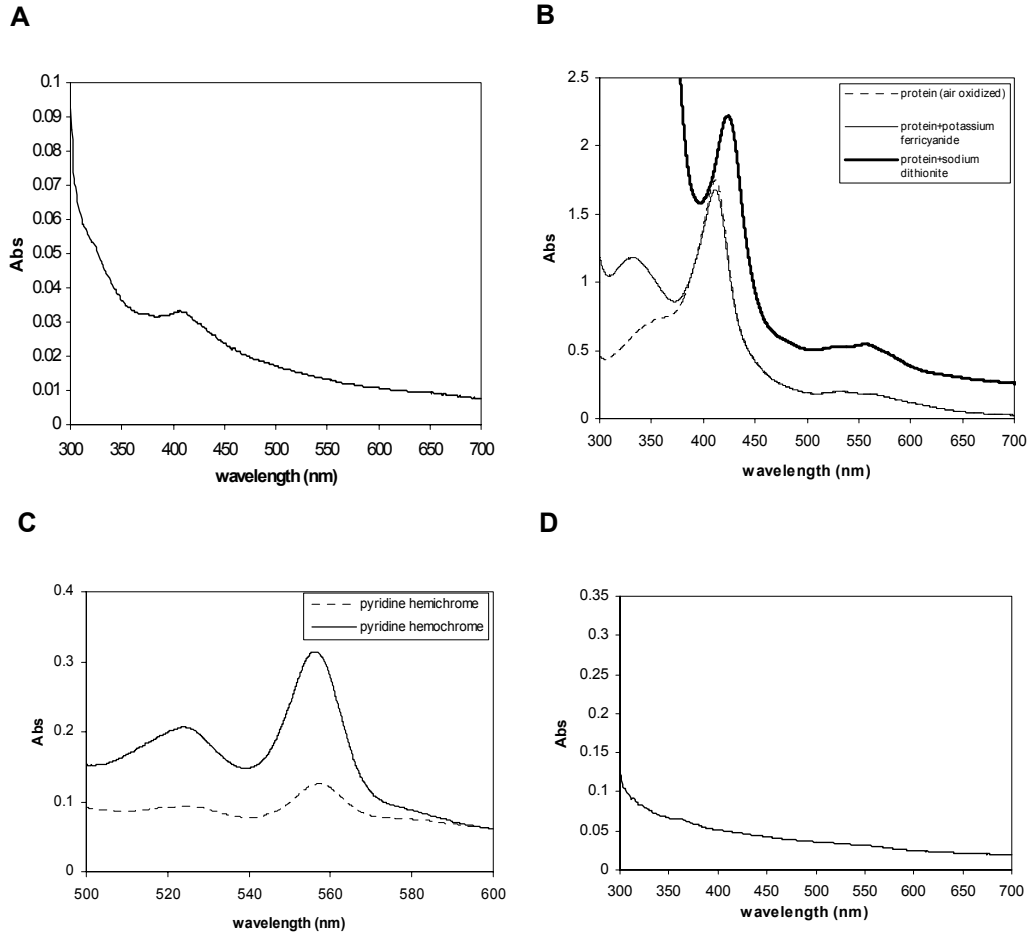

Figure 4.20 Absorption spectra of purified His-AppAΔN.

Spectra of purified His-AppAΔN before reconstitution **(A)** and reconstituted with hemin (**B**, dotted line). **(B)** Spectra of reconstituted His-AppAΔN in oxidized (thin line) and reduced (bold line) states. The oxidized spectra were measured upon the addition of potassium ferricyanide. The reduced spectra were measured upon the addition of sodium dithionite. **(C)** Spectra of pyridine hemichromoes (dotted line) and pyridine hemochromoes (thin line). **(D)** Spectra of purified His-AppAΔN incubated with vitamin B_{12}.

4.2.4.3 Binding of the C-terminal part of AppA to hemin-agarose or vitamin B_{12}-agarose

The heme-binding property of the C-terminal part of AppA (AppAΔN) was analyzed using hemin-agarose and vitamin B_{12}-agarose. After inducing overexpression in the *E. coli* strain JM109(pQEAppAΔN), the cells were sonicated in the storage buffer (Chapter 3.5.1). The cell extracts were incubated either with vitamin B_{12}-agarose or with hemin-agarose at 25°C for 1.5 hours with end-over-end rotation. As a control, cell extracts of the strain *E. coli* JM109(pQE30), which does not contain the *appA* gene, were also applied to both agaroses. After extensive washing, the agarose was loaded on an SDS gel. As shown in Figure 4.21A, the protein patterns were identical for extracts of the AppAΔN expressing strain and the control strain when applied to vitamin B_{12}-agarose. Very strong protein bands around 30 kDa in size were detected when the extract of the AppAΔN expression strain was incubated with hemin-agarose. These bands were missing when extracts of the control strain were applied. Western blot analysis confirmed that these bands indeed contain the C-terminal part of AppA (Figure 4.21B). Western blot also detected very low amounts of AppAΔN bound to the vitamin B_{12}-agarose (Figure 4.21B). Since both agaroses are based on the same matrix, it can be concluded that AppAΔN can specifically bind to hemin but not to the agarose. These results indicate that AppAΔN encompasses a heme binding domain, reflecting well the binding of the purified AppAΔN to hemin after reconstitution. To assure that binding of wild type AppAΔN to the hemin-agarose was not due to unspecific interaction of the His-tag to the column, the cell extract of *E. coli* JM109(pGEXAppAΔN), which expresses the GST-tagged AppAΔN, was also incubated with the hemin-agarose. The result showed that the GST-AppAΔN can also bind to the hemin-agarose (data not shown).

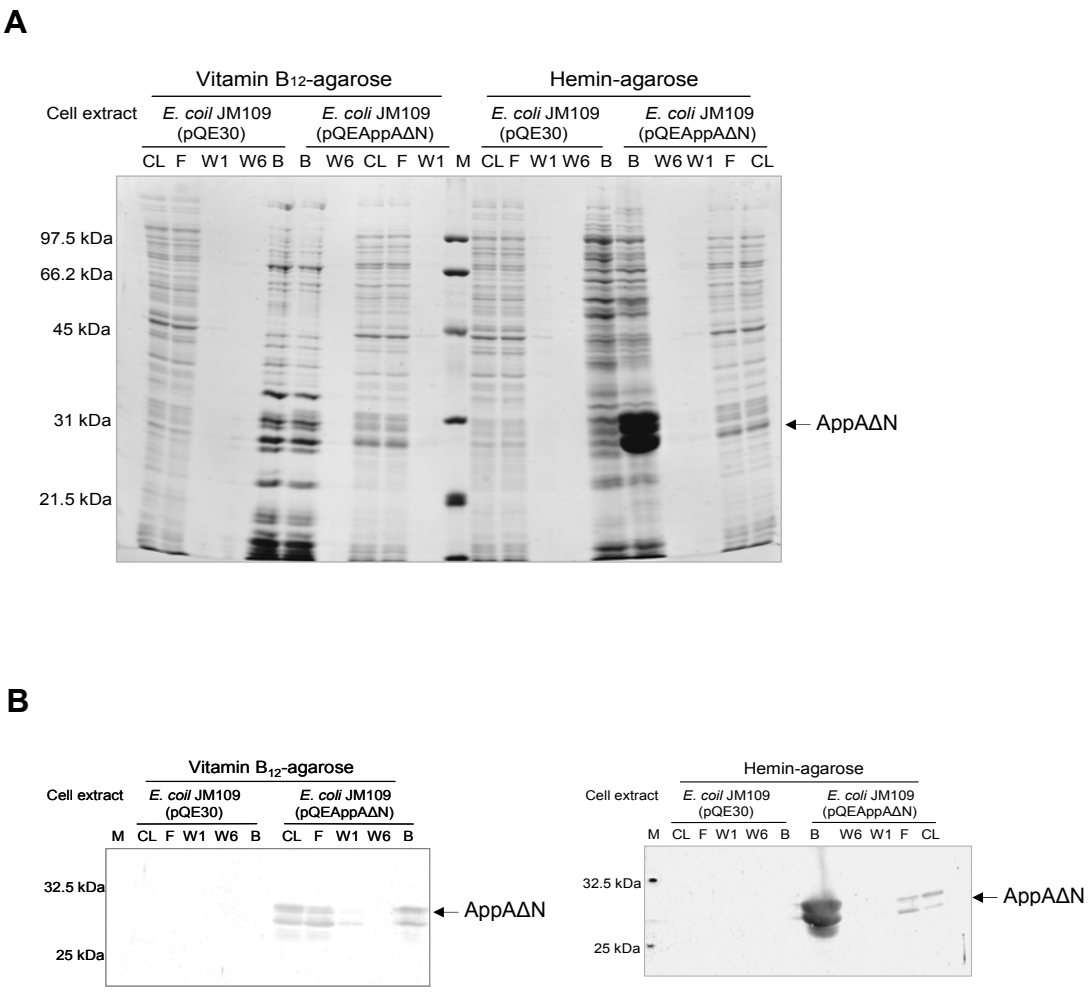

Figure 4.21 The C-terminal domain of AppA encompasses a heme binding domain.

1 ml cell extract containing 1 mg total protein was incubated with 40 µl vitamin B_{12}-agarose or hemin-agarose at 4°C for one hour. After extensive washing, the agarose was loaded on a 12% SDS-polyacrylamide gel, and the signals were analyzed by Coomassie blue staining **(A)** and Western blot **(B)** using an AppAΔN-specific antibody. The arrows indicate the expected size of AppAΔN. Abbreviations: M, molecular mass standards (also shown in the left of figures); CL, clear lysate before incubation; F, flow-through; W1, the first wash fraction; W6, the last wash fraction; B, agarose after extensive washing.

4.2.4.4 Heme strengthens the AppAΔN-PpsR interaction

To find out the role of heme in the binding of AppAΔN and PpsR, the interference of AppA with DNA binding of the PpsR protein was analyzed previously by gel retardation analysis in the presence of hemin. Unfortunately, hemin might affect the DNA-binding affinity of PpsR (Figure 4.18B). Therefore, the gel retardation analysis was further performed with His-AppAΔN which was reconstituted with hemin. When a 259 bp DNA fragment spanning the *puc* promoter region was incubated with increasing concentrations of GST-PpsR, the two retarded bands were observed in a native gel (Figure 4.22A). It

could be due to the facts that the DNA probe contains two consensus PpsR-binding sequences and that PpsR forms tetramers or dimers *in vitro* (Masuda and Bauer, 2002). When the DNA fragment (15.4 fmol) was incubated with 9 pmol of PpsR and increasing amounts of His-AppAΔN which was not reconstituted with hemin, a small increase in the amount of unbound DNA was observed (Figure 4.22B). When His-AppAΔN was reconstituted with hemin, the amount of shift 2 clearly decreased with increasing protein amount, while the amount of DNA in shift 1 and unbound DNA increased (Figure 4.22C). These *in vitro* data suggest that binding of heme strengthens the AppAΔN-PpsR interaction.

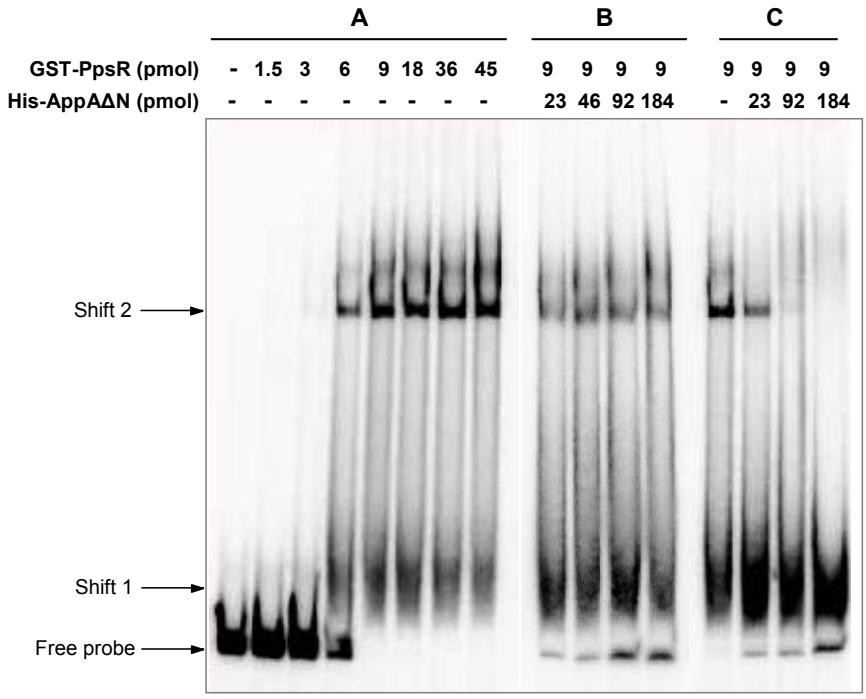

Figure 4.22 Heme strengthens the AppA-PpsR interaction.

Reduced PpsR (amount as indicated in the figure) was pre-incubated without AppAΔN or with AppAΔN at room temperature for one hour and then incubated for further 40min at 30°C with the ^{32}P-labeled *puc* DNA probe. The samples were then analyzed on a 4% native polyacrylamide gel. **(A)** PpsR can bind to the 259 bp *puc* promoter region. **(B)** PpsR was pre-incubated with AppAΔN which was not reconstituted with hemin. **(C)** PpsR was pre-incubated with AppAΔN which was reconstituted with hemin.

To test whether heme redox state affects the PpsR-binding affinity of AppAΔN, the DNA fragment spanning the *puc* promoter region was incubated with GST-PpsR, which was pre-incubated with reconstituted AppAΔN in the presence of $Na_2S_2O_4$. $Na_2S_2O_4$ can keep heme in a reduced state (Figure 4.20). The two incubation steps were performed in an anoxic box and the samples were analyzed in a native polyacrylamide gel. It was

supposed that AppAΔN with bound heme in reduced state exhibits higher affinity with PpsR. Surprisingly, the amount of shift1 and shift2 increased with increasing AppAΔN amount up to 92 pmol. When the amount of AppAΔN was more than 92 pmol, the decreasing shift1 amount was observed (Figure 4.23B). Comparing to the control experiment (Figure 4.23A), $Na_2S_2O_4$ appeared to inhibit the DNA-binding affinity of PpsR in the absence of AppAΔN. These results indicate that PpsR might also be a heme-binding protein which competes for the consumption of $Na_2S_2O_4$ with AppAΔN.

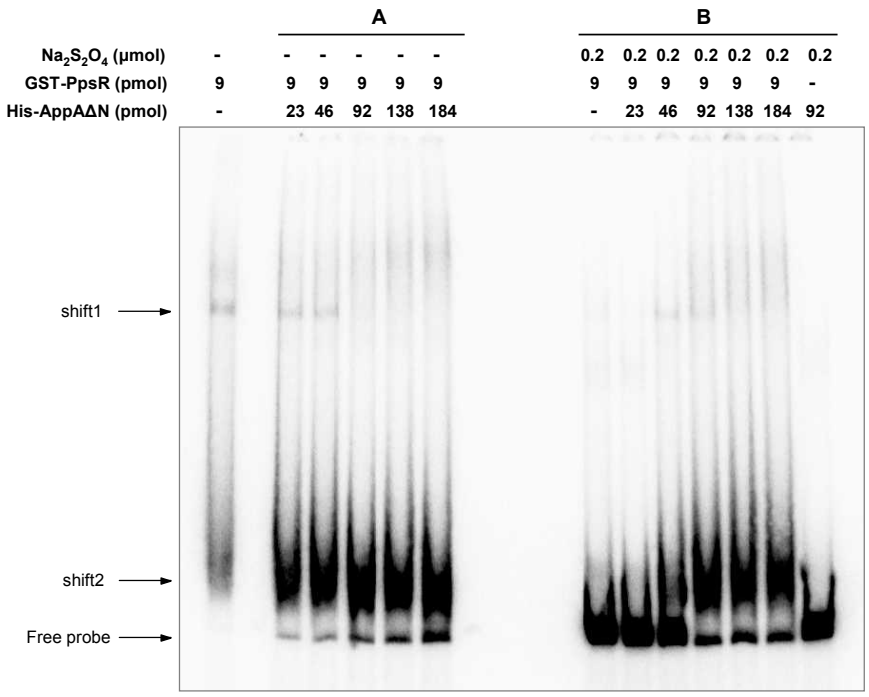

Figure 4.23 Influence of $Na_2S_2O_4$ in the binding of AppAΔN and PpsR.

Reduced PpsR (amount as indicated in the figure) was pre-incubated with reconstituted AppAΔN in the absence of $Na_2S_2O_4$ **(A)** or in the presence of $Na_2S_2O_4$ **(B)** at room temperature for one hour and then incubated for further 40min at 30°C with the ^{32}P-labeled *puc* DNA probe. Two incubation steps were performed in an anoxic box. The samples were then analyzed on a 4% native polyacrylamide gel.

4.2.4.5 Binding studies of PpsR and vitamin B_{12}-agarose or hemin-agarose

The central region of PpsR contains two PAS domains, which were reported to be critical for proper confirmation and repressor activity (Gomelsky *et al.*, 2000). Some PAS domains are found to bind the cofactor heme and to be involved in signal sensing and transduction (Gilles-Gonzalez and Gonzalez, 2004). However, it was not reported that PpsR purified after overproduction in *E. coli* contained any cofactor. To find out whether PpsR binds heme or not, the cell extracts of *E. coli* strains expressing the GST-PpsR were

also applied to either vitamin B_{12}-agarose or hemin-agarose. The Western blot using PpsR-specific antibody showed that PpsR can bind to very low amount of vitamin B_{12}-agarose and moderate amount of hemin-agarose (Figure 4.24), suggesting that PpsR may bind to hemin but not to vitamin B_{12}. Because PpsR was also detected in the last wash fraction after incubation with hemin-agarose and PpsR was not accumulated in a larger amount on the hemin-agarose compared to the amount of PpsR present in the clear lysate, it can not be excluded that the binding of PpsR to hemin-agarose is unspecific.

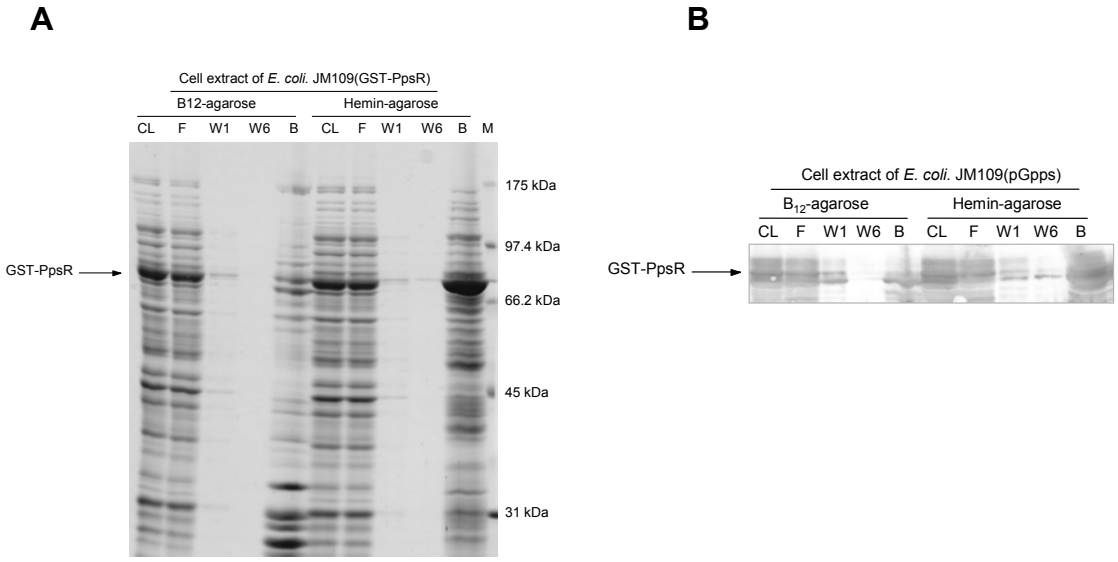

Figure 4.24 Binding studies of PpsR with vitamin B_{12} or heme.

1 ml cell extract containing 1 mg total protein was incubated with 40 µl vitamin B_{12}-agarose or hemin-agarose at 4°C for one hour. After extensive washing, the agarose was loaded on a 10% SDS-polyacrylamide gel, and the signals were analyzed by Coomassie blue staining **(A)** and Western blot **(B)** using a PpsR-specific antibody. Abbreviations: M, molecular mass standards (also shown in the right of figure); CL, clear lysate before incubation; F, flow-through; W1, the first wash fraction; W6, the last wash fraction; B, agarose after extensive washing.

4.2.5 Identification of a heme binding site in AppA

AppA can sense both light and redox signals and antagonize the repressor activity of PpsR through interaction with PpsR. The previous results suggested that the interaction site of AppA and PpsR is located in the C-terminal domain of AppA. Moreover, the gel mobility shift analysis showed that the C-terminal domain of AppA is sufficient to release PpsR from the DNA fragment (Chapter 4.2.3). The binding studies suggested the C-terminal domain of AppA carries cofactor heme as redox prosthetic group. Since the cysteine-rich domain of AppA is not involved in the light- and redox-dependent

regulation, the heme-binding site should not be located in this region. Therefore, the mutagenesis was performed in the C-terminal part of AppA except the cysteine-rich domain in order to find out the heme-binding site.

4.2.5.1 Construction and phenotype of strain APP11(pRK*appA*ΔM) expressing the AppA protein lacking heme-binding domain

A *Hin*dIII-*Sph*I DNA fragment, containing the promoter region of *appA* and the DNA fragment encoding the N-terminal BLUF domain of AppA, was amplified by PCR using primers AppA_up and AppASph (Table 2.4) and cloned into the *Hin*dIII and *Sph*I sites of vector pRK415, resulting in plasmid pRKAPBLUF. The DNA fragment encoding the cysteine-rich domain was amplified by PCR using primers AppACSph and AppA_down (Table 2.4) and cloned into the *Sph*I and *Kpn*I sites of plasmid pRKAPBLUF, creating plasmid pRK*appA*ΔM. This plasmid was conjugated into the *appA*$^-$ strain *R. sphaeroides* APP11, resulting in strain APP11(pRK*appA*ΔM). This strain expresses a shorter AppA protein with deletion of amino acids 135-378. The cells are unpigmented and the amount of BChl is 0.016 ± 0.006 μM/OD_{660}, which is slightly higher than that in the strain APP11 (0.004 ± 0.002 μM/OD_{660}) and much lower than that in the strain APP11(p484-Nco5) (0.69 ± 0.04 μM/OD_{660}) which expresses wild-type AppA. Strain APP11(pRK*appA*ΔM) exhibits similar spectroscopic characteristic to that of the negative control strain APP11 (Figure 4.28). All these phenotypes indicate that the middle part of AppA (amino acids 135-378) is essential for the function of AppA.

4.2.5.2 Strategies of mutagenesis

Random mutagenesis of the *appA* central part (nucleotides 403-1134, *i.e. appA* codons 135-378) was performed by error-prone PCR using primers: AppAL and AppAR (Table 2.4). The pool of PCR products was used to in-frame replace the original wild type sequence. The resulting 1.95 kb-DNA fragments, containing the full length *appA* gene pool and the promoter region of *appA*, were cloned into the *Hin*dIII and *Kpn*I sites of vector pRK415, creating plasmids pRK*appA*RM (Figure 4.25A). These plasmids were conjugated into the *appA*$^-$ strain *R. sphaeroides* APP11.

The site-directed mutagenesis was performed by overlap PCR according to standard protocols (Sambrook and Russell, 2001) shown in Figure 4.25B. The 1.95 kb *Hin*dIII-*Kpn*I DNA fragment, containing the full length *appA* gene with desired mutations and the

appA promoter region, were cloned into vector pRK415. The consequent plasmid was conjugated into the *appA*$^-$ strain *R. sphaeroides* APP11.

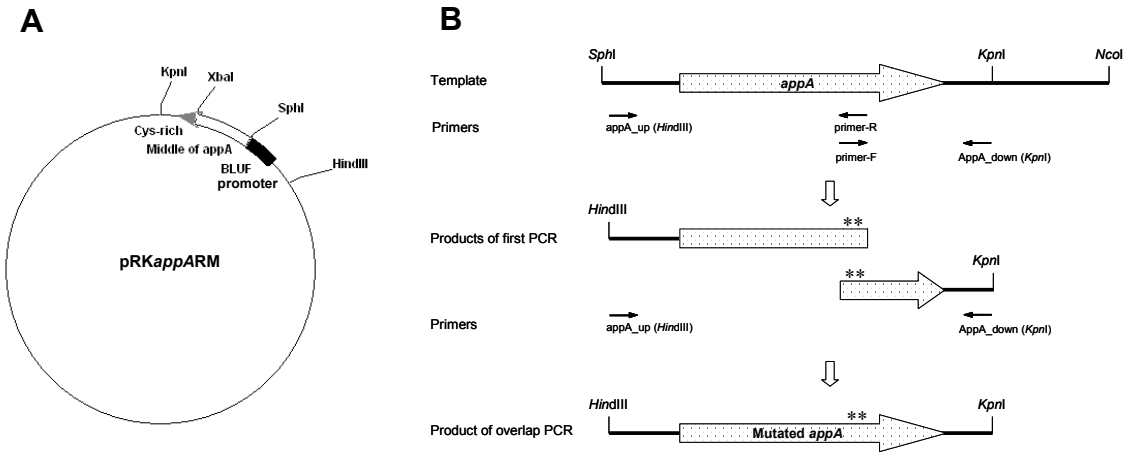

Figure 4.25 Mutagenesis strategies.

(A) Map of plasmid pRK*appA*RM. The middle part of *appA* (nucleotides 403-1134) was in-frame replaced by the pool of error-prone PCR products (*Sph*I-*Xba*I fragments); **(B)** Site-directed mutagenesis of *appA* by overlap PCR. A 2.5 kb *Sph*I-*Nco*I fragment from plasmid p484-Nco50 was used as template, which contained the *appA* promoter region followed by a wild-type *appA* sequence. The primer-F and primer-R contained the mutations and they were exactly complementary to each other. The 1.95 kb *Hin*dIII-*Kpn*I product was cloned into vector pRK415. The stars in the figure represent the mutation sites.

4.2.5.3 Identification of strains expressing AppA variants

The transconjugants constructed by the random mutagenesis were analyzed in regard to the color of the colonies. Colonies that exhibited a color, which was clearly different from that of the control strain App11(p484-Nco5) (dark red) and from the majority of the transconjugants (Figure 4.26), were selected for further analysis. The *appA* sequence was confirmed by *in situ* hybridization. The site of mutation was identified by DNA sequencing and the amino acid exchanges for the individual strains are listed in Table 4.2. The candidate strains were grown at low oxygen tension ($pO_2 \approx 3$ µM) and the BChl contents were quantified. All selected strains accumulated less BChl at low oxygen tension than the control strain having wild type *appA* on a plasmid (Figure 4.27A & B). The absorbance spectra of RM3 (L292R/A349V/P357L), RM9 (V306A/A349V/P357L), RM12 (V307G/A349V/P357L) and RM13 (S348P/A349V/P357L) are similar to the negative control strain APP11 (Figure 4.28). In strain RM14 (P282Q/A314V), RM17 (I263T/A349V/P357L) and RM21 (L204P/Q257R), the absorption at 800 nm, 850 nm and 875 nm is much lower than that of the positive control strain APP11(p484Nco5)

(Figure 4.28), suggesting that these strains form less photosynthetic apparatuses than the wild-type-like strain.

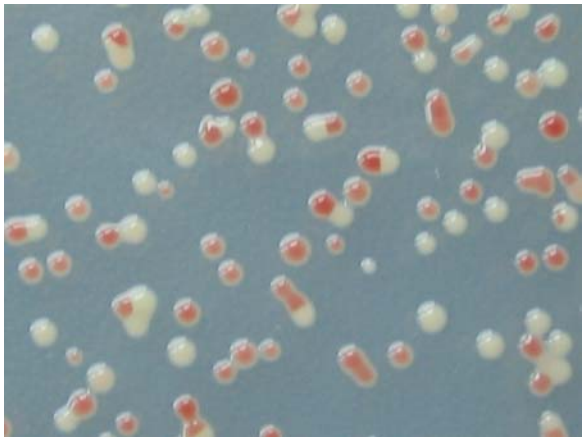

Figure 4.26 Colonies of strains expressing AppA variants.

The mixture of the transconjugants was spread on the RÄ-agar plate and incubated at 32°C in dark for three days. (Photographed by Andreas Jäger)

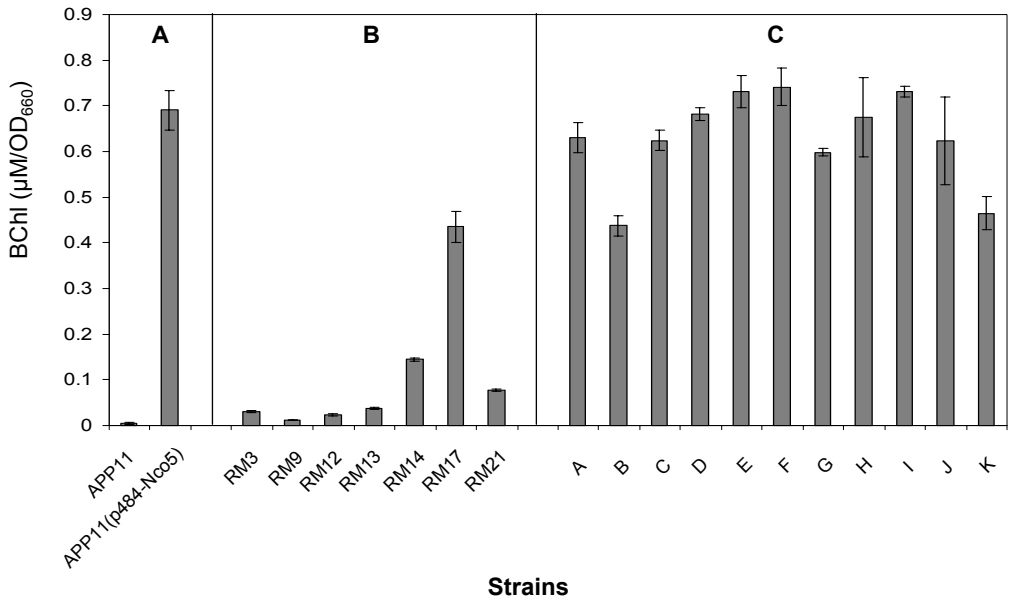

Figure 4.27 Relative bacteriochlorophyll (BChl) concentrations of strains expressing AppA variants.

Relative BChl concentrations shown represent the mean and standard deviation of three independent measurements of cultures grown in low oxygen ($pO_2 \approx 3$ µM). **(A)** APP11 as negative control and APP11(p484-Nco5) as positive control; **(B)** AppA variants screened after random mutagenesis; **(C)** AppA variants constructed by site-directed mutagenesis. For strain description, refer to Table 4.2.

All *appA* sequences in the selected strains harbored more than one amino acid exchange. Remarkably, all these exchanges clustered in a domain spanning from amino acid 204 to amino acid 357. The Pfam data base identified the amino acid sequence 274 to 393 from

AppA as a putative vitamin B_{12} binding domain. It is also suggested that this domain binds another tetrapyrrole like heme (Chapter 4.2.4), which is known to be involved in redox sensing by other proteins, like FixL, *Ec*Dos, *Ax*PDEA1 (Gilles-Gonzalez and Gonzalez, 2004).

Table 4.2 Redox- and light-dependent *puf* and *puc* expression in strains expressing AppA variants.

	Strain	Characteristics of AppA	Expression level		Redox regulation		Blue light effect	
			puf	*puc*	*puf*	*puc*	*puf*	*puc*
I	APP11	null AppA	+	n.d.	+++	+[a]	-	n.d.
	APP11(p484-Nco5)	AppA(without mutation)	+++	+++	+++	+++	+++	+++
II	RM3	L292R, A349V, P357L	+	+	+++	++	-	-[a]
	RM9	V306A, A349V, P357L	+	n.d.	+++	+[a]	-	-[a]
	RM12	V307G, A349V, P357L	+	+	+++	+++	-	-[a]
	RM13	S348P, A349V, P357L	+	n.d.	+++	+[a]	+	n.d.
	RM14	P282Q, A314V	++	+	+++	+[a]	-	n.d.
	RM17	I263T, A349V, P357L	++	++	+++	+	++	++
	RM21	L204P, Q257R	++	+	+++	+[a]	-	-[a]
III	A	L204P	+++	+++	+++	+++	+++	+++
	B	P282Q	++	++	+++	+++	++	++
	C	P357L	+++	+++	++	+++	+++	+++
	D	S348P	+++	+++	++	+++	+++	+++
	E	A349V	+++	+++	++	+++	+++	+++
	F	V306A	+++	+++	++	++	++	+++
	G	V307G	+++	++	+++	+++	+++	+++
	H	A314V	+++	+++	++	+++	+++	+++
	I	A349V, P357L	+++	+++	++	+++	+++	+++
	J	V306A, P357L	+++	+++	++	+++	+++	+++
	K	V306A, A349V	++	++	+++	+++	+	++

The parental strain APP11 is impaired in the production of photosynthetic complexes because of an insertional inactivation of the chromosomal *appA* gene (Gomelsky and Kaplan, 1995). The sites of mutation in each AppA variant are shown in the table. The *puf* and *puc* mRNA expression levels in control strains (I), AppA variants screened after random mutagenesis (II) and AppA variants constructed by site-directed mutagenesis (III) were monitored by Northern blot analyses from the cultures grown in low oxygen ($pO_2 \approx 3\mu M$) at OD_{660} within 0.7–0.9. Redox- and light-dependent *puf* and *puc* transcript levels were also monitored by Northern blot analyses except the ones marked by "a" at the top right corner, which were monitored by semi-quantitative RT-PCR. All the expression levels and regulation effects were normalized by the positive control strain APP11(p484-Nco5), for which the expression levels and regulation effects were set as 100%. +++, more than 70%; ++, 30% to 70%; +, less than 30%; -, no effect; n.d., no detectable signal by Northern blot analysis.

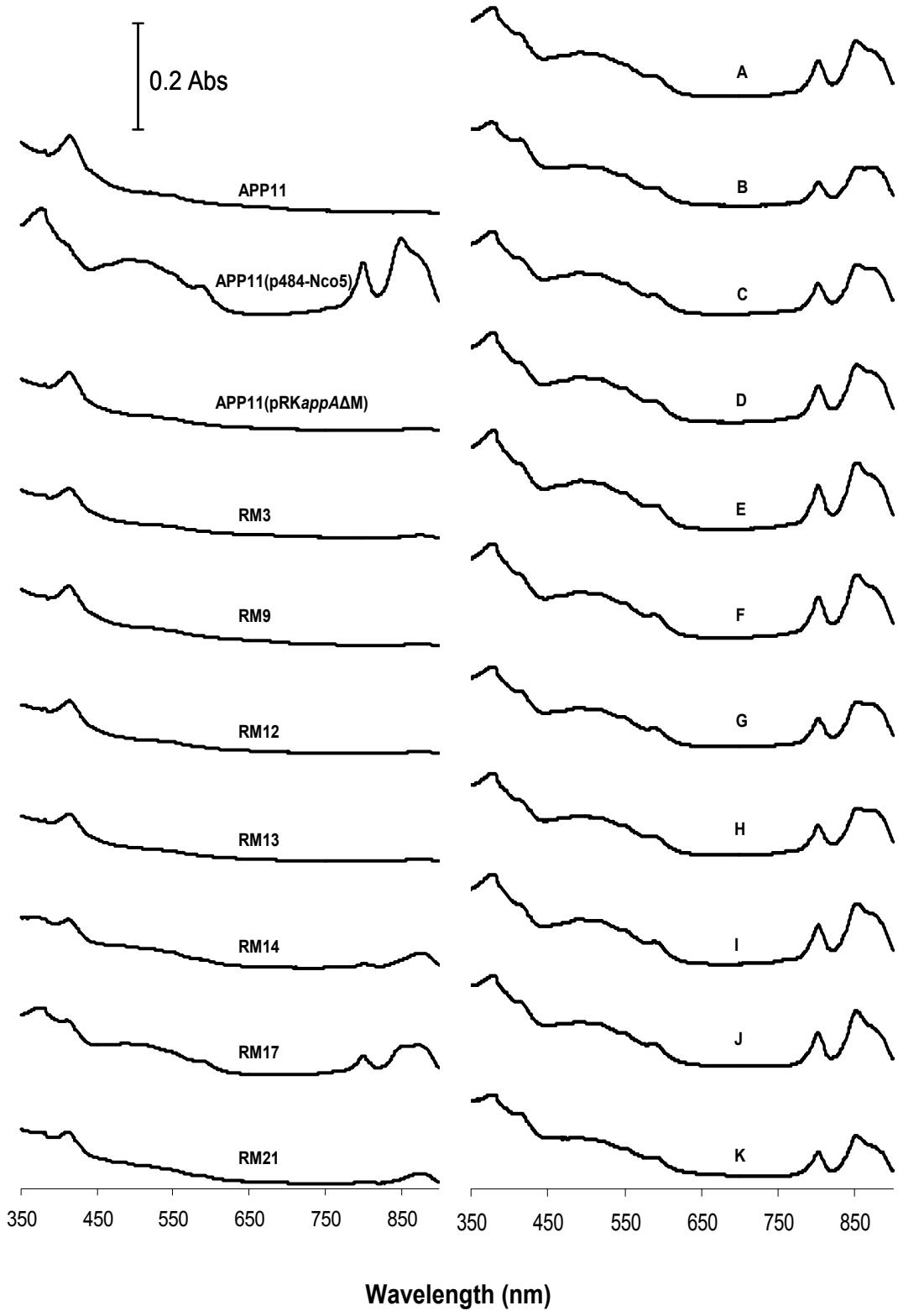

Figure 4.28 Absorbance spectra of the cell extracts from exponentially grown APP11 derived strains under low oxygen tension ($pO_2 \approx 3$ µM).

The absorbance maximum of BChl associated with the light harvesting complex (LH) I is 875 nm, and those of BChl associated with the LH II complex are 800 and 850 nm. Colored carotenoids absorb in the maxima of 450 to 550 nm. For strain description, refer to Table 4.2

Based on the identified amino acid exchanges, further AppA variants were constructed by site-directed mutagenesis. For all amino acid exchanges observed in variants obtained by random mutagenesis in combination with other amino acid exchanges, the variants containing only a single amino acid exchange were constructed by site-directed mutagenesis. The variants having two of the three amino acid exchanges, which were observed in mutants stemming from random mutagenesis, were also constructed. All these mutants had considerably higher BChl content than the strains selected after random mutagenesis (Figure 4.27C). The spectroscopic characteristics of these strains are similar to those of control strain APP11(p484-Nco5), except that the absorption at 850 nm of the cell extracts from strain B (P282Q) and G (V307G) is lower than that of other strains (Figure 4.28). In strain K (V306A/A349V), both absorbance maximum of BChl associated with the LH I and that of BChl associated with the LH II complex are lower than in control strain APP11(p484Nco5) (Figure 4.28), indicating that strain K form less photosynthetic apparatus than the control strain. In other proteins a His residue was shown or predicted to be involved in tetrapyrrole binding (Gilles-Gonzalez and Gonzalez, 2004; Sato *et al.*, 2004; Ebihara *et al.*, 2005). Therefore, the His at position 284 of AppA was exchanged to Ala, but no any significant change in phenotype was observed in comparison of this mutant and the control strain.

4.2.5.4 Redox regulation of PS genes in strains expressing AppA variants

For all mutant strains listed in Table 4.2, the redox dependent expression of the *puf* and *puc* operons, which encode pigment binding proteins, were determined by either Northern blot or semi-quantitative RT-PCR. Two PpsR binding sites are localized upstream of the *puc* operon (Choudhary and Kaplan, 2000). Thus, *puc* genes are under direct control of the AppA/PpsR system. No PpsR binding sites are found in close proximity of the *puf* promoter, even though several studies revealed AppA/PpsR dependent expression of *puf* (Braatsch *et al.*, 2002; 2004; Moskvin *et al.*, 2005 and Chapter 4.3.1). All strains were cultivated under high oxygen tension (200 μM) and then shifted to growth under low oxygen tension. Cells were harvested at the time of transition, 90 and 180 min after the oxygen shift and *puf* and *puc* mRNA levels were quantified by Northern blot hybridization. In some mutants *puc* expression was too low for Northern blot quantification (Table 4.2 and Figure 4.29). For those strains, *puc* mRNA levels were quantified by semi-quantitative RT-PCR at the annealing temperature of 59°C using primers Puc2AB-F and Puc2AB-R (Table 2.4).

As shown for some representative strains in Figure 4.29 and as summarized in Table 4.2, all strains that were selected after random mutagenesis of the *appA* central part (nucleotides 403-1134 from the start codon of *appA*) showed very low *puc* mRNA levels, even after shifting the cells to low oxygen. Low *puc* mRNA levels and moderate to strong increases in the transcript level were observed after the reduction of oxygen tension for some strains (*e.g.* RM3, RM12, RM14, RM17, and RM21). For those strains with very low *puc* mRNA levels, semi-quantitative RT-PCR was performed to detect *puc* mRNA (*e.g.* RM9 and RM13). This revealed that *puc* mRNA levels in these strains increase after a shift to low oxygen tension, although the total level remains very low. At low oxygen tension, all these strains showed *puf* mRNA levels which were reduced by more than 50% compared to the control strain APP11(p484-Nco5) expressing the wild type *appA* gene from a plasmid. The *puf* mRNA levels in the mutants, however, were less affected than *puc* mRNA levels. All mutants showed a strong increase in *puf* mRNA levels after the reduction of oxygen tension, which was also observed in control cells.

All strains harbouring *appA* sequences with only a single amino acid exchange accumulated similar *puf* mRNA levels and only moderately reduced *puc* mRNA levels. These strains showed similar redox regulation compared to the control strain expressing the wild type *appA* gene from a plasmid. The same was observed for the double mutants I (A349V/P357L), J (V306A/P357L), and K (V306A/A349V).

4.2.5.5 Blue light dependent regulation of PS genes in strains expressing AppA variants

At high oxygen tension, the PpsR protein represses transcription of PS genes. When the oxygen tension drops to 104 ± 24 µM or below, the AppA protein releases PpsR repression in dark grown cultures (Gomelsky and Kaplan, 1997; Braatsch *et al.*, 2002). In the presence of blue light, however, AppA does not interfere with the repressing effect of PpsR (Braatsch *et al.*, 2002; Masuda *et al.*, 2005b; Happ *et al.*, 2005). We quantified *puf* and *puc* mRNA levels in *R. sphaeroides* strains expressing the different AppA variants after blue light illumination of cultures grown at 104 ± 24 µM oxygen. Results for some representative strains are shown in Figure 4.29 and results for all strains are summarized in Table 4.2. All strains that expressed AppA proteins with only one amino acid exchange and the double mutants I (A349V/P357L), J (V306A/P357L), and K (V306A/A349V) showed blue light dependent repression of *puf* and *puc* genes similar to that observed in control strains. Some of the strains, which express AppA variants with three amino acid

exchanges and show only very low *puc* mRNA levels, failed to show blue light inhibition of *puf* expression: RM3 (L292R/A349V/P357L), RM9 (V306A/A349V/P357L) and RM12 (V307G/A349V/P357L). The same was observed for the double mutant RM14 (P282Q/A314V) and RM21 (L204P/Q257R). Two of the AppA variants with three amino acid exchanges were able to support blue light repression of *puf* genes, even though *puc* mRNA levels were quite low: RM13 (S348P/A349V/P357L) and RM17 (I263T/A349V/P357L). AppA variants that resulted in light-independent *puf* or *puc* expression still showed redox regulation, even though total *puf* and *puc* mRNA levels were reduced.

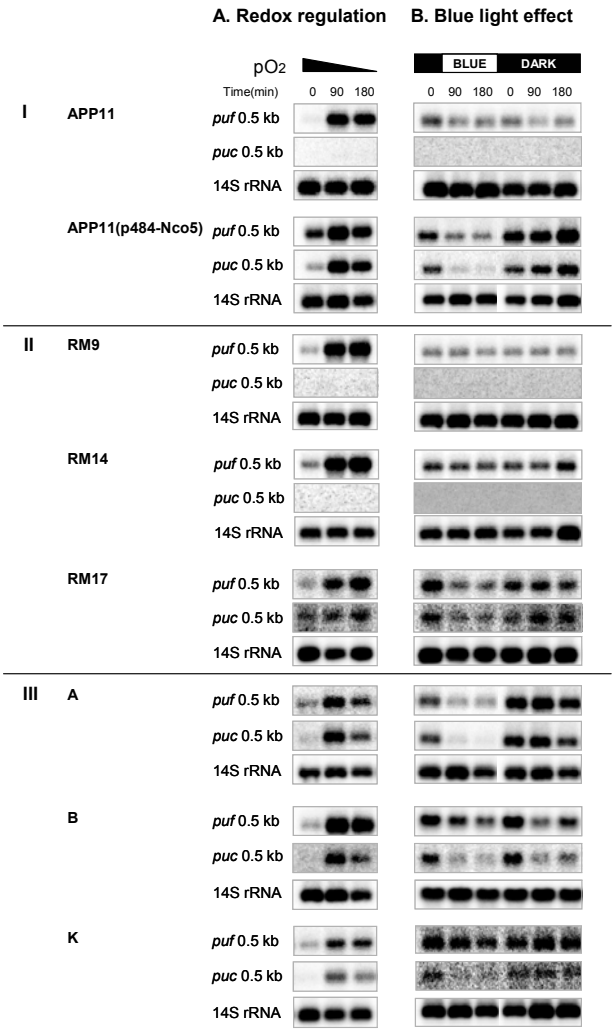

Figure 4.29 *puf* and *puc* expression in strains expressing representative AppA variants.

Kinetics of *puf* and *puc* expression in control strains (I), AppA variants screened after random mutagenesis (II) and AppA variants constructed by site-directed mutagenesis (III). Total RNA was isolated at indicated time points, and *puf* and *puc* transcript levels were monitored by RNA gel-blot analysis. A 14S rRNA-specific probe was used as internal standard. **(A)** The cells were cultivated under high oxygen tension ($pO_2 \approx 200$ µM) and then shifted to growth under low oxygen tension ($pO_2 \approx 3$ µM) when the optical densities of the cultures at 660 nm were around 0.12. **(B)** Cells were grown at 104 ± 24 µM dissolved oxygen and shifted from the dark into blue light at time point zero or kept in the dark.

4.2.6 Expression levels of *appA* and *ppsR* in strains expressing AppA variants

4.2.6.1 Protein levels of AppA in strains expressing AppA variants

The *puf* and *puc* expression and redox- and light-dependent regulation in strains RM3 (L292R/A349V/P357L) and RM9 (V306A/A349V/P357L) were very similar to the low expression levels in strain App11, which does not express AppA. This could be due to the malfunction of AppA variants or to low expression levels of these AppA variants. Therefore, the AppA levels in the different strains were tested by Western blot analysis. The AppA variants could not be detected in strains RM3, RM9, RM12 and RM13 (Figure 4.30). The protein levels detected by the AppA-specific antibody in strain RM14 and RM21 were moderately reduced compared to the positive control strain APP11(p484-Nco5). This could be due to the facts that i) the AppA variants are produced in different amount in the mutants, ii) these mutant proteins are highly unstable in comparison of wild-type AppA, or iii) these AppA variants are folded differently and not detected by the antibody. For the strains constructed by site-directed mutagenesis, no significant difference of AppA levels was detected.

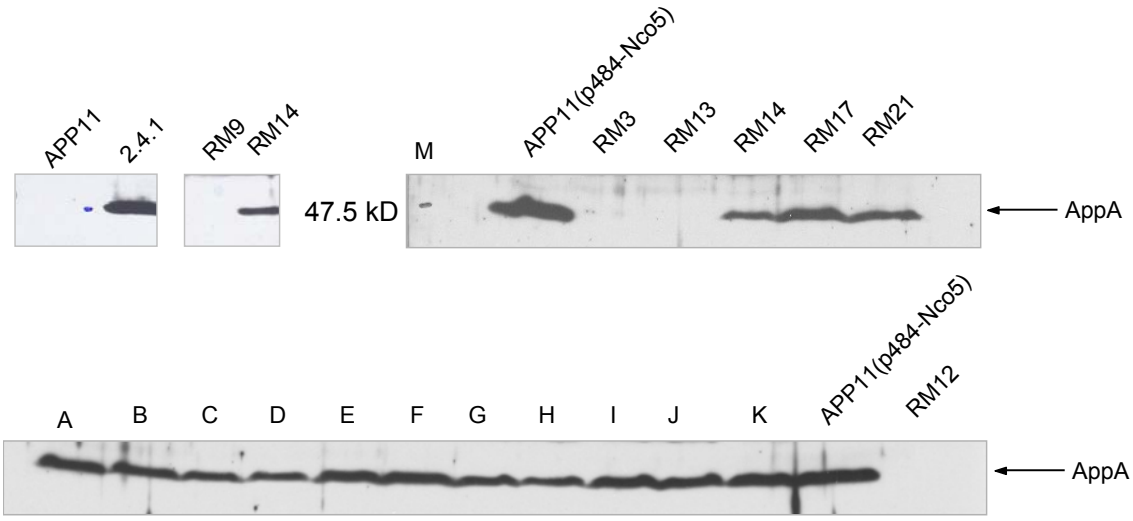

Figure 4.30 Protein levels of AppA in strains expressing AppA variants.

Cells grown under low oxygen conditions ($pO_2 \approx 3$ µM) were collected at an optical density of 0.8 at 660 nm. Each cell free extract containing 50 µg total proteins was loaded on the 10% SDS-polyacrylamide gel, and the AppA protein levels were determined by Western blot analysis using an AppA-specific antibody, which was raised in rabbit against the gel-purified His-AppAΔN (Chapter 4.2.4).

4.2.6.2 *appA* and *ppsR* mRNA levels in strains expressing AppA variants

The lower protein levels of AppA could be due to lower transcription levels. Therefore, the *appA* and *ppsR* mRNA levels in strains 2.4.1, APP11(p484-Nco5), RM9 and RM14 were quantified by semi-quantitative RT-PCR at the annealing temperature of 59°C using primer pair appA403F/appA755R (Table 2.4) for *appA* and primer pair ppsR-F/ppsR-R (Table 2.4) for *ppsR*. The result showed no significant differences in *appA* and *ppsR* mRNA levels among the tested strains (Figure 4.31). Therefore, it can be concluded that the *appA* and *ppsR* transcription levels are similar in strains 2.4.1, APP11(p484-Nco5), RM9 and RM14.

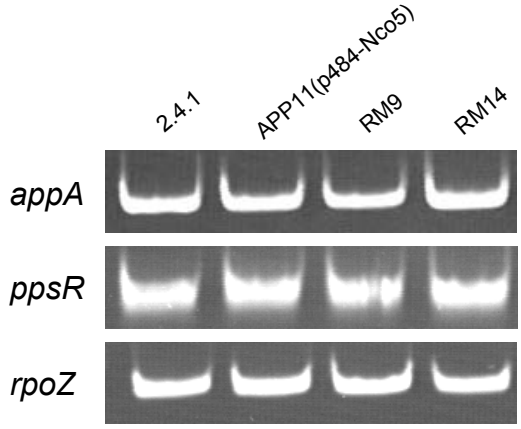

Figure 4.31 *appA* and *ppsR* mRNA levels in strains expressing AppA variants.

Cells grown under low oxygen conditions ($pO_2 \approx 3$ µM) were collected at an optical density of 0.8 at 660 nm. Total RNA was isolated. *appA* and *ppsR* transcript levels were monitored by semi-quantitative RT-PCR analysis. *rpoZ* transcript level was used as internal standard.

4.2.6.3 Stability of AppA in strains expressing AppA variants

The lower protein levels of AppA in the strains constructed by random mutagenesis could also be due to the fact that the protein is highly unstable. Hence, the stability of AppA for strains 2.4.1, APP11(p484-Nco5) and RM14 was checked after blocking translation by chloramphenicol. However, no significant difference in AppA turn-over was detected by Western blot (Figure 4.32).

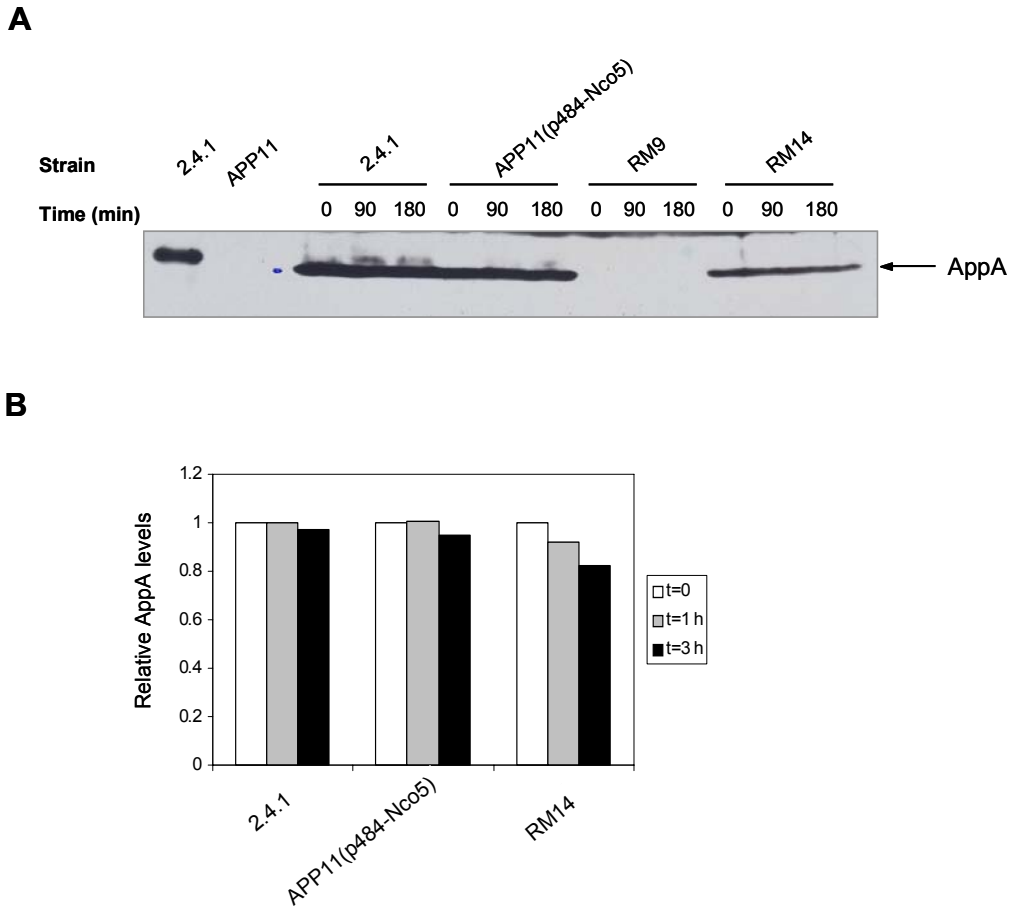

Figure 4.32 Stability of AppA in strains expressing AppA variants.

Chloramphenicol (500 µg/ml) was added at time point zero. **(A)** Cells were harvested at the indicated times and each cell free extract containing 50 µg total proteins was loaded on the 10% SDS-polyacrylamide gel. The AppA protein levels were determined by Western blot analysis using an AppAΔN-specific antibody. **(B)** The intensities of AppA signals were quantified and normalized to the intensities of AppA signals at time point zero (= 1, open bars).

4.2.6.4 Affinities between AppA variants and the AppAΔN-specific antibody

As shown above, the AppA protein levels are quite different in strains APP11(p484-Nco5), RM9 and RM14 (Figure 4.30), while the RT-PCR analysis showed that the *appA* transcription levels are similar in these strains (Figure 4.31). The possibility that different AppA protein levels are due to the different stability of AppA variants could also be excluded (Figure 4.32). The other possibility could be that the protein is folded differently and not detected by the antibody. To explore this possibility, the AppAΔN variants AppAΔN9(V306A/A349V/P357L) and AppAΔN14(P282Q/A314V) were expressed in *E. coli*. The 0.76 kb *Bgl*II-*Sma*I DNA fragments, containing *appA* codons 197-450 with the mutation sites, were amplified by PCR using primers DeltaNup and DeltaNdown (Table 2.4) and cloned into the *Bam*HI and *Sma*I sites of vector pQE30. The recombinant plasmids designated pQEAppAΔN9 and pQEAppAΔN14, respectively, were transformed

into *E. coli* JM109. Then His-AppAΔN9 and His-AppAΔN14 were produced in *E. coli* JM109(pQEAppAΔN9) and *E. coli* JM109(pQEAppAΔN14), respectively, induced at 17°C overnight with 0.5 mM IPTG. The Western blot analysis was performed after partial purification using an AppAΔN-specific antibody, which was raised in rabbit against the wild-type His-AppAΔN. It was observed that AppAΔN9 and AppAΔN14 were not detected by this AppAΔN-specific antibody, even though they were visible after staining (Figure 4.33). This strongly suggests that amino acid exchanges in the C-terminal part of AppA cause a structural change of AppA. Previously, the Western blot showed that the mutants contain variable amounts of AppA (Figure 4.30), while the *appA* expression levels are quite similar in those strains (Figure 4.31). Since the AppA variants were not detectable by the antibody used for Western blot, this suggests that the different amounts of AppA detected by Western blot were not due to different amounts of protein expressed in those mutants, but due to the misfolding of proteins and their low affinities with the antibody.

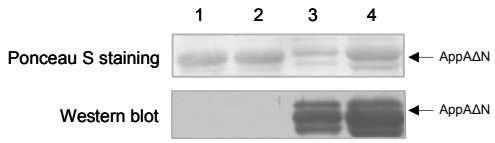

Figure 4.33 Affinities between AppA variants and the AppAΔN-specific antibody

5 µg AppAΔN9 (lane 1), 5 µg AppAΔN14 (lane 2), 2.5 µg AppAΔN (wild type, lane 3) and 5 µg AppAΔN (wild type, lane 4) were loaded on a 12% SDS-polyacrylamide gel and transferred on a nitrocellulose membrane. The signals were analyzed by Ponceau S staining (upper panel) and Western blot (lower panel) using an AppAΔN-specific antibody.

4.2.7 Binding of AppA variants to hemin-agarose

To test the heme-binding activity of AppAΔN mutant proteins, the cell extracts of *E. coli* strains expressing the AppAΔN variants AppAΔN9 and AppAΔN14 were also incubated with hemin-agarose. As seen in Figure 4.34, no significant amounts of mutated AppAΔN were bound to the agarose, suggesting that the mutant AppAΔN proteins can not bind significant amounts of heme, in contrast to the wild type protein (Figure 4.21). Therefore, the mutations in AppAΔN9 and AppAΔN14 are important for the heme-binding.

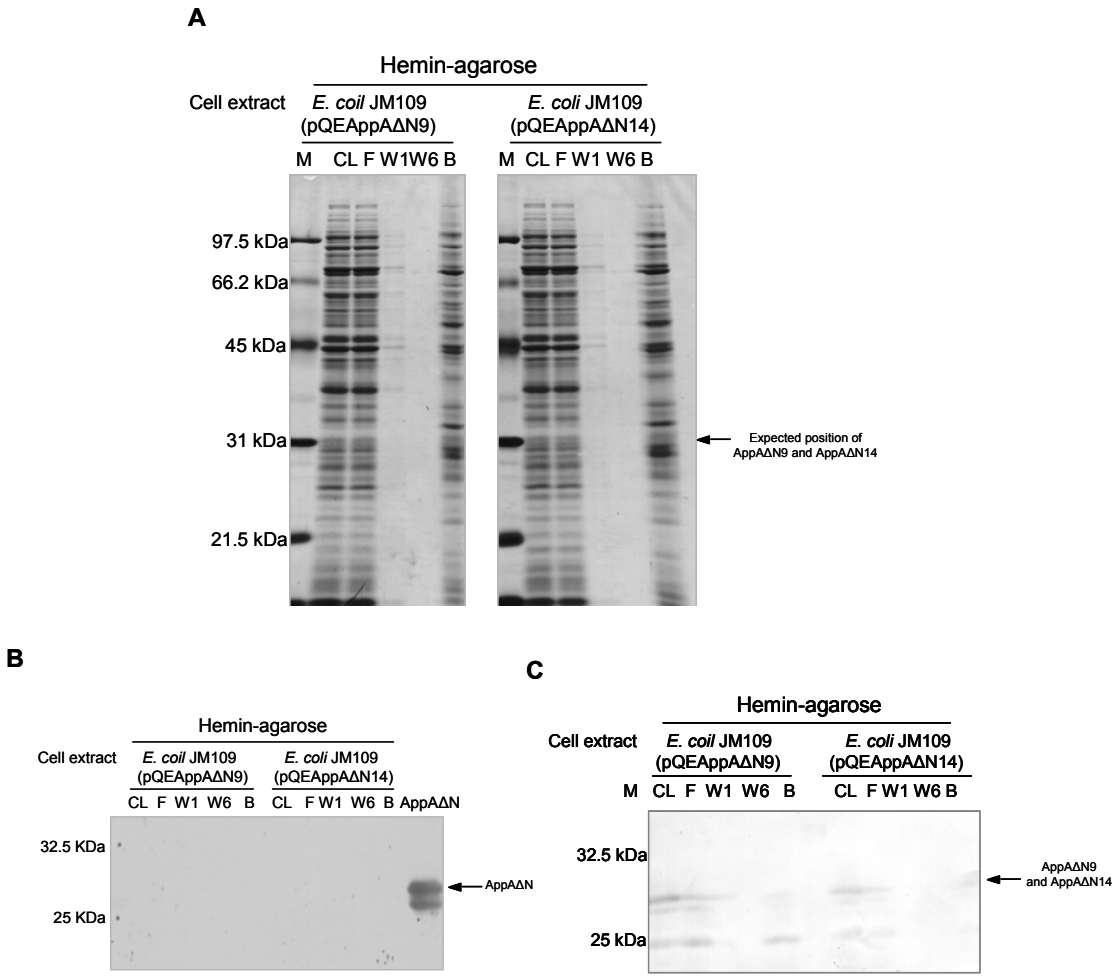

Figure 4.34 AppAΔN9 and AppAΔN14 lose the ability to bind heme.

1 ml cell extract containing 1 mg total protein was incubated with 40 µl hemin-agarose at 4°C for one hour. After extensive washing, the agarose was loaded on a 12% SDS-polyacrylamide gel, and the signals were analyzed by Coomassie blue staining **(A)** and Western blot using an AppAΔN-specific antibody **(B)** or a His-tag-specific antibody **(C)**. The arrows indicate the expected size of AppAΔN. Abbreviations: M, molecular mass standards (also shown in the left of figures); CL, clear lysate before incubation; F, flow-through; W1, the first wash fraction; W6, the last wash fraction; B, agarose after extensive washing.

4.2.8 SPR-based determinations of the BLUF-AppAΔN interaction and the PpsR-AppAΔN interaction

To better understand how light signals are transmitted from the BLUF domain to the C-terminal part of AppA (AppAΔN), and how changes in the light or redox signals from the C-terminal part of AppA affect the binding of AppA to PpsR, the BLUF-AppAΔN interaction and the PpsR-AppAΔN interaction were studied by the pull-down assays. But the results were unclear because i) the solubilities of these proteins were too low for the assays; or ii) the proteins can unspecifically bind the matrix (data not shown). Using

surface plasmon resonance (SPR)-based technique allows to study protein-protein interactions at much lower concentration. Another advantage of SPR spectroscopy is the ability to obtain kinetic data, *i.e.* the microscopic rate constants for an interaction between macromolecules.

4.2.8.1 Expression and purification of the BLUF domain

The protein AppAΔN (Chapter 4.2.4), BLUF and PpsR (Chapter 4.2.2) and were purified from *E. coli* cells and used in the SPR-based interaction analysis. For overexpression the BLUF domain, the 0.64 kb *Bgl*II-*Kpn*I DNA fragment, containing *appA* codons 1-168, was amplified by PCR (primers: appAup2 and A170down, Table 2.4) using plasmid pBBRAppA170 as template and cloned into the *Bam*HI and *Kpn*I sites of vector pQE30. The recombinant plasmid designated pQEBLUF was transformed into *E. coli* M15(pREP4). His-BLUF was produced in *E. coli* M15(pQEBLUF/pREP4) cells induced at 17°C overnight with 0.5 mM IPTG and the cells turned into yellow color after induction. The purification was performed by Ni-NTA agarose either under native conditions (Figure 4.35A) or under denaturing conditions (Figure 4.35C).

His-BLUF (22.6 kDa) purified under native conditions was dialyzed in storage buffer (Chapter 3.5.1) and it was yellow. The absorption spectrum was recorded from 300 nm to 600 nm. The spectrum of this protein appeared to be typical of a flavoprotein, with absorption maxima at 378 nm and 452 nm (Figure 4.35B). The amount of FAD was calculated based on the Lambert-Beer's law and using the extinction coefficient of 11,300 $M^{-1} \cdot cm^{-1}$ at 450 nm (Gomelsky and Kaplan, 1998). The result showed that 1 mol purified BLUF protein contained 0.49 mol FAD, indicating that only half of the BLUF proteins bind the cofactor FAD. This low FAD content may be due to the fact that the cofactor FAD was partly lost during the purification process.

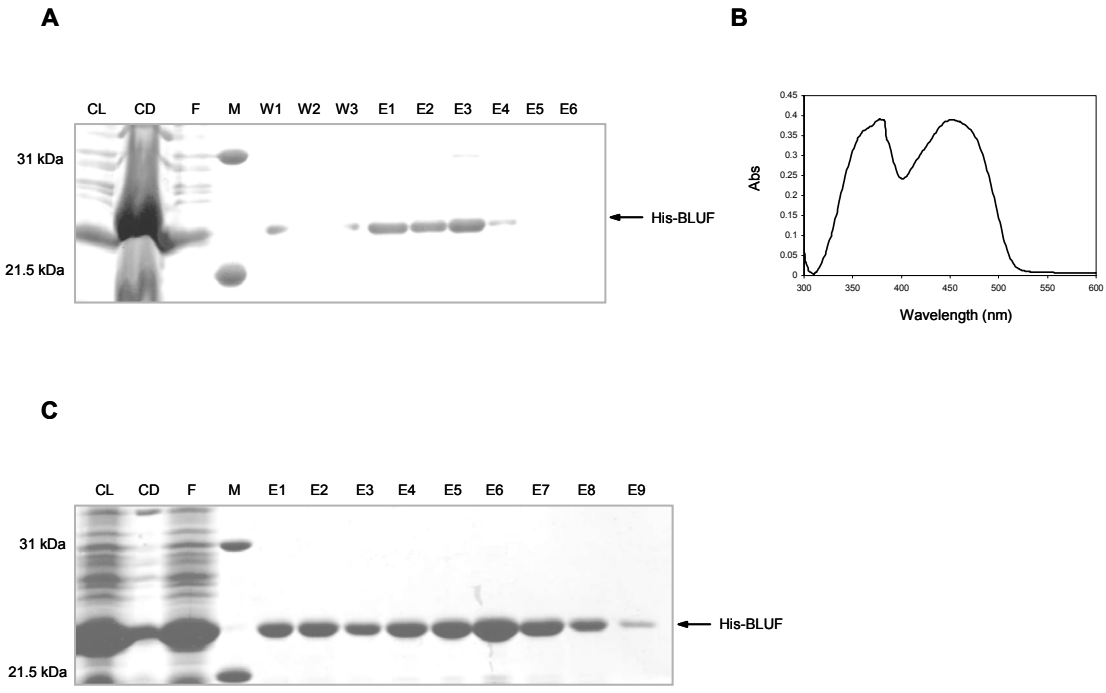

Figure 4.35 Purification of His-BLUF from crude extract of *E. coli* M15(pQEBLUF/pREP4).

(A) Purification of His-BLUF under native condition. Proteins were loaded on a 15% SDS-polyacrylamide gel, and the signals were analyzed by Coomassie blue staining; **(B)** Absorption spectrum of purified His-BLUF; **(C)** Purification of His-BLUF under denaturing condition. Proteins were eluted by an imidazole gradient and loaded on a 15% SDS-polyacrylamide gel. The signals were analyzed by Coomassie blue staining. Abbreviations: M, molecular mass standards (also shown in the left of figures); CL, clear lysate; CD, cell debris; F, flow-through; W, wash fraction; E, eluate.

4.2.8.2 Analysis of the interaction between PpsR and AppAΔN by a BIACORE® X system

To analyze the interaction of PpsR and AppAΔN, His-AppAΔN was immobilized on the Ni-NTA biosensor surface, resulting in an increase of resonance units (RU, a resonance unit is arbitrarily defined as 1/3000 of a degree in the angular change.) of approximately 1000, and then the same amount of PpsR was applied at different flow rates. As shown in Figure 4.36, the highest response difference was observed when PpsR was injected at a flow rate of 1 µl/min or 3 µl/min. When the flow rate was increased, most of the PpsR protein was not captured by the AppAΔN protein on the sensor chip and very low response difference was measured. These results indicate that longer incubation time allows more PpsR to bind AppAΔN. When His-BLUF was immobilized on the Ni-NTA surface and the same amount of PpsR was applied at a flow rate of 1 µl/min, no interaction was observed. This suggests that PpsR binds the C-terminal part of AppA

instead of the BLUF domain. This result is in agreement with the previous data (Chapter 4.1.3 and Chapter 4.2.3).

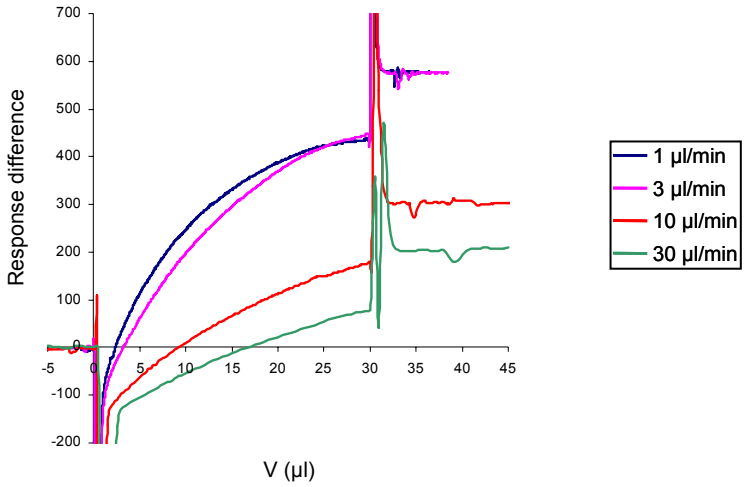

Figure 4.36 Analysis of the interaction between PpsR and AppAΔN by a BIACORE® X system.

His-AppAΔN was immobilized on a Ni-NTA biosensor surface, resulting in an increase of resonance units of approximately 1000. Then 30 µl of 500 nM PpsR was injected at a flow rate of 1 µl/min (blue), 3 µl/min (pink), 10 µl/min (red), and 30 µl/min (green), respectively.

The previous *in vivo* data provided evidence for a direct interaction of the two AppA domains, even without covalent linkage (Han *et al.*, 2004 and Chapter 4.1.4). Therefore, the interaction between the two domains of AppA was also tested using this BIACORE® X system. Unfortunately, no interaction was detected. This may be due to the lack of a certain factor or to the factor that the binding site was not exposed on the top for recognition. When hemin was applied on the Ni-NTA surface, the resonance units increased strongly, suggesting that hemin can bind to the Ni-NTA surface. Additionally, the BLUF domain is a blue light photoreceptor which can relay the light signal to the C-terminal part of AppA. Thus, light might be critical for the interaction between the two domains of AppA. But light can not reach the proteins during the measurement using the BIACORE® X system. Therefore, this BIACORE® X system with the NTA-chip is not suitable for determination of the interaction between the two domains of AppA.

4.2.8.3 Analysis of the BLUF-AppAΔN interaction and the PpsR-AppAΔN interaction using a Plasmonic® spectroscope

The Plasmonic® SPR system is based on the micro-cuvette technology. Up to eight measurements can be performed at the same time. The proteins to be assayed can be

incubated for the desired time and then the unbound protein can be washed out. Unlike the NTA-surface, the hydrophobic C18-suface used in this work allows the protein bind to the surface in random orientations. Thus, some of the binding sites can be exposed and recognized by their interacting partners.

The following SPR-measurements were performed by Martin H.F. Meyer in the group of Prof. Michael Keusgen at Philipps University of Marburg.

When PpsR (100 µg/ml) was immobilized to a C18-matrix and increasing concentrations of AppAΔN were applied, the association constant (k_{ass}) was 18.8 $s^{-1}{\cdot}mM^{-1}$ for this interaction (Figure 4.37). When AppAΔN was immobilized and PpsR was applied in solution, similar results were obtained (data not shown). In the presence of heme, the association constant of PpsR-AppAΔN increased 2.4-fold to a value of 44.6 $s^{-1}{\cdot}mM^{-1}$ (Figure 4.37), suggesting that the heme cofactor increases the PpsR-binding activity of AppAΔN.

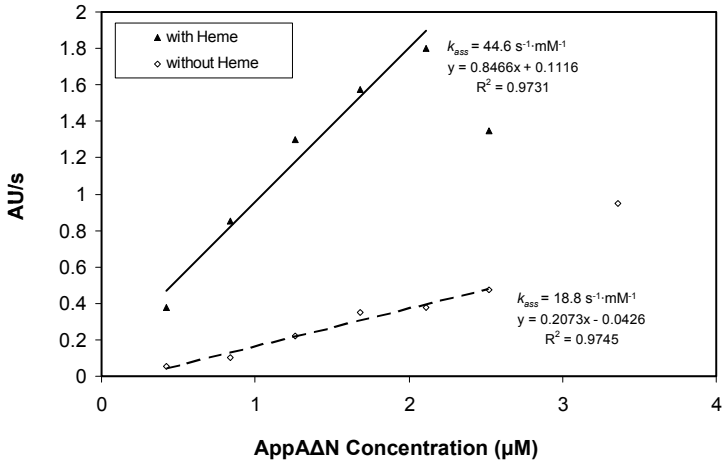

Figure 4.37 Concentration dependency curve of the interaction between PpsR and AppAΔN.

PpsR (100 µg/ml) was immobilized to the C18-matrix and variable amount of AppAΔN were applied in the presence of 1 µg/ml heme (filled triangles) or without heme (open diamonds). The interactions were analyzed using an SPR spectroscope (Plasmonic®, HSS Systeme, Wallenfels).

The interaction between the BLUF domain and AppAΔN was also tested using the Plasmonic® spectroscope. The same binding kinetics were observed when AppAΔN was immobilized with variation of the BLUF concentration or vice versa. An association constant of 9.9 $s^{-1}{\cdot}mM^{-1}$ was detected (Figure 4.38A), indicating a very weak interaction. The presence of heme increased this value by a factor of 3.1 (31.2 $s^{-1}{\cdot}mM^{-1}$, Figure

4.38A), suggesting that the heme cofactor influences the BLUF-binding activity of the AppAΔN. Illumination of the samples in the presence of heme did not significantly change the association constant (33.3 $s^{-1} \cdot mM^{-1}$, Figure 4.38B). It could be due to the fact that only half of the BLUF domain binds cofactor FAD (Chapter 4.2.8.1).

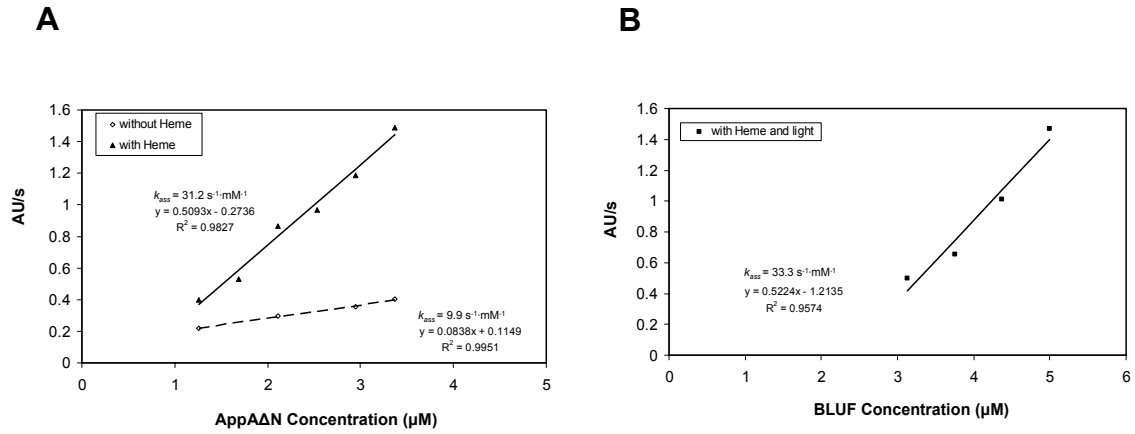

Figure 4.38 Concentration dependency curve of the interaction between the BLUF domain and AppAΔN.

(A) The BLUF domain (200 µg/ml) was immobilized to the C18-matrix and variable amount of AppAΔN were applied in the presence of 1 µg/ml heme (filled triangles) or without heme (open diamonds). The interactions were **(B)** AppAΔN (200 µg/ml) was immobilized to the C18-matrix and variable amount of the BLUF domain were applied in the presence of 1 µg/ml heme and light illumination (filled squares). The interactions were analyzed using an SPR spectroscope (Plasmonic®, HSS Systeme, Wallenfels).

As described in Chapter 4.2.7, the AppAΔN-mutants lost the ability to bind heme. To find out whether the mutation sites in these AppAΔN-mutants are crucial for the interactions, the binding kinetics between the AppAΔN-mutants and the BLUF domain in the presence of heme were determined using the Plasmonic® spectroscope. The association constants of the interactions between the AppAΔN-mutants and the BLUF domain are 24.5 $s^{-1} \cdot mM^{-1}$ and 18.7 $s^{-1} \cdot mM^{-1}$ for AppAΔN9 and AppAΔN14, respectively (Figure 4.39A). These results show that the AppAΔN-mutants in the presence of heme have a reduced binding capacity for the BLUF domain in comparison to the wild type protein AppAΔN (31.2 $s^{-1} \cdot mM^{-1}$), indicating that the mutation sites in the heme-binding domain are important for the interaction between the two domains of AppA.

For the binding of AppAΔN variants to PpsR, the kinetics showed tendencies similar to that seen for binding to the BLUF domain. In the presence of the heme cofactor association constants of 20.9 $s^{-1}\cdot mM^{-1}$ (AppAΔN9) and 21.4 $s^{-1}\cdot mM^{-1}$ (AppAΔN14) were determined (Figure 4.39B). These results show that the AppAΔN-mutants have a reduced binding capacity for PpsR in comparison to the wild type protein AppAΔN (44.6 $s^{-1}\cdot mM^{-1}$), indicating that the mutation sites in the heme-binding domain are important for the interaction between AppAΔN and PpsR.

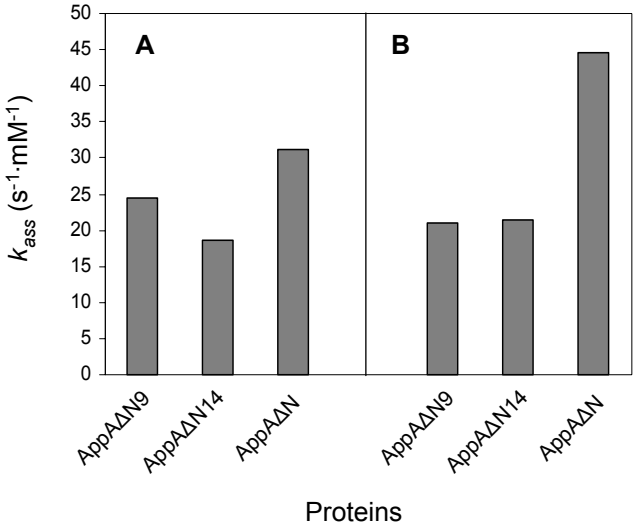

Figure 4.39 Comparison of association constant (k_{ass}).

(A) Association constant of the interactions between BLUF and AppAΔN variants; **(B)** Association constant of the interactions between PpsR and AppAΔN variants. The interactions were analyzed using an SPR spectroscope (Plasmonic®, HSS Systeme, Wallenfels).

To test whether the interaction of AppAΔN to the BLUF domain interferes with its interaction to PpsR, PpsR was coupled to the matrix and control experiments confirmed that no significant interaction of PpsR to the BLUF domain occurs. When AppA alone together with heme was added to the coupled PpsR, an increase of about 26 arbitrary units (AU, the arbitrary units are calculated based on the angular shift of the resonance angles.) was observed (Figure 4.40). When the two AppA domains were preincubated in the presence of heme and then added to the coupled PpsR, an increase of only 15.5 AU occurred (Figure 4.40). It can be concluded that the presence of BLUF interferes with the AppAΔN-PpsR interaction. When the two AppA domains were mixed in the presence of heme and illuminated, an increase of only 11 AU was observed (Figure 4.40), suggesting that the interference of the BLUF domain with the AppAΔN-PpsR interaction is stronger in the presence of light. In all experiments including both AppA domains, a big part of

AppAΔN (about 50%) was released from PpsR during washing, indicating that the formed complexes are not very stable.

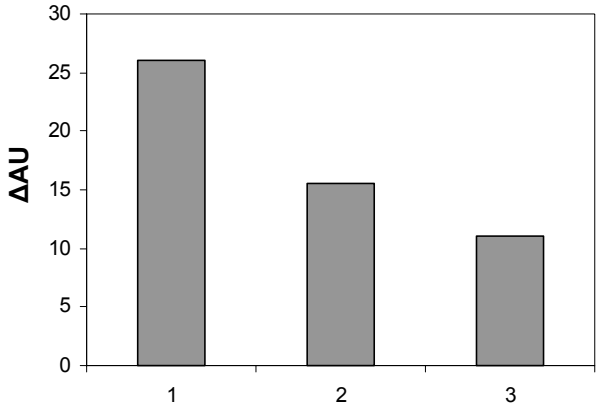

Figure 4.40 BLUF interferes with the interaction between AppAΔN and PpsR.

PpsR was immobilized to the C18 matrix. Column 1, AppAΔN was applied together with heme; Column 2, AppAΔN and BLUF were preincubated in the presence of heme and then applied to the coupled PpsR; Column 3, AppAΔN and BLUF were preincubated in the presence of heme, illuminated, and then applied to the coupled PpsR. The interactions were analyzed using an SPR spectroscope (Plasmonic®, HSS Systeme, Wallenfels). For each binding, the difference (ΔAU) between the arbitrary unit before applying protein mixture and the arbitrary unit after applying protein mixture and extensive washing was shown in the figure.

4.3 How does the AppA/PpsR system affect the *puf* expression?

The flavoprotein AppA in *R. sphaeroides* can sense light and oxygen signals and control the PS gene expression through the repressor protein PpsR. The consensus PpsR-binding sequence, TGT-N_{12}-ACA, is found in the promoter region of most PS genes (Figure 1.2B), such as *pucAB*, but not in the upstream region of the *puf* operon, although several studies showed that *pufBA* is indeed repressed by PpsR (Braatsch *et al.*, 2002; 2004; Moskvin *et al.*, 2005). How does the AppA/PpsR system affect the expression of the *puf* operon? One possibility is that the other regulatory systems present can control *puf* gene expression in parallel with the AppA-PpsR system; another possibility is that PpsR affects expression of a regulatory factor which controls *puf* expression. The second hypothesis could explain well why the responses of *puf* are always delayed comparing to the *puc* genes directly repressed by PpsR. To clarify this point, several candidate regulatory systems had been investigated in this work. The light- and redox-dependent *puf* and *puc* gene expression was analyzed by Northern blot and shown in Figure 4.41 and Figure 4.42.

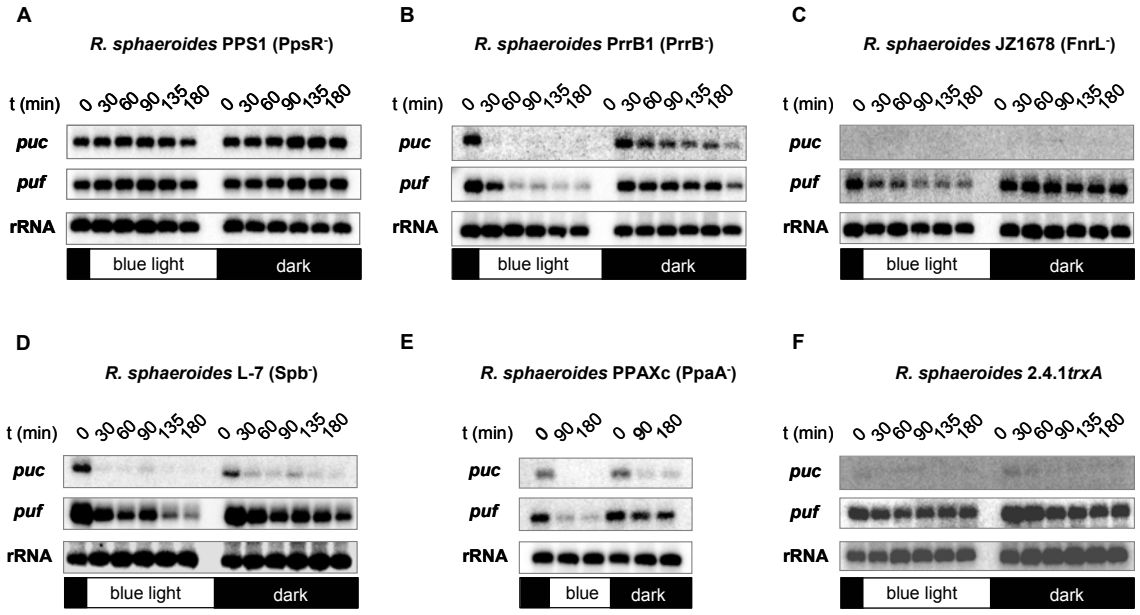

Figure 4.41 Kinetics of *puf* and *puc* expression in *R. sphaeroides* strain PPS1 (A), PrrB1 (B), JZ1678 (C), L-7 (D), PPAXc (E) and 2.4.1*trxA* (F) caused by blue light irradiation.

Cells grown at 104 ± 24 µM dissolved oxygen were shifted from the dark into blue light or kept in the dark. The 0.5 kb *puc* and the 0.5 kb *puf* signals were determined by RNA gel blot analyses. A 14S rRNA specific probe was used to show relative RNA loadings.

4.3.1 Role of the PpsR regulator in light- and redox-dependent regulation of PS genes

The PpsR null mutant, strain PPS1, is deeply pigmented even grown under aerobic conditions. In this strain, the PS genes are derepressed and the expressions of *puc* and *puf* genes are at very high level. No blue light repression could be detected in strain PPS1 under semi-aerobic conditions (Figure 4.41A) and *puf* genes were not induced when cells were shifted from high oxygen tension to low oxygen tension (Figure 4.42). These results were quite different from that of wild type strain *R. sphaeroides* 2.4.1 (Braatsch *et al.*, 2002 and Figure 4.42) and suggest that the expression of the *puf* operon is indeed under control of PpsR.

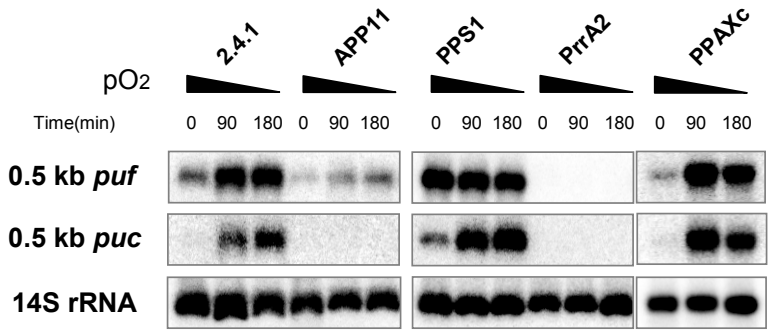

Figure 4.42 Redox-dependent *puf* and *puc* expression.

The cells were cultivated under high oxygen tension ($pO_2 \approx 200$ μM) and then shifted to growth under low oxygen tension ($pO_2 \approx 3$ μM) when the optical densities of the cultures at 660 nm were around 0.5. Total RNA was isolated at indicated time points, *puc* and *puf* transcript levels were monitored by RNA gel blot analyses. A 14S rRNA specific probe was used to show relative RNA loadings.

4.3.2 Role of the PrrB/PrrA two-component system in light- and redox-dependent regulation of PS genes

The PrrB/PrrA two-component system can activate the PS genes expression at low oxygen concentration. PrrA is a response regulator and PrrB functions as a sensor histidine-kinase/phosphatase. The consensus PrrA-binding site was found upstream of the *puf* operon. To test whether the PrrB/PrrA system also influences the light repression on *puf* genes, the same light-shift experiment was performed with *R. sphaeroides* PrrB1 (PrrB null mutant) under semi-aerobic conditions. The result showed a stronger decrease of *puf* expression in illuminated cells than the cells kept in dark (Figure 4.41B). A slight decrease of *puf* expression was also detected in dark cells. This might be caused by slight increase of oxygen tension during the experiment. Nevertheless, strain PrrB1 showed

around 70% inhibition on *puf* expression by blue light. A similar value was reported for the wild type strain (Braatsch *et al.*, 2002). It can be concluded that PrrB is not essential for light repression. Strain PrrA2 (PrrA null mutant) is unpigmented and no *puf* expression was detected by Northern blot even when cells were grown at very low oxygen concentration (Figure 4.42). The RT-PCR analysis confirmed no light inhibition on *pufBA* expression in strain PrrA2 (Metz, 2006). This implies that PrrA might be involved in the light repression on *pufBA* genes under semi-aerobic conditions. The light signal may be transmitted to PrrA via the electron transport chain as revealed under anaerobic conditions (Zeilstra-Ryalls & Kaplan, 2004; Happ *et al.*, 2005). Since the kinase PrrB is not required for light repression, the response regulator PrrA might be activated without phosphorylation or phosphorylated by other phosphodonors.

4.3.3 Role of the FnrL regulator in light-dependent regulation of PS genes

R. sphaeroides FnrL regulates the PS gene expression in response to the changes in oxygen levels (Zeilstra-Ryalls & Kaplan, 1995). It is a DNA-binding protein and increases the transcription of some PS genes when oxygen tension is reduced. The FnrL protein contains an iron-sulfur cluster, which is important for the FnrL DNA-binding activity (Lazazzera *et al.*, 1996; Khoroshilova *et al.*, 1997). The loss of FnrL results in inability to grow under photosynthetic or dark-DMSO conditions, while aerobic growth remains similar to that of wild-type 2.4.1 (Zeilstra-Ryalls & Kaplan, 1995). The *puf* and *puc* expression in the FnrL mutant strain JZ1678 under semi-aerobic conditions was also determined by Northern blot analysis. As shown in Figure 4.41C, the *puc* and *puf* expression levels are much lower than in wild-type 2.4.1, suggesting that the mutant form less photosynthetic apparatus than wild-type 2.4.1. Under semi-aerobic conditions, Northern blot analysis showed that *puf* expression level in the illuminated cells was reduced by 53% in comparison to dark cells (Figure 4.41C). Although this value was a little bit less than wild type strain (around 65%, Braatsch *et al.*, 2002), it still suggests that FnrL has no major role in such blue light inhibition at intermediate oxygen concentration.

4.3.4 Role of the Spb protein in light-dependent regulation of PS genes

The Spb protein is an H-NS protein, which elicits changes in DNA topology in response to the changes in the environment and consequently alters the pattern of gene expression.

In *R. sphaeroides*, it was described that Spb can bind to the promoter region of the *puf* operon and functions as a high-light repressor (Shimada *et al.*, 1996; Nishimura *et al.*, 1998). When grown photosynthetically under high-intensity light conditions, *R. sphaeroides* L-7 (Spb null mutant) formed less photopigments than the cells grown under low-intensity light conditions (Nishimura *et al.*, 1998). In order to test whether Spb influences the blue light repression of the *puf* operon, the blue light-shift experiment was performed with strain L-7 under semi-aerobic conditions. The Northern blot analysis showed around 59% blue light inhibition of *puf* expression (Figure 4.41D), which is similar to that in the wild type strain. Thus, Spb is not involved in the blue light-dependent regulation of *puf* operon under semi-aerobic conditions. Some decreases of *puf* and *puc* expression were also detected in dark cells. This could due to slight increase of oxygen tension during experiment.

4.3.5 Role of the PpaA regulator in light- and redox-dependent regulation of PS genes

The *ppaA* gene is located within the PS gene cluster of *R. sphaeroides* (Figure 1.2). It was shown that PpaA can activate photopigment production and *puc* operon expression under aerobic conditions (Gomelsky *et al.*, 2003). Moskvin *et al.* (2005) suggested that PpaA might be a prime candidate for a PpsR-affected regulatory factor that controls *puf* gene expression, even though no direct evidence showed that *puf* expression is under control of PpaA. So the *puf* and *puc* expressions were determined in PpaA mutant strain PPAXc by Northern blot analysis. The results showed that the *puf* and *puc* expressions in strain PPAXc are regulated the same way as in wild-type 2.4.1 in response to blue light irradiation and oxygen reduction (Figures 4.41E and 4.42), suggesting that PpaA is not involved in the blue light-dependent regulation of the *puf* operon under semi-aerobic conditions.

4.3.6 Role of the TrxA regulator in light-dependent regulation of PS genes

4.3.6.1 Kinetic of *puf* expression in the TrxA mutant caused by blue light irridation under semi-aerobic conditions

In *R. sphaeroides*, thioredoxin 1 (TrxA) is involved in the redox-dependent regulation of PS genes (Pasternak *et al.*, 1999; Li *et al.*, 2003). The TrxA protein level and the redox

status of TrxA are crucial for the control of the photosynthetic apparatus formation (Pasternak *et al.*, 1999). Since the TrxA-negative mutant is lethal in *R. sphaeroides* (Pasternak *et al.*, 1997), strain 2.4.1*trxA* expressing lower level of the TrxA protein was constructed. In strain 2.4.1*trxA*, the chromosomal *trxA* is disrupted and an integrated *trxA* is under control of IPTG inducible promoter. To find out whether the TrxA protein is involved in the light-dependent regulation of PS gene expression, the kinetic of *puf* and *puc* expression in strain 2.4.1*trxA* caused by blue light irridation under semi-aerobic conditions were determined by Northern blot analysis (Figure 4.41F). Surprisingly, the *puf* expression in this *trxA* mutant strain was not repressed by blue light under semi-aerobic conditions (Figure 4.41F), indicating that the TrxA protein might influence the blue light repression of *puf* expression. The *puc* mRNA level in strain 2.4.1*trxA* was too low for the quantification, indicating that the decreased levels of the TrxA protein lead to lower expression of *puc* genes. The same phenomenon was observed in the study of Pasternak *et al.* (1999). To test whether the *trxA* expression was regulated by blue light, the *trxA* mRNA levels in blue-light illuminated cells and the cells kept in dark were determined in wild-type strain 2.4.1 by Northern blot analysis (Figure 4.43). The specific *trxA* probe was amplified by PCR using C22 and C23 as primers (Table 2.4). The result showed that *trxA* gene does not respond to blue light at intermediate oxygen concentration. This result confirms the microarray data from Braatsch *et al.* (unpublished data). Since the expression of *trxA* is not directly controlled by PpsR and the *puf* expression in strain 2.4.1*trxA* shows different kinetic from that in wild-type strain in response to blue light under semi-aerobic conditions, there should be a certain link between the AppA-PpsR system and the TrxA regulator.

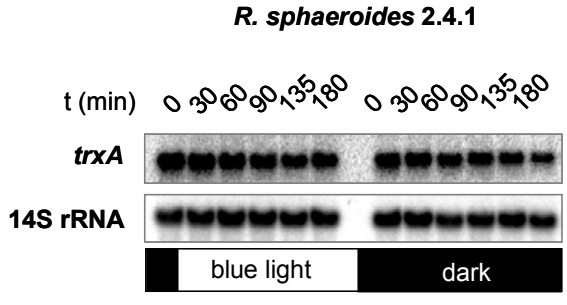

Figure 4.43 Kinetic of *trxA* expression in *R. sphaeroides* 2.4.1 caused by blue light irradiation.

Cells grown at 104 ± 24 µM dissolved oxygen were shifted from the dark into blue light or kept in the dark. *trxA* mRNA level was determined by RNA gel blot analysis. A 14S rRNA specific probe was used to show relative RNA loadings.

4.3.6.2 Role of gyrase in light-dependent regulation of PS genes

Li *et al.* (2004) showed the TrxA protein can affect the gene expression by modifying gyrase activity. The redox status of the cell determines the ratio of reduced to oxidized thioredoxin. In *R. sphaeroides*, the reduced TrxA binds the gyrase B subunit and increases supercoiling activity of gyrase, which influences transcription by bending and folding DNA (Malik *et al.*, 1996; Li *et al.*, 2004). Li *et al.* (2004) showed that the gyrase in the *trxA* mutant strain exhibits lower supercoiling activity than in the wild-type strain and the *puf* mRNA level in the *trxA* mutant strain is also lower than that in the wild-type strain. Moreover, it was shown that the *puf* mRNA level decreases in wild type cells treated by the gyrase inhibitor-novobiocin (Li *et al.*, 2004), suggesting that the gyrase activity is important for the *puf* gene expression in *R. sphaeroides*. To find out whether gyrase is involved in the light-dependent regulation of PS gene expression, the *puf* expression was determined in wild-type 2.4.1 in the presence of novobiocin. Around 30% blue light inhibition of the *puf* expression under semi-aerobic conditions was detected by Northern blot analysis (Figure 4.44). This value was much less than that of wild-type 2.4.1 (around 65%, Braatsch *et al.*, 2002), implying that the gyrase might be involved in the light-dependent regulation of *puf* gene expression.

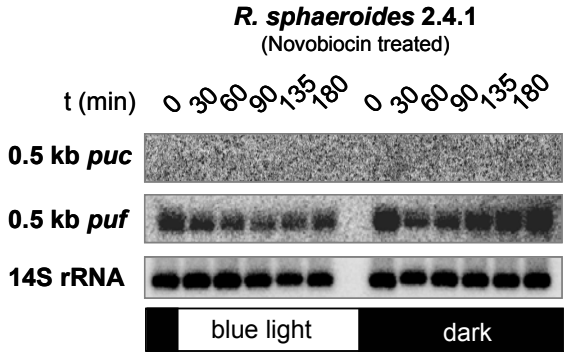

Figure 4.44 Kinetics of *puf* and *puc* expression in *R. sphaeroides* 2.4.1 caused by blue light in the presence of novobiocin.

Cells grown at 104 ± 24 µM dissolved oxygen were shifted from the dark into blue light or kept in the dark. At time point zero, novobiocin was added in the medium to a final concentration of 100 ng/ml. *puc* and *puf* mRNA levels were determined by RNA gel blot analyses. A 14S rRNA specific probe was used to show relative RNA loadings.

To determine the gyrase activity in the cell free extracts, the relaxed plasmid pBluescript SK (+) was used as the substrate for the supercoiling assay. Part of plasmid pBluescript SK (+) isolated from *E. coli* cells were highly supercoiled. Because the supercoiled plasmids were more compact than the relaxed ones, they migrated more rapidly during the gel electrophoresis (Figure 4.45A, lane 1). After the treatment with topoisomerase I, the highly supercoiled plasmids were relaxed. The plasmids in the different degree of supercoiling can be separated in the TAE-agarose gel (Figure 4.45A, lane 2).

In order to compare the gyrase activity in light irradiated cells and the dark cells, the same amounts of total proteins from cell free extracts of the wild-type 2.4.1 at each time point were incubated with relaxed plasmid pBluescript SK (+) at 37°C for 2 hours and the products in the different degree of supercoiling were separated by the 0.8% TAE-agarose gel electrophoresis (Figure 4.45B). Since DNA gyrase catalyzes the ATP-dependent supercoiling of covalent circular DNA, the high amounts of supercoiled plasmids indicate the high supercoiling activity of gyrase in the cell extracts. As shown in Figure 4.45B, the plasmids treated with the cell extracts from illuminated cells showed the similar patterns as the ones treated with the cell extracts from dark cells, indicating that there was no significant difference of supercoiling activity between the illuminated cells and the dark cells. Therefore, it can be concluded that blue light does not affect the gyrase activity. The decreased inhibition of *puf* expression by blue light in novobiocin treated cells could due to the lower *puf* expression level.

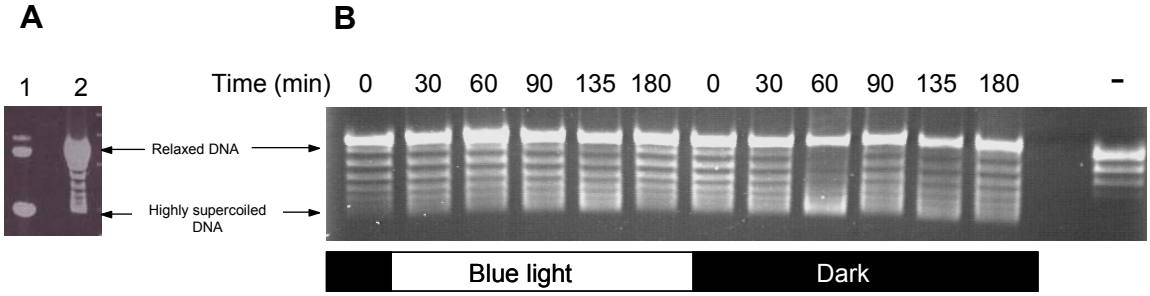

Figure 4.45 Supercoiling activity of gyrase in cell extracts of *R. sphaeroides* 2.4.1.

(A) Different topological conformations of plasmid pBluescript SK (+). The plasmid pBluescript SK (+) was isolated from *E. coli* cells (lane 1) and then relaxed by the treatment with topoisomerase I (lane 2). The relaxed plasmid pBluescript SK (+) was used as the substrate of supercoiling assay. **(B)** Supercoiling activity of gyrase in cell extracts of *R. sphaeroides* 2.4.1. Cells grown at 104 ± 24 µM dissolved oxygen were shifted from the dark into blue light or kept in the dark. Cells were harvested and extracted at indicated time points. Relaxed plasmid pBluescript SK (+) was used as substrate and shown in the right of figure. The plasmids in the different degree of supercoiling were separated by the 0.8% TAE-agarose gel electrophoresis.

4.3.6.3 Role of redox potential in light-dependent regulation of PS genes

The AppA protein, as a heme-binding protein (see previous chapter), regulates the PS gene expression in response to the change in the redox potential. It was assumed that the different kinetics of the *puf* expression between strain 2.4.1*trxA* and the wild-type strain

in response to blue light under semi-aerobic conditions may be caused by different redox potential in these two strains.

The transcription factor OxyR can directly sense the oxidative stress and be activated by reversible disulfide bond formation under high redox potential conditions (Zheng *et al.*, 1998; Åslund *et al.*, 1999). OxyR transcriptionally induces the expression of some catalases (hydroxyperoxidase), which is involved in the detoxification of hydrogen peroxide during the oxidative stress (Zeller & Klug, 2004 and reviewed in Chelikani *et al.*, 2004). The catalases in *R. sphaeroides* are encoded by the *katE* and *katC* genes. Zeller & Klug (2004) showed that the expression of *katE* gene was strongly induced after addition of H_2O_2 to exponentially growing cultures or after shifting the cells from low oxygen conditions to high oxygen conditions, while the *katC* gene shows no significant response to H_2O_2. The gel-shift experiment demonstrated that the transcription regulator OxyR in *R. sphaeroides* binds the *katE* promoter region and regulates the *katE* expression (Zeller & Klug, 2004). In brief, the previous studies showed that the OxyR regulator in *R. sphaeroides* is activated under high redox potential and consequently induces the *katE* expression. Therefore, high *katE* mRNA level indicates high redox potential in the cells.

To compare the redox potential in strain 2.4.1*trxA* and the wild-type strain, the *katE* expression was determined by quantitative real-time RT-PCR. The annealing temperatures were 62°C for *katE*, and 59°C for *rpoZ*, which encodes the ω-subunit of the *R. sphaeroides* RNA polymerase (Pappas *et al.*, 2004) and was used as internal standard. The real-time RT-PCR efficiencies were 2.00 for *katE* and 2.02 for *rpoZ*. The result showed that the expression of *katE* in strain 2.4.1*trxA* was reduced about 3.2-fold under semi-aerobic conditions in comparison of aerobic conditions (Figure 4.46A). This value was similar as reported in wild-type 2.4.1 (Zeller & Klug, 2004). Under both semi-aerobic and aerobic growth conditions, the *katE* mRNA level in strain 2.4.1*trxA* was significantly higher than in the wild type strain (Figure 4.46B), indicating that the redox potential in the strain 2.4.1*trxA* is much higher than in wild-type strain. This result confirmed the assumption that the different kinetics of *puf* expression between strain 2.4.1*trxA* and the wild type strain are caused by different redox potential in the cells.

Usually, the expression of the *rpoZ* gene is used as internal standard in RT-PCR experiment because it was supposed to be housekeeping gene in *Rhodobacter*. Its expression in *R. sphaeroides* is indeed constant in variable growth conditions (Pappas *et al.*, 2004 and studies in our group). However, it was observed that the *rpoZ* expression in wild-type 2.4.1 was 10-fold higher than in strain 2.4.1*trxA*, indicating that the *rpoZ*

expression might be regulated by the TrxA protein in *R. sphaeroides*. So far, no any evidence showed there is a relationship between *rpoZ* expression and *trxA* expression. This finding requires further verification.

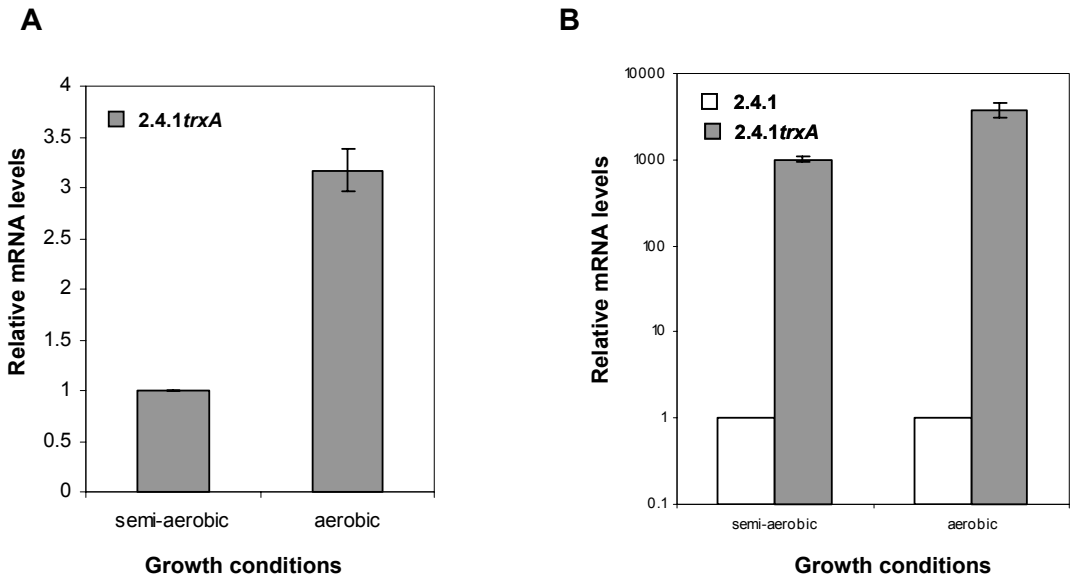

Figure 4.46 Expression of the *katE* gene in *R. sphaeroides* 2.4.1*trxA*.

Cells grown under either semi-aerobic or aerobic conditions were collected at an optical density of 0.8 at 660 nm. Total RNA was isolated, and *katE* transcript levels were quantified by real-time RT-PCR analyses and normalized to the *rpoZ* mRNA level (See Chapter 3.4.3.2). The data represent three independent experiments and error bars indicate the standard deviation. **(A)** Effect of oxygen tension on the expression of the *katE* gene in *R. sphaeroides* 2.4.1*trxA*. The values represent the relative *katE* transcript levels. The *katE* expression level under semi-aerobic conditions was set as 1. The *katE* transcript level under aerobic conditions was normalized to the one under semi-aerobic conditions and shown in the figure. **(B)** Comparison of the expression of *katE* genes in *R. sphaeroides* 2.4.1*trxA* and *R. sphaeroides* 2.4.1 (wild type strain). The filled bars represent the fold change of the *katE* mRNA level compared to that in the wild-type strain, for which the *katE* expression levels were set as 1 (open bars). The scale of Y-axis is the logarithmic scale.

5 Discussion

5.1 The BLUF domain: a novel blue-light photoreceptor

Blue light controls a wide variety of biological activities through various types of photoreceptors and signaling systems (Lin, 2000; Crosson *et al.*, 2003; Sancar, 2003; van der Horst & Hellingwerf, 2004). Recently, the BLUF domains have been identified, which use FAD as their chromophore. Their sequences, structures and photo-excitation processes are different from those of other flavoproteins (Gomelsky & Klug, 2002; Laan *et al.*, 2003; Kraft *et al.*, 2003; Gauden *et al.*, 2005; Unno *et al.*, 2005). These differences define the BLUF domain as a new family of the blue light photoreceptors.

5.1.1 The BLUF domain is fully modular and can relay signals to completely different output domains

So far, six BLUF proteins have been characterized, which are the following:

- AppA from *Rhodobacter sphaeroides* (Gomelsky & Kaplan, 1998; Kraft *et al.*, 2003; Laan *et al.*, 2003; Masuda *et al.*, 2005; Anderson *et al.*, 2005)
- PAC from *Euglena gracilis* (Iseki *et al.*, 2002; Ito *et al.*, 2005)
- YcgF from *Escherichia coli* (Rajagopal *et al.*, 2004; Hasegawa *et al.*, 2006)
- BlrB from *R. sphaeroides* (Jung *et al.*, 2005; Zirak *et al.*, 2006)
- Slr1694 from *Synechocystis* sp. PCC6803 (Masuda, *et al.*, 2004; Hasegawa *et al.*, 2004; 2005)
- Tll0078 from *Thermosynechococcus elongatus* BP-1 (Kita *et al.*, 2005; Fukushima *et al.*, 2005)

The first three proteins are multidomain proteins, which contain common blue-light sensing domains (the BLUF domains) with different sets of carboxyl-terminal effector domains. The last three proteins belong to the group of the small BLUF domain proteins, which only consist of the BLUF domain with an extension of 30-70 amino acids. Despite little sequence similarity outside of the BLUF domain, all of these BLUF domains showed red-shifted UV-visible spectral changes upon illumination (Masuda & Bauer, 2002; Jung *et al.*, 2005; Ito *et al.*, 2005; Masuda, *et al.*, 2004; Rajagopal *et al.*, 2004; Kita *et al.*, 2005), suggesting that the fundamental photocycle reaction is common to all BLUF domains irrespective of their downstream parts. The isolated N-terminal BLUF domain

exhibits a photocycle identical to that observed with full length AppA (Kraft *et al.*, 2003), indicating that the BLUF domain is directly responsible for the light-induced photocycle in the AppA protein. Therefore, it was assumed that the BLUF domain is a module functioning as a transducer of light signal and mediates the activities of different set of regulatory output domains.

Before this study started, the function of AppA and PAC had been well characterized. The AppA protein from *R. sphaeroides* integrates light and redox signals and functions as a transcriptional antirepressor, controlling the expression of the photosynthesis (PS) genes via redox and light-modulated interaction with the repressor PpsR (Gomelsky *et al.*, 2000; Masuda & Bauer, 2002; Braatsch *et al.*, 2002). The N-terminal BLUF domain of AppA modulates the PpsR-binding activity of the C-terminal part of AppA in response to blue light (Chapter 4.2 and later discussion). Like the AppA protein, the PAC protein in *E. gracilis* is also a multidomain protein. It contains four BLUF domains. Each BLUF domain is connected to an adenylate cyclase with blue light excitation controlling cyclase activity that subsequently mediates photoavoidance and phototaxis (Iseki *et al.*, 2002; Ntefidou *et al.*, 2003). To test whether the BLUF domain can transmit signals to different output domains, the PACα1-BLUF domain (the BLUF1 domain of the α-subunit of the PAC protein, Figure 4.1) was fused to the C-terminal part of AppA and the function of this hybrid protein was investigated in this study (Chapter 4.1.2). As shown in Figure 4.6, 4.7 and 4.8, the hybrid protein is fully functional in light-dependent gene regulation in *R. sphaeroides*, despite only around 30% identity between the PACα1-BLUF domain and the AppA-BLUF domain. This proofs that the BLUF domain from the PAC protein can fully replace its homologue, the AppA-BLUF domain, in the light-dependent signaling in *R. sphaeroides*. As described above, the output domains of the PAC protein and the AppA protein are functionally clearly different. The PACα1-BLUF domain can not only regulate the activity of an adenylate cyclase in *E. gracilis* but also control the ability of the C-terminal domain of AppA to bind the PpsR repressor protein in *R. sphaeroides*. This implies that the BLUF domain creates a light-dependent output signal, which can be recognized and processed by different protein domains fused to the BLUF domain. The amino acids conserved between the PACα1-BLUF domain and the AppA-BLUF domain (Gomelsky & Klug, 2002; Iseki *et al.*, 2002) define the BLUF sequence sufficient to generate this light dependent signal and to transmit it to the output domains.

Interestingly, different from the AppA and PAC proteins, some proteins only consist of the BLUF domains without any linked output domains, *e.g.*, BlrB, Slr1694 and Tll0078

(Gomelsky & Klug, 2002). Therefore, this study addresses the question whether the BLUF domain proteins can relay the light signals to other noncovalently linked proteins. To this end, the BLUF domain of AppA and the C-terminal domain of AppA were expressed as separated domains in *R. sphaeroides* strain APP11(pBBRAppA170)(p484-Nco5Δ). The light signal transduction in strain APP11(pBBRAppA170)(p484-Nco5Δ) is similar to that in the strain expressing the wild-type AppA protein (Figure 4.9), suggesting that the signal transmission by AppA does not require covalent linkage of the BLUF domain and the C-terminal domain. This finding leads to the conclusion that the BLUF domain functions as a module that can transduce a light dependent signal to a C-terminally fused output domain or to a separately expressed protein. This was confirmed further by a recent study on the function of the short BLUF protein Slr1694. Okajima *et al.* (2005) reported that the Slr1694 protein from *Synechocystis* sp. PCC6803 interacts with a response regulator Slr1693 and subsequently regulates the positive phototaxis of this bacterium. Because the Slr1694 protein does not contain any functional domain outside of the BLUF domain, the BLUF domain of Slr1694 is directly responsible for the light sensing and transmits the light-dependent signal to other regulatory protein. This suggests that the BLUF domain (or protein) indeed functions as a module that can relay signals to a wide variety of output domains or proteins.

5.1.2 Mechanism of light signal transduction via the BLUF domain

As discussed above, the BLUF domains can relay signals to functionally diverse output units. However, it is not well understood how the BLUF domains sense the light-dependent signals and how they transmit signals to the output domains (or proteins).

In many photoreceptors, the light absorbed by a chromophore induces structural changes in the chromophore and the apoprotein for further signaling (van der Horst & Hellingwerf, 2004). In the AppA protein, the photochemical excitation of the flavin results in strengthening of a hydrogen bond between the flavin and the apoprotein that leads to a conformational change in the BLUF domain (Kraft *et al.*, 2003; Masuda *et al.*, 2005; Anderson *et al.*, 2005; Unno *et al.*, 2005; Masuda *et al.*, 2005). Similar structural change has been reported for other BLUF domains, *e.g.*, Slr1694 (Masuda *et al.*, 2004) and YcgF (Hasegawa *et al.*, 2006), suggesting that the light-induced structural change is common for the BLUF domains. It was previous presumed that the BLUF domain functions as a sensory module affecting the downstream processes through protein-protein interaction (Gomelsky & Klug, 2002). This view can be supported by i) the interaction between the

BLUF domain and the C-terminal domain of AppA revealed in this study (Figure 4.38), and ii) the interaction between the small BLUF protein Slr1694 and the regulator Slr1693 revealed from the yeast two-hybrid screening (Okajima *et al.* 2005). Since the BLUF domain can transmit the signals to output units by protein-protein interactions, the conformational changes of the BLUF domain induced by the blue-light excitation is assumed to be responsible for controlling the interactions.

To date, the best characterized signal transduction pathway via the BLUF domain is the blue light response via the AppA/PpsR system in *R. sphaeroides*. Based on the studies of the function and photochemistry of AppA, the mechanism of light signal transduction via the BLUF domain of AppA is summarized and illuminated in Figure 5.1. Mutant analysis in this study revealed that the C-terminal domain of AppA is sufficient for redox-dependent regulation and it is also required for the light-dependent regulation together with the BLUF domain (Chapter 4.1.3). Further studies showed that the C-terminal domain of AppA is sufficient to release the repressor activity of PpsR *in vitro* (Figure 4.17). Taken together, these *in vivo* and *in vitro* data strongly suggest that the binding site between AppA and PpsR must be located at the C-terminal domain of AppA and that the BLUF domain does not participate in the complex formation with PpsR to inhibit the repressor activity of PpsR. Surface plasmon resonance (SPR) based interaction studies demonstrated that the C-terminal domain of AppA does interact with PpsR in the absence of the BLUF domain (Figure 4.36 and 4.37). Interestingly, the C-terminal domain of AppA can also interact with the BLUF domain (Figure 4.38) and this interaction interferes with the association of the C-terminal domain of AppA with PpsR (Figure 4.40), indicating that the BLUF-binding site and the PpsR-binding site overlap somehow in the C-terminal domain of AppA. When the C-terminal domain of AppA is occupied by the BLUF domain, PpsR can not bind the C-terminal domain of AppA any longer. As shown in Figure 5.1, light-induced conformational change of the BLUF domain allows the BLUF domain to be bound to the C-terminal domain of AppA and consequently leads to disjunction of the AppA-PpsR complex. However, this study failed to show that light illumination does increase the association of the BLUF domain with the C-terminal domain of AppA (Figure 4.38). Since the chromophore flavin is essential for light sensing and the structural change in the BLUF domain, the amount of flavin bound to the BLUF domain studied in this work could be an important factor for the light excitation process. As shown in Figure 4.35B, only half of the purified BLUF proteins contain the FAD, while Gomelsky & Kaplan (1998) reported that 1 mol of the BLUF domain is capable of

binding 1 mol of FAD. Therefore, it is likely that the low amount of FAD causes the light-excited change only in part of the BLUF domains that is not sufficient to influence the detectable association between two domains of AppA. Moreover, Zirak *et al.* (2006) reported that the BlrB protein (a small BLUF protein) containing only FAD but not the combination of FAD, FMN and riboflavin can achieve high photo-excitation efficiency, suggesting that the flavin content is also important for the photocycle process. Unfortunately, in most cases, the purified BLUF protein contains three types of flavins (Gomelsky & Kaplan, 1998; Masuda *et al.*, 2005; Zirak *et al.*, 2006; Laan *et al.*, 2006). Because these flavins exhibit similar absorption feature, they can not be distinguished by their absorbance spectra. Hence, thin-layer chromatography should be applied to determine the flavin content of the BLUF protein assayed in this work. In addition, Masuda *et al.* (2005) supposed that the interaction between two domains of AppA could be intramolecular or intermolecular (Figure 5.1). It is more likely that this interaction is intramolecular because the size-exclusion chromatography revealed that both light-illuminated AppA and the AppA protein kept in dark are monomers in solution (Masuda & Bauer, 2002). However, Hazra *et al.* (2006) have reported recently that AppA also exists as a dimeric form. The dimeric AppA proteins are dominated by the monomeric ones and the size-exclusion chromatography is not sensitive enough to detect the dimers. They observed the AppA dimers using the pulsed laser-induced transient grating technique, which is more sensitive than the size-exclusion chromatography. Thus, the intermolecular interaction between two domains of AppA can not be excluded.

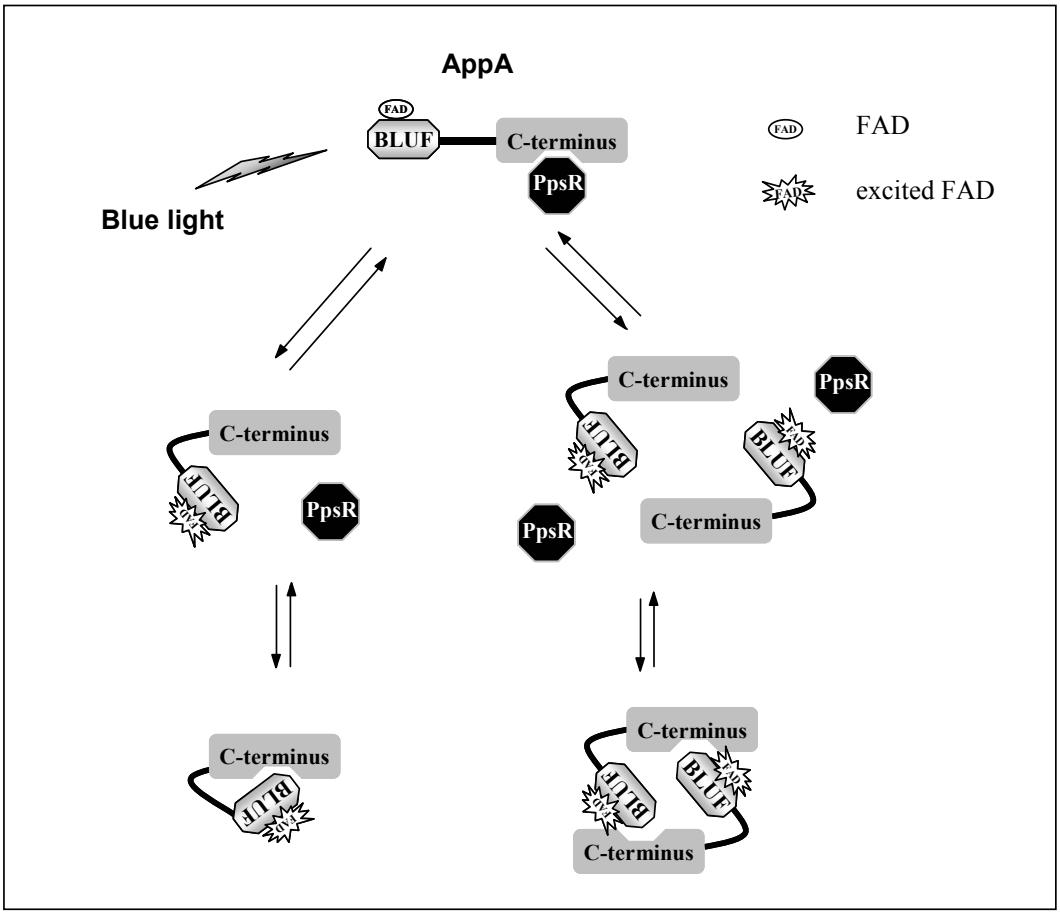

Figure 5.1 Model of light signal transduction via the BLUF domain of AppA.

The photochemical excitation of the flavin results in a conformational change in the apoprotein of the BLUF domain of AppA. The BLUF domain in the light-state structure is able to be bound to the C-terminal domain of AppA to prevent the binding of PpsR through the intramolecular or intermolecular interaction. (Modified from Masuda *et al.*, 2005)

5.2 A heme cofactor is required for redox and light signaling by the AppA protein

AppA has been shown to play a role in controlling PS gene expression in *R. sphaeroides* in response to both light and oxygen. As discussed above, the C-terminal domain of AppA can interact with either the BLUF domain or the PpsR repressor protein. Interestingly, this work revealed that the C-terminal domain is sufficient for redox-dependent regulation. To date, how the C-terminal domain of AppA senses the oxygen and how the redox signal is transferred to PpsR are unknown. This work revealed that the C-terminal domain of AppA binds heme (Chapter 4.2), which is known to be involved in redox sensing by other proteins, like FixL, *Ec*Dos, *Ax*PDEA1 (Gilles-Gonzalez and Gonzalez, 2004).

Heme proteins have been known to play important roles in biology as oxygen carriers (*e.g.*, hemoglobin), oxygen activator (*e.g.*, cytochrome P450 and peroxidase), and mediator of electron transfer (*e.g.*, cytochrome *c*) (Antonini & Brunori, 1971; Poulos, 1988; Sono *et al.*, 1996). Recently, a new class of heme proteins, designated heme-based sensor proteins (Rodgers, 1999; Gilles-Gonzalez & Gonzalez, 2005), have been identified. Specifically, heme functions as a biological sensor, and signals in response to changes in heme electronic and ligand binding states are transferred to domains that regulate catalytic functions, such as kinase activity for FixL, guanylate cyclase activity for sGC, phosphodiesterase activity for *Ec*DOS, chemotaxis by HemAT, and transcription by CooA and NPAS2 (Puranik *et al.*, 2004; Gilles-Gonzalez & Gonzalez, 2004; 2005; Sasakura *et al.*, 2006). In these proteins, association (or dissociation) of the external gaseous axial ligand (the input signal) such as O_2, NO, or CO to (or from) the heme iron or changes in the heme redox state lead to protein conformational changes in the heme environment, which transmit signals to the other functional domains to initiate catalytic function or DNA binding (the output signal) (Figure 5.2). For example, heme oxidation/reduction is associated with global structural changes in *Ec*DOS. *Ec*DOS is a protein sensing the environmental O_2 concentration by modulating the cellular cAMP concentration, thus altering the transcription of specific proteins. The structural changes in the FGloop region cause alterations in the pattern of hydrogen bonding around the heme cofactor, as well as global movement of one subunit relative to the other, which triggers movements of the catalytic domain that initiate catalysis (Kurokawa *et al.*, 2004). A similar mechanism has been reported for FixL, whose kinase activity can be inactivated by the binding of O_2 to the heme-PAS domain (Amezcua *et al.*, 2002).

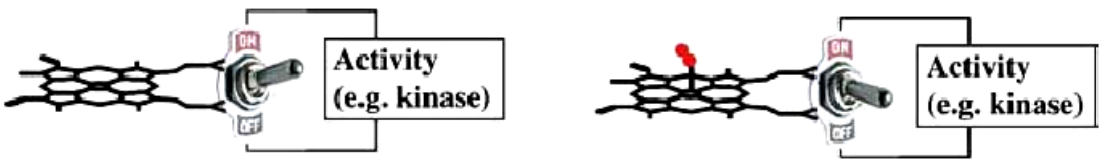

Figure 5.2 Switching by heme-based sensors.

This cartoon illustrates the possible responses to the signal (red circles) by a hypothetical sensor that is normally active in the unliganded state. To apply the same figure to a hypothetical sensor that is normally inactive in the unliganded state, reverse all the switches. (Modified from Gilles-Gonzalez & Gonzalez, 2005)

In this work, the binding of heme by the C-terminal part of AppA is supported by the binding of the C-terminal domain of AppA (AppAΔN) to hemin-agarose (Figure 4.21), by an absorbance typical for bound heme when hemin was added to isolated AppAΔN protein (Figure 4.20), and by the effect of heme in AppA/PpsR binding studies (Figure 4.22, 4.37 and 4.38A). The importance of heme in signal transduction via the AppA/PpsR system can be inferred by the facts i) that the reconstituted C-terminal part of AppA more effectively binds PpsR (Figure 4.22), ii) that the presence of heme increased the association constant of the AppAΔN-PpsR interaction *in vitro* (Figure 4.37), and iii) that the mutations leading to a loss of heme binding resulted in reduced interactions between AppAΔN and PpsR (Figure 4.39). The AppA variants RM9 and RM14 resemble the APP11 strain which lacks AppA, and they lost the ability to bind heme. The mutations in their heme binding domain affect their local conformation (Figure 4.33). It is likely that the binding of oxygen to the heme cofactor alters the structure of AppAΔN and, consequently, its affinity in binding to PpsR. As outlined in Figure 5.3 (status C→A), the binding of O_2 to the heme bound by AppA in direct response to the increase of oxygen tension in the dark causes the dissociation of the AppA-PpsR complex, which results in down regulation of PS gene expression.

Interestingly, heme also affects the interaction of AppAΔN and the AppA N-terminal BLUF domain (Figure 4.38A). This suggests that depending on the redox status AppAΔN gains the potential to bind to PpsR and at the same time to interact with the BLUF domain. Whether an interaction with the BLUF domain takes place or not is determined by the light signal, which can be relayed from the BLUF domain to AppAΔN (Chapter 5.1.1). The interaction studies support the view that the BLUF domain can interfere with the binding of AppAΔN to PpsR and that this interfering effect is clearly stimulated by light (Figure 4.40). Therefore, blue-light-excited AppA is unable to effectively associate with PpsR and consequently allows PpsR to bind to the promoter regions of PS genes under both high oxygen and low oxygen concentrations (Figure 5.3, status B and D). At high oxygen tension, the binding of O_2 to the heme keeps AppAΔN in a conformation that does not allow the interaction with the light-excited BLUF domain (Figure 5.3, status B). At low oxygen tension, status C→D illustrated in Figure 5.3 is the same as shown in Figure 5.1.

Taken together, the model shown in Figure 5.3 proposes a light switch of AppA mediated by the BLUF photoreceptor domain that only affects PS gene expression when a heme

dependent redox switch confers the capacity for PpsR interaction. The combination of these two events leads to the integration of the two stimuli by AppA.

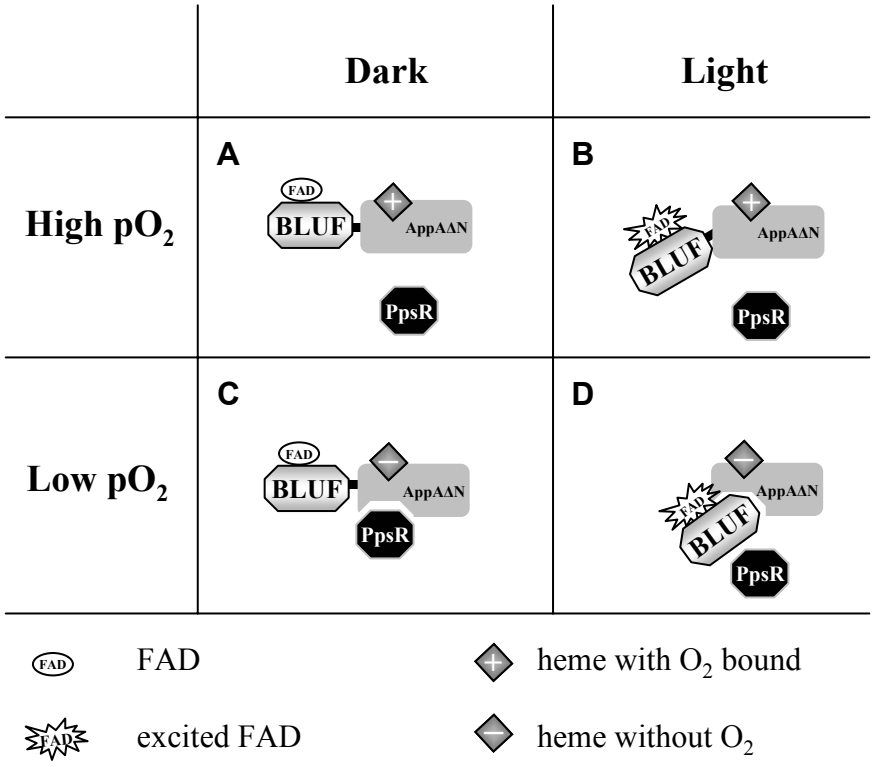

Figure 5.3 Model for the integration of redox and light responses by the AppA protein

The AppA protein contains two functional domains: the BLUF domain (FAD as cofactor, sensing light signal) and AppAΔN (heme as cofactor, sensing redox signal). AppA can antagonize the repressor activity of PpsR by forming an AppA-PpsR complex, and the PpsR binding site is located at the AppAΔN part. The cofactors of AppA influence the conformation of the BLUF domain and AppAΔN under different oxygen and light conditions, thus controlling the binding of AppAΔN to the BLUF domain, to PpsR or neither of them. See the text for other details.

However, this work could not test whether the heme redox state affects the interaction of the C-terminal domain of AppA with the BLUF domain or PpsR since redox state of the proteins cannot be controlled with the existing set-up in gel retardation assays and the SPR-based interaction studies. Therefore, it can not be excluded that AppA may be a heme-sensing protein which senses the amount of heme in the cell instead of bound oxygen. The heme-sensing proteins, such as the transcription regulator Bach1 (Sun *et al.*, 2004), HbrL (Smart and Bauer, 2006), and the eukaryotic initiation factor 2a (eIF2a) kinase HRI (Inuzuka *et al.*, 2004), sense heme per se and become active (or inactive) upon heme binding. In *R. sphaeroides*, the *hem* genes encode the enzymes which are involved in the biosynthesis of heme and other tetrapyrrole-related products (*e.g.*, bacteriochlorophyll). The redox-responding transcription regulators FnrL, the PrrB/PrrA

system and the AppA/PpsR system control the expression of *hem* genes in response to changes in oxygen tension (Moskvin *et al.*, 2005). Smart and Bauer (2006) found that the regulation of *hem* gene expression in *R. capsulatus* is a feedback control involving the heme binding protein HbrL, which functions as an activator of *hemA* and *hemZ* expression in the absence of heme and as a repressor of *hemB* expression in the presence of heme. Therefore, it is also possible that AppA applies the same mechanism as HbrL. AppA may indirectly sense the redox potential by sensing the overproduced heme in response to changes in cellular redox and consequently controls the expression of *hem* genes and other PS genes.

The primary sequence of the C-terminal domain of AppA shows no significant homology to any known heme-binding protein and no conserved histidine residues are present. Therefore, it was assumed that the C-terminal domain of AppA might bind heme precursors without the central iron. However, no binding of protoporphyrin IX could be detected after incubating purified AppAΔN protein with protoporphyrin IX. Nevertheless, the binding of the C-terminal domain of AppA to hemin agarose and the redox activity of the bound heme strongly support the presence of iron, suggesting that AppA harbours a new type of heme binding domain.

5.3 How does PpsR regulate the PS gene expression in response to oxygen tension and light quality in the phototrophic bacteria?

The PpsR proteins have been mainly characterized in the two closely related species *Rhodobacter sphaeroides* and *Rhodobacter capsulatus*. PpsR blocks the transcription of several PS gene operons by binding to the target sequence (TGT-N_{12}-ACA) found in tandom in the promoter region of many PS genes (Gomelsky and Kaplan, 1995; Ponnampalam and Bauer, 1997). Recently, the PpsR proteins have been found in diverse species of anoxygenic photosynthetic bacteria, such as *Bradyrhizobium* (Jaubert *et al.*, 2004), *Rhodopseudomonas (Rps.) palustris* (Giraud *et al.*, 2002), *Rubrivivax gelatinosus* (Steunou *et al.*, 2004), suggesting that PpsR may be a global regulator of photosynthetic apparatus biosynthesis genes in anoxygenic photosynthetic bacteria. The sequence analysis revealed that the *ppsR* genes are in all cases localized within the photosynthetic gene cluster.

5.3.1 DNA-binding mechanism of PpsR

Two mechanisms involved in controlling the DNA-binding affinity of PpsR are well characterized. One mechanism involves oxidation-reduction of two cysteine residues. For example, CrtJ (counterpart of PpsR) in *R. capsulatus* undergoes a dithiol-disulfide switch when oxygen tension increases (Ponnampalam and Bauer, 1997; Masuda *et al.*, 2002). In aerobically grown cells, two cysteine residues (marked in Figure 5.4) are believed to be oxidized and form an intramolecular disulfide bond, whereas in the anaerobically grown cells, they exist as free thiols. The oxidized CrtJ shows a higher DNA binding affinity (Ponnampalam and Bauer, 1997; Masuda *et al.*, 2002). However, a comparison with the other PpsR sequences indicates that only the Cys residue located in the HTH domain (the DNA-binding domain) is well conserved (Figure 5.4). Among the different PpsR proteins characterized, *Bradyrhizobium* PpsR1 and *Thiocapsa roseopersicina* PpsR1 contain only one Cys residue in the HTH domain, while *Bradyrhizobium* PpsR2, *Rps. palustris* PpsR2 and *T. roseopersicina* PpsR2 lack the Cys residue (Figure 5.4). Jaubert *et al.* (2004) showed that PpsR1 of *Bradyrhizobium* OR278, in spite of its unique Cys residue, retains redox sensitivity via the formation of an intermolecular disulfide bond. Contrary to CrtJ, the DNA binding affinity of *Bradyrhizobium* PpsR1 was higher under reduced conditions (Jaubert *et al.*, 2004). In the case of *Bradyrhizobium* PpsR2, which lacks the Cys residue, no direct redox effect has been observed on its DNA-binding activity (Jaubert *et al.*, 2004). It was suggested that *Bradyrhizobium* PpsR2 is inactivated by forming a complex with bacteriophytochrome (BphP) (Giraud *et al.*, 2002; Jaubert *et al.*, 2004; and later chapter).

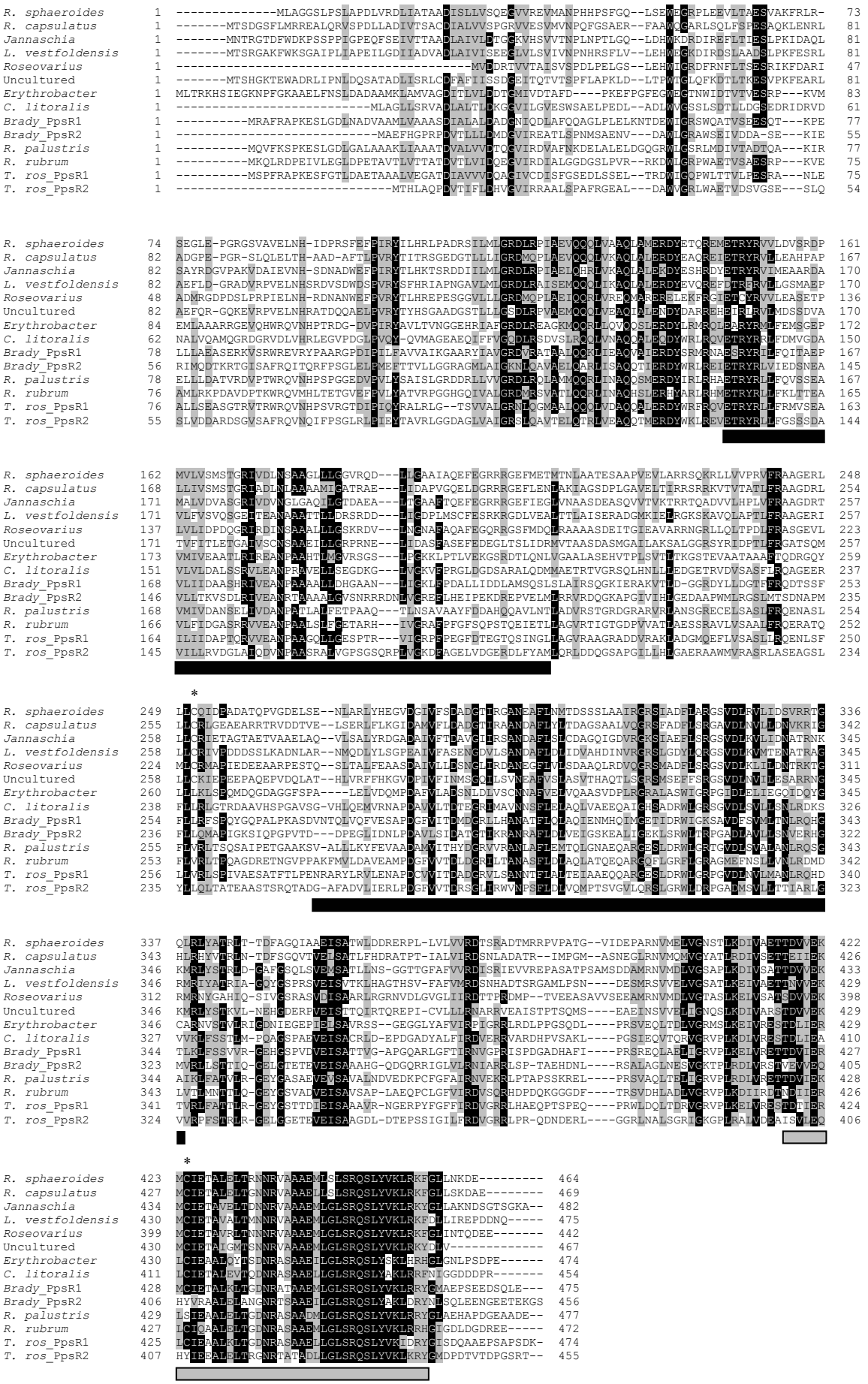
R. sphaeroides
R. capsulatus
Jannaschia
L. vestfoldensis
Roseovarius
Uncultured
Erythrobacter
C. litoralis
Brady_PpsR1
Brady_PpsR2
R. palustris
R. rubrum
T. ros_PpsR1
T. ros_PpsR2

Figure 5.4 Multiple sequence alignment of the PpsR homologues.

Sequence similarity search was performed at NCBI (http://www.ncbi.nlm.nih.gov/BLAST/) using BLASTP with default settings. The selected sequences shown in this figure have scores >150 and E-value $<1e^{-35}$. The multiple sequence alignment was generated by CLUSTAL W with default parameters. The similarity identification was performed using BioEdit sequence alignment editor with the shade threshold ≥ 60%. Region of similarity (grey) and identity (black) are highlighted. The stars (*) represent conserved cysteine residues in PpsR and CrtJ. The black boxes below the sequences represent the PAS domains and the grey box below the sequences represents the HTH domain. The organisms listed from top to bottom and their respective GenBank accession numbers are *Rhodobacter sphaeroides* 2.4.1 YP_353356; *Rhodobacter capsulatus* S17813; *Jannaschia* sp. CCS1 YP_508106; *Loktanella vestfoldensis* SKA53 ZP_01002308; *Roseovarius* sp. 217 ZP_01034603; uncultured proteobacterium AAM48684; *Erythrobacter* sp. NAP1 ZP_01041674; *Congregibacter litoralis* KT71 EAQ96254; *Bradyrhizobium* sp. ORS278 AAT78846; *Bradyrhizobium* sp. ORS278 AAL68701; *Rhodopseudomonas palustris* BisB5 YP_570870; *Rhodospirillum rubrum* ATCC 11170 YP_425717; *Thiocapsa roseopersicina* AAX53585; *Thiocapsa roseopersicina* AAX53580.

The second mechanism of controlling DNA-binding affinity of PpsR involves interactions between PpsR and an antagonist, such as the AppA protein in *R. sphaeroides*, which was mainly discussed in this work. PpsR contains two conserved Cys residues as CrtJ (Figure 5.4), therefore, it was previously assumed to undergo a dithiol-disulfide switch when oxygen tension changes. However, the study on the *in vivo* redox sates of the two cysteines of PpsR in *R. sphaeroides* showed that the thiol group of the two cysteines in PpsR exists in a reduced state irrespective of oxygen (Figure 4.15), which is in agreement with the findings from Cho *et al.* (2004). This suggests that the cysteine residues in *R. sphaeroides* PpsR are not involved in PpsR DNA-binding activity in contrast to those of CrtJ. Actually, the repressive activity of the PpsR protein is modulated by the flavoprotein AppA (Gomelsky & Kaplan, 1997), which is unique in its ability to sense and transmit both redox and light signals (Braatsch *et al.*, 2002; Masuda and Bauer, 2002; Han *et al.*, 2004; and this work). A model for the integration of redox and light responses by the AppA/PpsR system was proposed in the previous chapter (Figure 5.3). AppA contains an N-terminal BLUF domain responsible for the light dependent signaling and a C-terminal heme-binding domain responsible for both light and redox dependent signaling. The DNA-binding activity of PpsR is inhibited by establishing AppA-PpsR complex.

However, the AppA protein is not found in other purple bacteria. Interestingly, a new type of bacteriophytochrome (BphP) was reported to control the synthesis of the entire photosynthetic apparatus of *Bradyrhizobium* ORS278 (Giraud *et al.*, 2002). A similar behaviour is observed for the closely related species *Rps. palustris*, but not for the more distant anoxygenic photosynthetic bacteria of the genus *Rhodobacter*, *Rubrivivax* or

Rhodospirillum. Like the AppA protein, BphP is also a photoreceptor protein. The light regulation of BphP is associated to their capability to exist in two photo-interconvertible forms (the red-light-absorbing form and the far-red-light absorbing form). Based on the phenotypes of *Bradyrhizobium bphP* and *ppsR2* deletion mutants and on the action spectrum of the photosystem synthesis, the red form of BphP was proposed to antagonize the repressive effect of PpsR2 (Giraud *et al.*, 2002).

5.3.2 Dual roles of PpsR: repressor and activator

In *Rhodobacter*, PpsR was characterized as a repressor of PS genes. Two PpsR binding sites are located upstream of numerous photosystem genes (Choudhary & Kaplan, 2000) and overlap the -10 and -35 regions where RNA polymerase would normally bind. This indicates that PpsR represses PS gene transcription by competing with RNA polymerase for binding to DNA, which was confirmed by *in vitro* transcription assays with *R. capsulatus* housekeeping RNA polymerase (Bowman *et al.*, 1999).
Interestingly, Steunou *et al.* (2004) reported that PpsR in *Rubrivivax gelatinosus* is a dual regulator: repressor and activator. *Rubrivivax gelatinosus* PpsR acts as an aerobic repressor of the *crtI* gene, while it acts as an activator for the expression of *pucBA*. The duality of PpsR was also reported in *Bradyrhizobium* OR278 (Jaubert *et al.*, 2004). Different from *Rubrivivax gelatinosus*, there are two PpsR homologues present in *Bradyrhizobium* OR278, each possessing a single activity: PpsR1 is an activator whereas PpsR2 is a repressor.

In summary, PpsR is a global regulator in purple bacteria which controls the expression of PS genes according to redox and light conditions. In different organisms, PpsRs may exhibit different regulatory features: i) the DNA-binding affinity of PpsR is modulated either by the redox states of cysteine residue(s) or by the interaction with other specific regulators; ii) PpsR can function either as a repressor or as an activator of PS genes.

5.4 The AppA/PpsR system coordinately regulates PS gene expression together with the PrrB/PrrA system

In *R. sphaeroides*, a sophisticated regulatory circuit has been developed to control the photosystem biosynthesis in response to two external stimuli: oxygen and light. Several regulatory systems, including the AppA/PpsR system, the PrrB/PrrA system, FnrL, PpaA

TrxA and so on, have been shown to be involved in controlling PS gene expression. Among these regulatory proteins, the AppA protein is the only photoreceptor protein, indicating that AppA plays a key role in blue light repression on PS gene expression. Some of the mutants analysed in this study with 3 amino acid exchanges in the heme binding domain resemble the APP11 strain that lacks the AppA protein. All phenotypically APP11-like strains showed very low overall expression levels of *puf* and *puc* genes (Figure 4.29 and Table 4.2). No light regulated *puf* or *puc* expression was observed in the strains with strongly reduced *puc* mRNA levels (*e.g.*, APP11, RM3, RM9, RM12 and RM21). It can be concluded that the AppA/PpsR system is the major system that represses both the *puf* and the *puc* genes in the presence of light.

The PrrB/PrrA two-component system in *R. sphaeroides* activates the expression of photosynthesis genes at low oxygen tension. PrrB functions as a sensor histidine-kinase/phosphatase and PrrA functions as a response regulator through binding DNA targets. Happ *et al.* (2005) showed that light can activate the PS gene expression via the PrrB/PrrA system under anaerobic conditions. In the absence of PrrA, expression of *puc* and *puf* genes is very low under semi-aerobic conditions and no repression can be observed in the light (Metz, 2006). These results indicate that the AppA/PpsR system coordinately controls light-dependent regulation of PS gene expression together with the PrrB/PrrA system.

In this work, the AppA mutants were also analyzed with regard to redox-dependent regulation of the *puf* and *puc* genes (Figure 4.29 and Table 4.2). When the strains lack the functional AppA (*e.g.*, APP11, RM3, RM9, RM12 and RM13), the basal expression levels of *puf* and *puc* are much lower than those of the wild-type strain (Table 4.2 and Figure 4.29). It could be due to the fact that *puf* and *puc* genes are repressed by PpsR. Despite this repressive effect, some activation by PrrA at low oxygen concentration takes place. Hence, the *puf* and *puc* genes in the strains expressing malfunctional AppA still exhibit redox-dependent expression, suggesting that the PrrB/PrrA system is sufficient for the redox control of *puf* and *puc* transcription. When the response regulator PrrA is lacking, the transcripts of *puf* and *puc* in the cells grown under all growth conditions were no longer detectable by Northern blot analysis (Figure 4.29). This suggests that PrrA is also important for the basal expression levels of *puf* and *puc* genes. Therefore, the redox-dependent regulation by the AppA/PpsR system requires the presence of the two-component PrrB/PrrA system.

So far, how the AppA/PpsR system and the PrrB/PrrA system communicate with each other to achieve coordinate regulation of photosystem development is not well understood in *R. sphaeroides*. Moskvin *et al.* (2005) suggested these two systems may control each other's synthesis or activities, because the expression of *prrA* indirectly depends on PpsR. Recently, Jaeger *et al.* (unpublished) have proposed a model of the competition for promoter binding between the PpsR repressor and the PrrA activator. *In vitro* footprint analysis showed that CrtJ (counterpart of PpsR) in *R. capsulatus* can effectively compete with RegA (counterpart of PrrA) for the binding of the *puc* promoter (Bowman *et al.*, 1999).

5.5 Perspectives

This study demonstrates that the BLUF domain of AppA is a sensory module that interacts with the C-terminal domain of AppA in response to light. The amino acids within the BLUF domain important for the photo-excitation were intensively investigated. Unfortunately, the amino acids essential for the interaction with the C-terminus of AppA are unknown yet. To make this clear, random mutagenesis can be performed in the BLUF domain and selection can be performed according to the colour of colonies.

The C-terminal part of AppA harbours a heme-binding domain. The PpsR-binding affinity of AppA may be controlled either by the association/disassociation of oxygen to the heme bound by AppA or by the amount of heme in the cell. To figure out which process is carried out in *R. sphaeroides*, the influence of heme redox state on the PpsR-binding affinity of AppA should be tested by *in vitro* binding assays under anoxic conditions. Since the primary sequence of AppA does not show a significant homology to a known heme binding protein, the structure model of the C-terminus of AppA would benefit the studies on the heme-binding properties and the mechanism for the regulation of PS gene expression via the AppA-PpsR system.

The central region of PpsR contains two PAS domains, which were reported to be critical for proper conformation and repressor activity (Gomelsky *et al.*, 2000). Some PAS domains are found to bind the cofactor heme and involved in signal sensing and transduction (Gilles-Gonzalez and Gonzalez, 2004). The PpsR PAS domains exhibit some sequence similarity to heme-binding PAS domains. Recently, CrtJ (counterpart of PpsR) in *R. capsulatus* was proved to be a heme-binding protein (Setterdahl and Bauer, 2006). Because no cofactor was detected in the GST-tagged PpsR purified after overproduction

in *E. coli* contained any cofactor, the overexpression of PpsR should be performed in the presence of the heme precursor δ-ALA to find out whether isolated PpsR protein binds heme. Moreover, mutagenesis of the PAS domains would be also helpful.

The consensus PpsR-binding sequence, TGT-N_{12}-ACA, is present in the promoter region of several PS genes (Figure 1.2B), such as the *puc*, *bch*, and *crt* operons, but not in the upstream region of the *puf* operon, which is also located in the PS gene cluster (Figure 1.2). The blue light repression on the *puf* genes is missing in *ppsR* null mutant strain PPS1 (Figure 4.41A), indicating that the expression of the *puf* operon is under the control of PpsR. This is in agreement of previous studies on the regulation of *puf* gene expression (Braatsch *et al.*, 2002; 2004; Moskvin *et al.*, 2005). It is likely that PpsR interacts with other regulators and indirectly controls *puf* gene expression. Therefore, the yeast two-hybrid assay can be performed to find out the putative PpsR interacting partners.

The mutant analysis in this work confirms the interdependence of the AppA/PpsR and PrrB/PrrA pathways. To know whether two systems regulate each other's synthesis or activities, the AppA or PrrA protein levels should be determined in wild-type strain and PrrA- or AppA-deficient strains under variable light and oxygen conditions. Another hypothesis is that PpsR and PrrA may competitively bind to the promoter region of target gene. Therefore, protein-DNA binding assays should be performed *in vivo* under variable light and oxygen conditions.

6 Summary

The AppA protein in *Rhodobacter sphaeroides* is an antagonist of the transcriptional repressor protein PpsR, which can block the transcription of several photosynthesis genes through binding to a consensus sequence. To date, the AppA protein is unique in its ability to sense and transmit both light and redox signals.

The AppA protein consists of an N-terminal FAD-binding domain, recently named BLUF (sensors of **b**lue **l**ight **u**sing **F**AD), and a C-terminal domain, which is involved in the light- and redox-dependent regulation of photosynthesis genes. The BLUF domain is a new family of blue light photoreceptors and it is present either in multidomain proteins or as a short protein only consisting of the BLUF domain. Recently, four BLUF domains have been found in the photoreceptor protein photoactivated adenylyl cyclase (PAC) from the eukaryotic organism *Euglena gracilis*. Each BLUF domain is linked to a downstream domain whose function is completely different from that of the C-terminal domain of AppA.

In this work, a hybrid protein containing one of the BLUF domains from the PAC protein and the C-terminal domain of AppA was expressed in *R. sphaeroides* and the function of this hybrid protein was investigated. The results showed that the BLUF domain from the PAC protein can fully replace the AppA-BLUF domain in the light-dependent signaling. Moreover, this work revealed that the signal transmission by AppA does not require covalent linkage of the BLUF domain and the C-terminal domain. These two observations demonstrate that the BLUF domain is fully modular and can relay signals to completely different output domains. It was previously assumed that the small BLUF-containing proteins transfer the light-dependent signals to other proteins by protein-protein interactions. The interaction between the BLUF domain and the C-terminal domain of AppA revealed in this work supports this assumption.

The previous studies have shown that AppA interacts with PpsR and inhibits the repressor activity of PpsR. However, the interacting domains of AppA and PpsR have not been determined. It was found in this study that the C-terminal domain of AppA is sufficient to inhibit the DNA-binding activity of PpsR *in vivo* and *in vitro*. This observation indicates that the binding site between AppA and PpsR must be located at the C-terminal domain of AppA. Furthermore, surface plasmon resonance (SPR) based interaction studies demonstrate that the C-terminal domain of AppA can interact with PpsR in the absence of

the BLUF domain. In addition, this work presented the first evidence that the C-terminal domain of AppA contains a heme as the redox sensitive prosthetic group. Mutant analysis revealed that some of the amino acids in the heme-binding domain are essential for the function of AppA. It was also found that the cofactor heme affects not only the interaction of the C-terminal domain of AppA with PpsR but also the interaction of the C-terminal domain of AppA with the BLUF domain. These data demonstrate that the cofactor heme plays a key role in the light- and redox-dependent signaling.

Besides the AppA/PpsR system, several other regulatory systems in *R. sphaeroides* also control the expression of photosynthesis genes according to light and redox conditions. Thus, the interplay between the AppA/PpsR system and other systems was investigated in this work. The results showed that i) the AppA/PpsR system is the major contributor that mediates the expression of photosynthesis genes in response to light, ii) the PrrB/PrrA system is sufficient to activate photosynthesis gene expression in response to the decrease of oxygen and the redox-dependent regulation by the AppA/PpsR system requires the presence of the PrrB/PrrA system, and iii) the deficiency of thioredoxin causes the increase in the redox potential and consequently affects the AppA-PpsR system in light-dependent signaling.

7 Zusammenfassung

Das AppA Protein aus *Rhodobacter sphaeroides* ist ein Antagonist des Transkriptions-repressor-Proteins PpsR, das die Transkription verschiedener Photosynthesegene durch Bindung an eine spezifische DNA Erkennungssequenz unterbindet. Die Fähigkeit, sowohl Licht- als auch Redox Signale zu messen und weiterzuleiten, ist bislang nur von AppA bekannt.

Das AppA Protein besteht aus einer N-terminalen FAD-Bindedomäne, die als BLUF (**b**lue **l**ight **u**sing **F**AD Sensor) bezeichnet wird, und einer C-teminalen Domäne, die an der licht- und redoxabhängigen Regulation von Photosynthesegenen beteiligt ist. Die BLUF Domäne stellt eine neue Familie innerhalb der Blaulichtrezeptoren dar und ist entweder Bestandteil eines Proteins mit mehreren Domänen oder ein kleines Protein, das nur die BLUF Domäne beinhaltet. Kürzlich wurden vier BLUF Domänen in dem Photorezeptor-Protein PAC (**P**hotoaktivierte **A**denyl **C**yclase) des eukaryotischen Organismus *Euglena gracilis* beschrieben. Jede der BLUF Domänen ist *downstream* an eine Domäne mit gänzlich anderer Funktion als der C-terminale Bereich von AppA gekoppelt.

In dieser Arbeit wurde ein Hybridprotein mit einer der BLUF Domänen des PAC Proteins und der C-terminalen Domäne des AppA Proteins in *R. sphaeroides* exprimiert und die Funktion dieses Hybridproteins untersucht. Die Ergebnisse zeigen, dass die BLUF Domäne des PAC Proteins die Funktion der lichtabhängigen Signalwahrnehmung und -weiterleitung der AppA-BLUF Domäne vollständig ersetzen kann. Darüberhinaus zeigt diese Arbeit, dass die Signalübertragung durch AppA keine kovalente Bindung der BLUF Domäne mit der C-terminalen Domäne erfordert. Diese beiden Beobachtungen demonstrieren, dass die BLUF Domäne gänzlich modular aufgebaut ist und Signale an unterschiedlichste Ausgabedomänen weitergeleitet werden können. Es wurde vermutet, dass kleine Proteine, die eine BLUF Domäne enthalten, lichtabhängige Signale mittels Protein-Protein Interaktion auf andere Proteine übertragen. Diese Vermutung wird durch die gezeigte Interaktion zwischen der BLUF Domäne und der C-terminalen Domäne von AppA unterstützt.

Frühere Arbeiten haben gezeigt, dass AppA mit PpsR interagiert und die Repressoraktivität von PpsR inhibiert. Die interagierenden Domänen von AppA und PpsR wurden jedoch noch nicht bestimmt. Diese Studie zeigt, dass die C-terminale

Domäne von AppA ausreicht, die DNA bindende Aktivität von PpsR sowohl *in vivo* als auch *in vitro* zu inhibieren. Diese Beobachtung deutet darauf hin, dass die Bindungstelle zwischen AppA und PpsR in der C-terminalen Domäne von AppA lokalisiert sein muss. Außerdem zeigten Oberflächenplasmonresonanz (SPR) basierte Interaktionsstudien, dass die C-terminale Domäne von AppA auch in der Abwesenheit der BLUF Domäne mit PpsR ineragieren kann. Darüberhinaus gibt diese Arbeit den ersten Hinweis darauf, dass die C-terminale Domäne des AppA Proteins ein Häm als redox-sensitive prosthetische Gruppe enthält. Mutationsanalysen zeigten, dass einige Aminosäuren in der Häm-bindenden Domäne essentiell für die Funktion von AppA sind. Es wurde auch gezeigt, dass der Kofaktor Häm nicht nur die Interaktion der C-terminalen Domäne von AppA mit PpsR beeinflusst, sondern auch die Interaktion zwischen der C-terminalen Domäne von AppA und der BLUF Domäne. Diese Daten verdeutlichen, dass Häm als Kofaktor eine Schlüsselrolle in der licht- und redoxabhängigen Signalübertragung zukommt.

Neben dem AppA/PpsR System sind mehrere andere Regulationssysteme in *R. sphaeroides* an der Kontrolle der Expression von Photosynthesegenen in Abhängigkeit von Licht und Redox Bedingungen beteiligt. Daher wurde die Wechselwirkung zwischen dem AppA/PpsR System und anderen Systemen in dieser Arbeit untersucht. Die Ergebnisse zeigen, dass a) das AppA/PpsR System der bedeutendste Regulator der Expression der Photosynthesegene im Rahmen einer Lichtantwort ist, b) das PrrB/PrrA System ausreicht, um die Expression der Photosynthesegene in Antwort auf ein Absenken des Sauerstoffgehalts zu aktivieren, wobei die Anwesenheit des PrrB/PrrA Systems für die redox-abhängige Regulation durch AppA/PpsR benötigt wird, und c) das Fehlen von Thioredoxin einen Anstieg des Redox-Potentials bewirkt und somit das AppA/PpsR System in der licht-abhängigen Signalwahrnehmung beeinflusst.

8 References

Amezcua, C.A., Harper ,S.M., Rutter, J., and Gardner, K.H. (2002) Structure and interactions of PAS kinase N-terminal PAS domain model for intramolecular kinase regulation. *Structure* **10**: 1349-1361.

Anderson, S., Dragnea, V., Masuda, S., Ybe, J., Moffat, K., and Bauer, C.E. (2005) Structure of a novel photoreceptor, the BLUF domain of AppA from *Rhodobacter sphaeroides*. *Biochemistry* **44**: 7998-8005.

Antonini, E., Brunori, M. (1971) *Hemoglobin and myoglobin in their reactions with ligands.* Amsterdam: Elsevier/North-Holland Biomedical Press.

Aslund, F., Zheng, M., Beckwith, J., and StorZ, G. (1999) Regulation of the OxyR transcription factor by hydrogen peroxide and the cellular thiol-disulfide status. *Proc. Natl. Acad. Sci. USA* **96**: 6161-6165.

Ausmees, N., Mayer, R., Weinhouse, H., Volman, G., Amikam, D., Benziman, M., and Lindberg, M. (2001) Genetic data indicate that proteins containing the GGDEF domain possess diguanylate cyclase activity. *FEMS Microbiol. Lett.* **204**: 163-167.

Barany, F. (1985) Two-condon insertion mutagenesis of plasmid genes by using single strained hexameric oligonucleotids. *Proc. Natl. Acad. Sci. USA* **82**: 4202-4206.

Berry, E.A., Trumpower, B.L. (1987) Simultaneous determination of hemes *a*, *b*, and *c* from pyridine hemochrome spectra. *Anal. Biochem.* **161**: 1-15.

Bowman, W.C., Du, S., Bauer, C.E., and Kranz, R.G. (1999) *In vitro* activation and repression of photosynthesis gene transcription in *Rhodobacter capsulatus*. *Mol. Microbiol.* **33**: 429-437.

Braatsch, S. (2002) Blaulichtabhängige Regulation von Photosynthesegenen in *Rhodobacter*. Doctorarbeit. Justus-Liebig-Universität, Giessen.

Braatsch, S., Gomelsky, M., Kuphal, S., and Klug, G. (2002) A single flavoprotein, AppA, integrates both redox and light signals in *Rhodobacter sphaeroides*. *Mol. Microbiol.* **45**: 827-836.

Braatsch, S., Klug, G. (2004) Blue light perception in bacteria. *Photosynth. Res.* **79**: 45-57.

Braatsch, S., Moskvin, O.V., Klug, G., and Gomelsky, M. (2004) Responses of the *Rhodobacter sphaeroides* transcriptome to blue light under semiaerobic conditions. *J. Bacteriol.* **186**: 7726-7735.

Bradford, M.M. (1976) A rapid and sensitive method for the quantitation of microgram quantities of protein utilizing the principle of protein-dye binding. *Anal. Biochem.* **72**: 248-254.

Briggs, W.R., Christie, J.M. (2002) Phototropins 1 and 2: versatile plant blue-light receptors. *Trends Plant Sci.* **7**: 204-210.

Briggs, W.R., Christie, J.M., and Salomon, M. (2001) Phototropin: a new family of flavin-binding blue light receptors in plants. *Antioxid. Redox Signal.* **3**: 775-788.

Cashmore, A.R., Jarillo, J.A., Wu, Y.-J., and Liu, D. (1999) Cryptochromes: blue light receptors for plants and animals. *Science* **284**: 760-765.

Chelikani, P., Fita, I., and Loewen, P.C. (2004) Diversity of structures and properties among catalases. *Cell. Mol. Life Sci.* **61**: 192-208.

Cho, S.-H., Youn, S.-H., Lee, S.-R., Yim, H.-S., and Kang, S.-O. (2004) Redox property and regulation of PpsR, a transcriptional repressor of photosystem gene expression in *Rhodobacter sphaeroides*. *Microbiol.* **150**: 697-705.

Choudhary, M., Kaplan, S. (2000) DNA sequence analysis of the photosynthesis region of *Rhodobacter sphaeroides* 2.4.1^{T}. *Nucleic Acids Res.* **28**: 862-867.

Christie, J.M., Salomon, M., Nozue, K., Wada, M., and Briggs, W.R. (1999) LOV (light, oxygen, or voltage) domains of the blue-light photoreceptor phototropin (nph1): binding sites for the chromophore flavin mononucleotide. *Proc. Natl. Acad. Sci. USA* **96**: 8779-8783.

Crosson, S., Rajagopal, S., and Moffat, K. (2003) The LOV domain family: photoresponsive signaling modules coupled to diverse output domains. *Biochemistry* **42**: 2-10.

Drews, G. (1985) Structure and functional organization of light-harvesting complexes and photochemical reaction centers in membranes of phototrophic bacteria. *Microbiol. Rev.* **49**: 59-70.

Drews, G., Imhoff, J.F. (1991) Phototrophic Purple Bacteria. In *Variations in Autotrophic Life*. Shively, J.M., Barton, L.L. (eds). London: Academic Press, pp. 51-97.

Edwards, P.R., Leatherbarrow, R.J. (1997) Determination of association rate constants by an optical biosensor using initial rate analysis. *Anal. Biochem.* **246**: 1-6.

Elsen, S., Jaubert, M., Pignol, D., and Giraud, E. (2005) PpsR: a multifaceted regulator of photosynthesis gene expression in purple bacteria. *Mol. Microbiol.* **57**: 17-26.

Eraso, J.M., Kaplan, S. (1994) *prrA*, a putative response regulator involved in oxygen regulation of photosynthesis gene expression in *Rhodobacter sphaeroides*. *J. Bacteriol.* **176**: 32-43.

Eraso, J.M., Kaplan, S. (1995) Oxygen-insensitive synthesis of the photosynthetic membranes of *Rhodobacter sphaeroides*: a mutant histidine kinase. *J. Bacteriol.* **177**: 2695-2706.

Eraso, J.M., Kaplan, S. (1996) Complex regulatory activities associated with the histidine kinase PrrB in expression of photosynthesis genes in *Rhodobacter sphaeroides* 2.4.1. *J. Bacteriol.* **178**: 7037-7046.

Eraso, J.M., Kaplan, S. (2000) From redox flow to gene regulation: role of the PrrC protein of *Rhodobacter sphaeroides* 2.4.1. *Biochemistry* **39**: 2052-2062.

Fukushima, Y., Okajima, K., Shibata, Y., Ikeuchi, M., and Itoh, S. (2005) Primary intermediate in the photocycle of a blue-light sensory BLUF FAD-protein, Tll0078, of *Thermosynechococcus elongatus* BP-1. *Biochemistry* **44**: 5149-5158.

Gauden, M., Yeremenko, S., Laan, W., van Stokkum, I.H.M., Ihalainen, J.A., van Grondelle, R., Hellingwerf, K.J., and Kennis, J.T.M. (2005) Photocycle of the flavin-binding photoreceptor AppA, a bacterial transcriptional antirepressor of photosynthesis genes. *Biochemistry* **44**: 3653-3662.

Gilles-Gonzalez, M.-A., Gonzalez, G. (2004) Signal transduction by heme-containing PAS-domain proteins. *J. Appl. Physiol.* **96**: 774-783.

Gilles-Gonzalez, M.-A., Gonzalez, G. (2005) Heme-based sensors: defining characteristics, recent development, and regulatory hypotheses. *J. Inorg. Biochem.* **99**: 1-22.

Giraud, E., Fardoux, J., Fourrier, N., Hannibal, L., Genty, B., Bouyer, P., Dreyfus, B., and Verméglio, A. (2002) Bacteriophytochrome controls photosystem synthesis in anoxigenic bacteria. *Nature* **417**: 202-205.

Gomelsky, L., Sram, J., Moskvin, O.V., Horne, I.M., Dodd, H.N., Pemberton, J.M., McEwan, A.G., Kaplan, S., and Gomelsky, M. (2003) Identification and *in vivo* characterization of PpaA, a regulator of photosystem formation in *Rhodobacter sphaeroides*. *Microbiol.* **149**: 377-388.

Gomelsky, M., Horne, I.M., Lee, H.-J., Pemberton, J.M., McEwan, A.G., and Kaplan, S. (2000) Domain structure, oligomeric state, and mutational analysis of PpsR, the *Rhodobacter sphaeroides* repressor of photosystem gene expression. *J. Bacteriol.* **182**: 2253-2261.

Gomelsky, M., Kaplan, S. (1995a) *appA*, a novel gene encoding a *trans*-acting factor involved in the regulation of photosynthesis gene expression in *Rhodobacter sphaeroides* 2.4.1. *J. Bacteriol.* **172**: 4609-4618.

Gomelsky, M., Kaplan, S. (1995b) Genetic evidence that PpsR from *Rhodobacter sphaeroides* 2.4.1 functions as a repressor of *puc* and *bchF* expression. *J. Bacteriol.* **177**: 1634-1637.

Gomelsky, M., Kaplan, S. (1995c) Isolation of regulatory mutants in photosynthesis gene expression in *Rhodobacter sphaeroides* 2.4.1 and partial complementation of a PrrB mutant by the HupT histidine-kinase. *Microbiol.* **141**: 1805-1809.

Gomelsky, M., Kaplan, S. (1997) Molecular genetic analysis suggesting interactions between AppA and PpsR in regulation of photosynthesis gene expression in *Rhodobacter sphaeroides* 2.4.1. *J. Bacteriol.* **179**: 128-134.

Gomelsky, M., Kaplan, S. (1998) AppA, a redox regulator of photosystem formation in *Rhodobacter sphaeroides* 2.4.1, is a flavoprotein. Identification of a novel FAD binding domain. *J. Biol. Chem.* **273**: 35319-35325.

Gomelsky, M., Klug, G. (2002) BLUF: a novel FAD-binding domain involved in sensory transduction in microorganisms. *TRENDS Biochem. Sci.* **27**: 497-500.

Gregor, J., Klug, G. (1999) Regulation of bacterial photosynthesis genes by oxygen and light. *FEMS Microbiol. Lett.* **179**: 1-9.

Grinstead, J.S., Hsu, S.-T.D., Laan, W., Bonvin, A.M.J.J., Hellingwerf, K.J., Boelens, R., and Kaptein, R. (2006) The solution structure of the AppA BLUF domain: insight into the mechanism of light-induced signaling. *ChemBioChem* **17**: 187-193.

Han, Y., Braatsch, S., Osterloh, L., and Klug, G. (2004) A eukaryotic BLUF domain mediates light-dependent gene expression in the purple bacterium *Rhodobacter sphaeroides* 2.4.1. *Proc. Natl. Acad. Sci. USA* **101**: 12306-12311.

Happ, H.N. (2002) Analyse der lichtabhängigen Expression von Photosynthesegenen in Purpurbakterien mit Hilfe eines Reportergensystems. Examensarbeit. Justus-Liebig-Universität, Giessen.

Happ, H.N., Braatsch, S., Broschek, V., Osterloh, L., and Klug, G. (2005) Light-dependent regulation of photosynthesis genes in *Rhodobacter sphaeroides* 2.4.1 is coordinately controlled by photosynthetic electron transport via the PrrBA two-component system and the photoreceptor AppA. *Mol. Microbiol.* **58**: 903-914.

Hartmann, M. (2004) Neue Ansätze in der biomolekularen Interaktionsanalyse unter besonderer Berücksichtigung pharmazeutischer und lebensmittelchemischer Fragestellungen. Doctorarbeit. University of Bonn, Germany.

Hasegawa, K., Masuda, S., and Ono, T. (2004) Structural intermediate in the photocycle of a BLUF (sensor of blue light using FAD) protein Slr1694 in a Cyanobacterium *Synechocystis* sp. PCC6803. *Biochemistry* **43**: 14979-14986.

Hasegawa, K., Masuda, S., and Ono, T. (2005) Spectroscopic analysis of the dark relaxation process of a photocycle in a sensor of blue light using FAD (BLUF) protein Slr1694 of the Cyanobacterium *Synechocystis* sp. PCC6803. *Plant Cell Physiol.* **46**: 136-146.

Hasegawa, K., Masuda, S., and Ono, T. (2006) Light induced structural changes of a full-length protein and its BLUF domain in YcgF(Blrp), a blue-light sensing protein that uses FAD (BLUF). *Biochemistry* **45**: 3785-3793.

Hazra, P., Inoue, K., Laan, W., Hellingwerf, K.J., and Terazima, M. (2006) Tetramer formation kinetics in the signaling state of AppA monitored by the time-resolved diffusion. *Biophys. J.* **91**: 654-661.

Heintzen, C., Loros, J.J., and Dunlap, J.C. (2001) The PAS protein VIVID defines a clock-associated feedback loop that represses light input, modulates gating, and regulates clock resetting. *Cell* **104**: 453-464.

Hellingwerf, K.J., Hendriks, J., and Gensch, T. (2003) Photoactive Yellow Protein, a new type of photoreceptor protein: Will this "yellow lab" bring us where we want to go? *J. Phys. Chem. A* **107**: 1082-1094.

Hendrischk, A.-K., Braatsch, S., Glaeser, J., and Klug, G. The *phrA* gene of *Rhodobacter sphaeroides* encodes a photolyase and is regulated by singlet oxygen and peroxide in a σ^E dependent manner. Submitted.

Hill, S., Austin, S., Eydmann, T., Jones, T., and Dixon, R. (1996) *Azotobacter vinelandii* NIFL is a flavoprotein that modulates transcriptional activation of nitrogen-fixation genes via a redox-sensitive switch. *Proc. Natl. Acad. Sci. USA* **93**: 2143-2148.

Hoff, W.D., Dux, P., Hard, K., Devreese, B., Nugteren-Roodzant, I.M., Crielaard, W., Boelens, R., Kaptein, R., Van Beeumen, J., and Hellingwerf, K.J. (1994) Thiol ester-linked *p*-coumaric acid as a new photoactive prosthetic group in a protein with rhodopsin-like photochemistry. *Biochemistry* **33**: 13595-13962.

Hughes, J., Lamparter, T., Mittmann, F., Hartmann, E., Gaertner, W., Wild, A., and Boerner, T. (1997) A prokaryotic phytochrome. *Nature* **386**: 663.

Hunter, C.N., Ashby, M.K., and Coomber, S.A. (1987) Effect of oxygen on levels of mRNA coding for reaction-centre and light-harvesting polypeptides of *Rhodobacter sphaeroides*. *Biochem. J.* **247**: 489-492.

Inuzuka, T., Yun, B.-G., Ishikawa, H., Takahashi, S., Hori, H., Matts, R.L., Ishimori, K., and Morishima, I. (2004) Identification of crucial histidines for heme binding in the N-terminal domain of the heme-regulated eIF2α Kinase *J. Biol. Chem.* **279**: 6778-6782.

Iseki, M., Matsunaga, S., Murakami, A., Ohno, K., Shiga, K., Yoshida, K., Sugai, M., Takahashi, T., Hori, T., and Watanabe, M. (2002) A blue-light-activated adenylyl cyclase mediates photoavoidance in *Euglena gracilis*. *Nature* **415**: 1047-1051.

Ito, S., Murakami, A., Sato, K., Nishina, Y., Shiga, K., Takahashi, T., Higashi, S., Iseki, M., and Watanabe, M. (2005) Photocycle features of heterologously expressed and assembled eukaryotic flavin-binding BLUF domains of photoactivated adenylyl cyclase (PAC), a blue-light receptor in *Euglena gracilis*. *Photochem. Photobiol. Sci.* **4**: 762-769.

Jaeger, A., Braatsch, S., Haberzettl, K., Metz, S., Osterloh, L., Han Y., and Klug, G. Light signalling but not redox signalling by the AppA and PpsR proteins from *Rhodobacter sphaeroides* requires a balanced interplay to the PrrA response regulator. Unpublished.

Jaubert, M., Zappa, S., Fardoux, J., Adriano, J.-M., Hannibal, L., Elsen, S., Lavergne, J., Verméglio, A., Giraud, E., and Pignol, D. (2004) Light and redox control of photosynthesis gene expression in *Bradyrhizobium*: dual roles of two PpsR. *J. Biol. Chem.* **279**: 44407-44416.

Jiang, Z., Swem, L.R., Rushing, B.G., Devanathan, S., Tollin, G., and Bauer, C.E. (1999) Bacterial photoreceptor with similarity to photoactive yellow protein and plant phytochromes. *Science* **285**: 406-409.

Joshi, H.M., Tabita, F.R. (1996) A global two component signal transduction system that integrates the control of photosynthesis, carbon dioxide assimilation, and nitrogen fixation. *Proc. Natl. Acad. Sci. USA* **93**: 14515-14520.

Jung, A., Domratcheva, T., Tarutina, M., Wu, Q., Ko, W., Shoeman, R.L., Gomelsky, M., Gardner, K.H., and Schlichting, I. (2005) Structure of a bacterial BLUF photoreceptor: insights into blue light-mediated signal transduction. *Proc. Natl. Acad. Sci. USA* **102**: 12350-12355.

Keen, N.T., Tamaki, S., Kobayashi, D., and Trollinger, D. (1988) Improved broad-host-range plasmids for DNA cloning in Gram-negative bactreia. *Gene* **70**: 191-197.

Kery, V., Elleder, D., and Kraus, J.P. (1995) δ-Aminolevulinate increases heme saturation and yield of human cystathionine β-synthase expressed in *Escherichia coli*. *Arch. Biochem. Biophys.* **316**: 24-29.

Khoroshilova, N., Popescu, C., Münck, E., Beinert, H., and Kiley, P.J. (1997) Iron-sulfur cluster disassembly in the FNR protein of *Escherichia coli* by O_2: [4Fe-4S] to [2Fe-2S] conversion with loss of biological activity. *Proc. Natl. Acad. Sci. USA* **94**: 6087-6092.

Kita, A., Okajima, K., Morimoto, Y., Ikeuchi, M., and Miki, K. (2005) Structure of a cyanobacterial BLUF protein, Tll0078, containing a novel FAD-binding blue light sensor domain. *J. Mol. Biol.* **349**: 1-9.

Kordes, E., Jock, S., Fritsch, J., Bosch, F., and Klug, G. (1994) Cloning of a gene involved in rRNA precursor processing and 23S rRNA cleavage in *Rhodobacter capsulatus*. *J. Bacteriol.* **176**: 1121-1127.

Kort, R., Crielaard, W., Spudich, J.L., and Hellingwerf, K.J. (2000) Color-sensitive motility and methanol release responses in *Rhodobacter sphaeroides*. *J. Bacteriol.* **182**: 3017-3021.

Kort, R., Phillips-Jones, M.K., van Aalten, D.M.F., Haker, A., Hoffer, S.M., Hellingwerf, K.J., and Crielaard, W. (1998) Sequence, chromophore extraction and 3-D model of the photoactive yellow protein from *Rhodobacter sphaeroides*. *Biochimica et Biophysica Acta* **1385**: 1-6.

Kovach, M.E., Elzer, P.H., Hill, D.S., Robertson, G.T., Farris, M.A., Roop II, R.M., and Peterson, K.M. (1995) Four new derivatives of the broad-host-range cloning vector pBBR1MCS, carrying different antibiotic-resistance cassettes. *Gene* **166**: 175-176.

Kraft, B.J., Masuda, S., Kikuchi, J., Dragnea, V., Tollin, G., Zaleski, J.M., and Bauer, C.E. (2003) Spectroscopic and mutational analysis of the blue-light photoreceptor AppA: a novel photocycle involving flavin stacking with an aromatic amino acid. *Biochemistry* **42**: 6726-6734.

Kunert, A., Hagemann, M., and Erdmann, N. (2000) Construction of promoter probe vectors for *Synechocystis sp.* PCC 6803 using the light-emitting reporter system Gfp and LuxAB. *J. Microbiol. Methods* **41**: 185-194.

Kuphal, S. (2001) Lichtabhängige Expression der Photosynthesegene des Purpurbakteriums *Rhodobacter sphaeroides*. Diplomarbeit. Justus-Liebig-Universität, Giessen.

Kurokawa, H., Lee, D.-S., Watanabe, M., Sagami, I., Mikami, B., Raman, C.S., and Shimizu, T. (2004) A redox-controlled molecular switch revealed by the crystal structure of a bacterial heme PAS sensor. *J. Biol. Chem.* **279**: 20186-20193.

Laan, W., Gauden, M., Yeremenko, S., van Grondelle, R., Kennis, J.T.M., and Hellingwerf, K.J. (2006) On the mechanism of activation of the BLUF domain of AppA. *Biochemistry* **45**: 51-60.

Laan, W., van der Horst, M.A., van Stokkum, I.H.M., and Hellingwerf, K.J. (2003) Initial characterization of the primary photochemistry of AppA, a blue-light–using flavin adenine dinucleotide–domain containing transcriptional antirepressor protein from *Rhodobacter sphaeroides*: a key role for reversible intramolecular proton transfer from the flavin adenine dinucleotide chromophore to a conserved tyrosine? *Photochem. Photobiol.* **78**: 290-297.

Laguri, C., Phillips-Jones, M.K., and Williamson, M.P. (2003) Solution structure and DNA binding of the effector domain from the global regulator PrrA (RegA) from *Rhodobacter sphaeroides*: insights into DNA binding specificity. *Nucleic Acids Res.* **31**: 6778-6787.

Lazazzera, B.A., Beinert, H., Khoroshilova, N., Kennedy, M.C., and Kiley, P.J. (1996) DNA binding and dimerization of the Fe-S-containing FNR protein from *Escherichia coli* are regulated by oxygen. *J. Biol. Chem.* **271**: 2762-2768.

Lee, H.J., Yan, Y.L., Marriott, G., and Corn, R.M. (2005) Quantitative functional analysis of protein complexes on surfaces. *J. Physiol. -London* **563**: 61-71.

Lee, J.K., Kaplan, S. (1992) *cis*-acting regulatory elements involved in oxygen and light control of *puc* operon transcription in *Rhodobacter sphaeroides*. *J. Bacteriol.* **174**: 1146-1157.

Lee, J.K., Wang, S., Eraso, J.M., Gardner, J., and Kaplan, S. (1993) Transcriptional regulation of *puc* operon expression in *Rhodobacter sphaeroides*. Involvement of an integration host factor-binding sequence *J. Biol. Chem.* **268**: 24491-24497.

Li, K., Pasternak, C., Härtig, E., Haberzettl, K., Maxwell, A., and Klug, G. (2004) Thioredoxin can influence gene expression by affecting gyrase activity. *Nucleic Acids Res.* **32**: 4563-4575.

Li, K., Pasternak, C., and Klug, G. (2003) Expression of the *trxA* gene for thioredoxin 1 in *Rhodobacter sphaeroides* during oxidative stress. *Arch. Microbiol.* **180**: 484-489.

Lin, C. (2000) Plant blue-light receptors. *Trends Plant Sci.* **5**: 337-342.

Lin, C., Shilitin, D. (2003) Cryptochrome structure and signal transduction. *Annu. Rev. Plant Biol.* **54** : 469-496.

Malik, M., Bensaid, A., Rouviere-Yaniv, J., and Drlica, K. (1996) Histone-like protein HU and bacterial DNA topology: suppression of an HU deficiency by gyrase mutations. *J. Mol. Biol.* **256**: 66-76.

Masuda, S., Bauer, C.E. (2002) AppA is a blue light photoreceptor that antirepresses photosynthesis gene expression in *Rhodobacter sphaeroides*. *Cell* **110**: 613-623.

Masuda, S., Dong, C., Swem, D.L., Setterdahl, A.T., Knaff, D.B., and Bauer, C.E. (2002) Repression of photosynthesis gene expression by formation of a disulfide bond in CrtJ. *Proc. Natl. Acad. Sci. USA* **99**: 7078-7083.

Masuda, S., Hasegawa, K., Ishii, A., and Ono, T. (2004) Light-induced structural changes in a putative blue-light receptor with a novel FAD binding fold sensor of blue-light using FAD (BLUF); Slr1694 of *Synechocystis* sp. PCC6803. *Biochemistry* **43**: 5304-5313.

Masuda, S., Hasegawa, K., and Ono, T. (2005a) Adenosine diphosphate moiety does not participate in structural changes for the signaling state in the sensor of blue-light using FAD domain of AppA. *FEBS Lett.* **579**: 4329-4332.

Masuda, S., Hasegawa, K., and Ono, T. (2005b) Light-induced structural changes of apoprotein and chromophore in the sensor of blue light using FAD (BLUF) domain of AppA for a signaling state. *Biochemistry* **44**: 1215-1224.

Masuda, S., Hasegawa, K., and Ono, T. (2005c) Tryptophan at position 104 is involved in transforming light signal into changes of β-sheet structure for the signaling state in the BLUF domain of AppA. *Plant Cell Physiol.* **46**: 1894-1901.

Messer, W. (1999) DNA, chromosomes, and plasmids. In *Biology of the prokaryotes.* Lengeler,J.W., Drews, G., and Schlegel, H.G. (eds). Stuttgart: Georg Thieme Verlag, pp. 343-361.

Meyer,T.E. (1985) Isolation and characterization of soluble cytochromes, ferredoxins and other chromophoric proteins from the halophilic phototrophic bacterium *Ectothiorhodospira halophila*. *Biochimica et Biophysica Acta* **806**: 175-183.

Metz, S. (2006) Einfluss von Blaulicht auf die Regulation von Photosynthesegenen in *Rhodobacter sphaeroides*: Die Rolle von PpsR bei der blaulichtabhängigen Regulation des *puf* -Operons in *Rhodobacter sphaeroides*. Diplomarbeit. Justus-Liebig-Universität, Giessen.

Moskvin, O.V., Gomelsky, L., and Gomelsky, M. (2005) Transcriptome analysis of the *Rhodobacter sphaeroides* PpsR regulon: PpsR as a master regulator of photosystem development. *J. Bacteriol.* **187**: 2148-2156.

Mosley, C.S., Suzuki, J.Y., and Bauer, C.E. (1994) Identification and molecular genetic characterization of a sensor kinase responsible for coordinately regulating light harvesting and reaction center gene expression in response to anaerobiosis. *J. Bacteriol.* **176**: 7566-7573.

Neidle, E.L., Kaplan, S. (1993) Expression of the *Rhodobacter sphaeroides hemA* and *hemT* genes, encoding two 5-aminolevulinic acid synthase isozymes. *J. Bacteriol.* **175**: 2292-2303.

Nishimura, K., Shimada, H., Hatanaka, S., Mizoguchi, H., Ohta, H., Masuda, T., and Takamiya, K. (1998) Growth, pigmentation, and expression of the *puf* and *puc* operons in a light-responding-repressor (SPB)-disrupted *Rhodobacter sphaeroides*. *Plant Cell Physiol.* **39**: 411-417.

Ntefidou, M., Iseki, M., Watanabe, M., Lebert, M., and Häder, D.-P. (2003) Photoactivated adenylyl cyclase controls phototaxis in the flagellate *Euglena gracilis*. *Plant Physiol.* **133**: 1517-1521.

Oh, J.-I., Eraso, J.M., and Kaplan, S. (2000) Interacting regulatory circuits involved in orderly control of photosynthesis gene expression in *Rhodobacter sphaeroides* 2.4.1. *J. Bacteriol.* **182**: 3081-3087.

Oh, J.-I., Kaplan, S. (2000) Redox signaling: globalization of gene expression. *EMBO J.* **19**: 4237-4247.

Oh, J.-I., Kaplan, S. (2001) Generalized approach to the regulation and integration of gene expression. *Mol. Microbiol.* **39**: 1116-1123.

Oh, J.-I., Ko, I.-J., and Kaplan, S. (2004) Reconstitution of the *Rhodobacter sphaeroides cbb3*-PrrBA signal transduction pathway in vitro. *Biochemistry* **43**: 7915-7923.

Okajima, K., Yoshihara, S., Fukushima, Y., Geng, X., Katayama, M., Higashi, S., Watanabe, M., Sato, S., Tabata, S., Shibata, Y., Itoh, S., and Ikeuchi, M. (2005) Biochemical and functional characterization of BLUF-type flavin-binding proteins of two species of Cyanobacteria. *J. Biochem.* **137**: 741-750.

Osterloh, L. (2003) Regulation von Photosynthesegenen durch Blaulicht in *Rhodobacter*. Diplomarbeit. Justus-Liebig-Universität, Giessen.

Ouchane, S., Kaplan, S. (1999) Topological analysis of the membrane-localized redox-responsive sensor kinase PrrB from *Rhodobacter sphaeroides* 2.4.1. *J. Biol. Chem.* **274**: 17290-17296.

Pappas, C.T., Sram, J., Moskvin, O.V., Ivanov, P.S., Mackenzie, R.C., Choudhary, M., Land, M.L., Larimer, F.W., Kaplan, S., and Gomelsky, M. (2004) Construction and validation of the *Rhodobacter sphaeroides* 2.4.1 DNA microarray: transcriptome flexibility at diverse growth modes. *J. Bacteriol.* **186**: 4748-4758.

Pasternak, C., Assemat, K., Clément-Métral, J.D., and Klug, G. (1997) Thioredoxin is essential for *Rhodobacter sphaeroides* growth by aerobic and anaerobic respiration. *Microbiol.* **143**: 83-91.

Pasternak, C., Haberzettl, K., and Klug, G. (1999) Thioredoxin is involved in oxygen-regulated formation of the photosynthetic apparatus of *Rhodobacter sphaeroides*. *J. Bacteriol.* **181**: 100-106.

Penfold, R.J., Pemberton, J.M. (1994) Sequencing, chromosomal inactivation, and functional expression in *Escherichia coli* of *ppsR*, a gene which represses carotenoid and bacteriochlorophyll synthesis in *Rhodobacter sphaeroides*. *J. Bacteriol.* **176**: 2869-2876.

Pfaffl, M.W. (2001) A new mathematical model for relative quantification in real-time RT–PCR. *Nucleic Acids Res.* **29**: e45.

Ponnampalam, S.N., Bauer, C.E. (1997) DNA binding characteristics of CrtJ. *J. Biol. Chem.* **272**: 18391-18396.

Poulos, T. (1988) Heme enzyme crystal structures. *Adv. Inorg. Biochem.* **7**: 1-36.

Puranik, M., Nielsen, S.B., Youn, H., Hvitved, A.N., Bourassa, J.L., Case, M.A., Tengroth, C., Balakrishnan, G., Thorsteinsson, M.V., Groves, J.T., McLendon, G.L., Roberts, G.P., Olson, J.S., and Spiro, T.G. (2004) Dynamics of carbon monoxide binding to CooA. *J. Biol. Chem.* **279**: 21096-21108.

Rajagopal, S., Key, J.M., Purcell, E.B., Boerema, D.J., and Moffat, K. (2004) Purification and initial characterization of a putative blue light regulated phosphodiesterase from *Escherichia coli*. *Photochem. Photobiol.* **80**: 542-547.

Rodgers, K.R. (1999) Heme-based sensors in biological systems. *Curr. Opin. Chem. Biol.* **3**: 158-167.

Sambrook, J., Russell, D.W. (2001) *Molecular Cloning: A Laboratory Manual.* New York, USA: Cold Spring Harbor Laboratory Press.

Sancar, A. (1994) Structure and function of DNA photolyase. *Biochemistry* **33**: 2-9.

Sancar, A. (2003) Structure and function of DNA photolyase and cryptochrome blue-light photoreceptors. *Chem. Rev.* **103**: 2203-2237.

Sasakura, Y., Yoshimura, T., Kurokawa, H., and Shimizu, T. (2006) Structure-function relationships of *Ec*DOS, a heme-regulated phosphodiesterase from *Escherichia coli*. *Acc. Chem.Res.* **39**: 37-43.

Sato, E., Sagami, I., Uchida, T., Sato, A., Kitagawa, T., Igarashi, J., and Shimizu, T. (2004) SOUL in mouse eyes is a new hexameric heme-binding protein with characteristic optical absorption, resonance Raman spectral, and heme-binding properties. *Biochemistry* **43**: 14189-14198.

Setterdahl, A., Bauer, C.E. (2006) *Rhodobacter capsulatus* transcriptional regulator CrtJ binds heme. ISPP2006, PAU, France

Sganga, M.W., Bauer, C.E. (1992) Regulatory factors controlling photosynthetic reaction center and light-harvesting gene expression in *Rhodobacter capsulatus*. *Cell* **68**: 945-954.

Shimada, H., Iba, K., and Takamiya, K. (1992) Blue-light irradiation reduces the expression of *puf* and *puc* operons of *Rhodobacter sphaeroides* under semi-aerobic conditions. *Plant Cell Physiol.* **33**: 471-475.

Shimada, H., Ohta, H., Masuda, T., Shioi, Y., and Takamiya, K. (1993) A putative transcription factor binding to the up stream region of the *puf* operon in *Rhodobacter sphaeroides*. *FEBS Lett.* **328**: 41-44.

Shimada, H., Wada, T., Handa, H., Ohta, H., Mizoguchi, H., Nishimura, K., Masuda, T., Shioi, Y., and Takamiya, K. (1996) A transcription factor with a leucine-zipper motif involved in light-dependent inhibition of expression of *puf* operon in photosynthetic bacterium *Rhodobacter sphaeroides*. *Plant Cell Physiol.* **37**: 515-522.

Simon, R., Priefer, U., and Pühler, A. (1983) A broad host range mobilization system for *in vivo* genetic engineering: transposon mutagenesis in Gram-negative bacteria. *Bio/Technology* **1**: 37-45.

Smart, J.L., Bauer, C.E. (2006) Tetrapyrrole biosynthesis in *Rhodobacter capsulatus* is transcriptionally regulated by the heme-binding regulatory protein, HbrL. *J. Bacteriol.* **188**: 1567-1576.

Sono, M., Roach, M.P., Coulter, E.D., and Dawson, J.H. (1996) Heme-containing oxygenases. *Chem. Rev.* **96** : 2841-2888.

Sprenger, W.W., Hoff, W.D., Armitage, J.P., and Hellingwerf, K.J. (1993) The eubacterium *Ectothiorhodospira halophila* is negatively phototactic, with a wavelength dependence that fits the absorption spectrum of the photoactive yellow protein. *J. Bacteriol.* **175**: 3096-3104.

Steunou, A.-S., Astier, C., and Ouchane, S. (2004) Regulation of photosynthesis genes in *Rubrivivax gelatinosus*: transcription factor PpsR is involved in both negative and positive control. *J. Bacteriol.* **186**: 3133-3142.

Sun, J., Brand, M., Zenke, Y., Tashiro, S., Groudine, M., and Igarashi, K. (2004) Heme regulates the dynamic exchange of Bach1 and NF-E2-related factors in the Maf transcription factor network. *Proc. Natl. Acad. Sci. USA* **101**: 1461-1466.

Suwanto, A., Kaplan, S. (1989) Physical and genetic mapping of the *Rhodobacter sphaeroides* 2.4.1 genome: presence of two unique circular chromosomes. *J. Bacteriol.* **171**: 5850-5859.

Swem, L.R., Kraft, B.J., Swem, D.L., Setterdahl, A.T., Masuda, S., Knaff, D.B., Zaleski, J.M., and Bauer, C.E. (2003) Signal transduction by the global regulator RegB is mediated by a redox-active cysteine. *EMBO J.* **22**: 4699-4708.

Taylor, B.L., Zhulin, I.B. (1999) PAS domains: internal sensors of oxygen, redox potential and light. *Microbiol. Mol. Biol. Rev.* **63**: 479-506.

Unno, M., Sano, R., Masuda, S., Ono, T., and Yamauchi, S. (2005) Light-induced structural changes in the active site of the BLUF domain in AppA by Raman spectroscopy. *J. Phys. Chem. B* **109**: 12620-12626.

van der Horst, M.A., Hellingwerf, K.J. (2004) Photoreceptor proteins, "Star actors of modern times": a review of the functional dynamics in the structure of representative members of six different photorecpttor families. *Acc. Chem. Res.* **37**: 13-20.

Yang, C.-C., Nash, H.A. (1989) The interaction of *E. coli* IHF protein with its specific binding sites. *Cell* **57**: 869-880.

Yanisch-Perron, C., Vieira, J., and Messing, J. (1985) Improved M13 phage cloning vectors and host strains: nucleotide sequences of the M13mp18 and pUC19 vectors. *Gene* **33**: 103-119.

Zeilstra-Ryalls, J.H., Gabbert, K., Mouncey, N.J., Kaplan, S., and Kranz, R.G. (1997) Analysis of the *fnrL* gene and its function in *Rhodobacter capsulatus*. *J. Bacteriol.* **179**: 7264-7273.

Zeilstra-Ryalls, J.H., Kaplan, S. (1995) Aerobic and anaerobic regulation in *Rhodobacter sphaeroides* 2.4.1: the role of the *fnrL* gene. *J. Bacteriol.* **177**: 6422-6431.

Zeilstra-Ryalls, J.H., Kaplan, S. (1996) Control of *hemA* expression in *Rhodobacter sphaeroides* 2.4.1: regulation through alterations in the cellular redox state. *J. Bacteriol.* **178**: 985-993.

Zeilstra-Ryalls, J.H., Kaplan, S. (1998) Role of the *fnrL* gene in photosystem gene expression and photosynthetic growth of *Rhodobacter sphaeroides* 2.4.1. *J. Bacteriol.* **180**: 1496-1503.

Zeilstra-Ryalls, J.H., Kaplan, S. (2004) Oxygen intervention in the regulation of gene expression: the photosynthetic bacterial paradigm. *Cell. Mol. Life Sci.* **61**: 417-436.

Zeller, T., Klug, G. (2004) Detoxification of hydrogen peroxide and expression of catalase genes in *Rhodobacter*. *Microbiol.* **150**: 3451-3462.

Zeller, T., Klug, G. (2006) Thioredoxins in bacteria: functions in oxidative stress response and regulation of thioredoxin genes. *Naturwissenschaften*. **93**: 259-266

Zeng, X., Kaplan, S. (2001) TspO as a modulator of the repressor/antirepressor (PpsR/AppA) regulatory system in *Rhodobacter sphaeroides* 2.4.1. *J. Bacteriol.* **183**: 6355-6364.

Zheng, M., Aslund, F., and StorZ, G. (1998) Activation of the OxyR transcription factor by reversible disulfide bond formation. *Science* **279**: 1718-1721.

Zhulin, I.B., Taylor, B.L., and Dixon, R. (1997) PAS domain S-boxes in archaea, bacteria and sensors for oxygen and redox. *TRENDS Biochem. Sci.* **22**: 331-333.

Zirak, P., Penzkofer, A., Schiereis, T., Hegemann, P., Jung, A., and Schlichting, I. (2006) Photodynamics of the small BLUF protein BlrB from *Rhodobacter sphaeroides*. *J. Photochem. Photobiol. B* **83**: 180-194.

Acknowledgements

First and foremost I would like to thank my supervisor Prof. Dr. Gabriele Klug for her constant support and excellent guidance. It is her encouragement and valuable suggestions that gave me motives and inspiration to make progress in my scientific research.

I also thank Prof. Dr. Rainer Renkawitz for being my co-supervisor and the referee of my dissertation. I thank HD Dr. Christoph Forreiter for being the referee on my defence.

I would like to express my sincere thanks to Andreas Jäger not only for his technical support but also for his friendship. It gave me great pleasure to work with him. Specially, I want to say "Vielen Dank" to him for translating many documents from German to English.

Further, I would like to thank my colleagues for providing tips in my experiments and also for the nice working atmosphere what they create. In particular I would like to express gratitude to Dr. Stephan Braatsch for initiating this project and his great help on my study; to Dr. Kuanyu Li and Dr. Tanja Zeller for sharing their experience and providing helpful comments; to the "RNA members", Steffen Wagner, Pamela Walter, Sonja Hundt, and Jasmin Weisel for their help in the protein-related work; to Dr. Hendrik Happ, Anne-Kathrin Hendrischk, Dr. Mobarak Abu Mraheil, Sebastian Metz, and Lisa Osterloh for sharing their materials with me; to Dr. Anke Treuner-Lange, Dr. Elena Evguenieva-Hackenberg and Dr. Jens Glaeser for their instructive suggestions; to Angelika Balzer and Kerstin Haberzettl for their technical assistance; to Sebastian Frühwirth for help in cloning; to Ramakanth Madhugiri for his good suggestions on my thesis; to Katrin Luehrsen and Susanne Weber for sequencing. "Ich danke Euch!"

My thanks also extend to Prof. Dr. Michael Keusgen and Martin Meyer for the cooperation in the SPR-based protein interaction assays; to Dr. Masakatsu Watanabe, Dr. Mineo Iseki and Dr. Mark Gomelsky for providing strains and plasmids; to Prof. Dr. Karl Forchhammer and Dr. Mani Maheswaran for help in initial plasmon resonance measurements; to Dr. Peter Friedhoff and Rohit Ghai for help in sequence analysis and protein structure modeling.

I sincerely express my gratitude to my Chinese friends for their kind help during my study. "感谢所有关心和帮助过我的中国朋友们!"

I want to thank Deutsche Forschungsgemeineschaft for the financial support, and thank Prof. Dr. Alfred Pingoud and Dr. Jamilah Michel for their help in Graduiertenkolleg.

Also I send my thanks to many other people, too numerous to mention, who helped in their own little way throughout this work.

Last, but not least, I would like to take this opportunity to thank my parents and my sister for providing me a sustained understanding and encouragement. I am forever grateful to my beloved husband Shaojun Lu for his personal care and support. I sincerely appreciate and thank him for sharing my happiness and sorrow.

Erklärung

Hiermit erkläre ich, dass ich die vorliegende Arbeit selbstständig verfasst habe und dabei keine anderen als die angegebenen Quellen und Hilfsmittel verwendet habe. Zitate sind als solche gekennzeichnet.

Giessen, den 27.10.2006

Yuchen Han